EUROPEAN ORGANISATION FOR NUCLEAR RESEARCH (CERN)

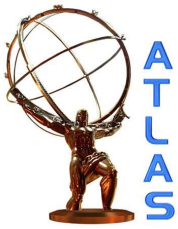

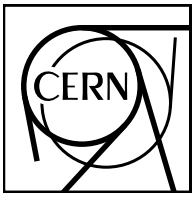

CERN-PH-EP-2012-310

Submitted to: Phys. Rev. D

Search for new phenomena in events with three charged leptons at $\sqrt{s} = 7$ TeV with the ATLAS detector

The ATLAS Collaboration

Abstract

A generic search for anomalous production of events with at least three charged leptons is presented. The search uses a pp-collision data sample at a center-of-mass energy of $\sqrt{s} = 7$ TeV corresponding to 4.6 fb^{-1} of integrated luminosity collected in 2011 by the ATLAS detector at the CERN Large Hadron Collider. Events are required to contain at least two electrons or muons, while the third lepton may either be an additional electron or muon, or a hadronically decaying tau lepton. Events are categorized by the presence or absence of a reconstructed tau-lepton or Z-boson candidate decaying to leptons. No significant excess above backgrounds expected from Standard Model processes is observed. Results are presented as upper limits on event yields from non-Standard-Model processes producing at least three prompt, isolated leptons, given as functions of lower bounds on several kinematic variables. Fiducial efficiencies for model testing are also provided. The use of the results is illustrated by setting upper limits on the production of doubly-charged Higgs bosons decaying to same-sign lepton pairs.

Search for new phenomena in events with three charged leptons at $\sqrt{s} = 7$ TeV with the ATLAS detector

The ATLAS Collaboration
(Dated: February 21, 2013)

A generic search for anomalous production of events with at least three charged leptons is presented. The search uses a pp-collision data sample at a center-of-mass energy of $\sqrt{s} = 7$ TeV corresponding to 4.6 fb^{-1} of integrated luminosity collected in 2011 by the ATLAS detector at the CERN Large Hadron Collider. Events are required to contain at least two electrons or muons, while the third lepton may either be an additional electron or muon, or a hadronically decaying tau lepton. Events are categorized by the presence or absence of a reconstructed tau-lepton or Z-boson candidate decaying to leptons. No significant excess above backgrounds expected from Standard Model processes is observed. Results are presented as upper limits on event yields from non-Standard-Model processes producing at least three prompt, isolated leptons, given as functions of lower bounds on several kinematic variables. Fiducial efficiencies for model testing are also provided. The use of the results is illustrated by setting upper limits on the production of doubly-charged Higgs bosons decaying to same-sign lepton pairs.

PACS numbers: 13.85Rm, 14.80.Fd, 14.65.Jk, 12.60.Cn

I. INTRODUCTION

Events with more than two energetic, prompt, and isolated charged leptons are rarely produced at hadron colliders. Such events offer a clean probe of electroweak processes at high center-of-mass energies, and their production at enhanced rates above Standard Model predictions would constitute evidence for new phenomena. Models predicting events with multiple leptons in the final state include excited neutrino models [1, 2], fourth-generation quark models [3], the Zee–Babu neutrino mass model [4–6], supersymmetry [7–15], and models with doubly-charged Higgs bosons [16, 17], including Higgs triplet models [18, 19].

The production of multilepton events in the Standard Model is dominated by WZ and ZZ production, where both bosons decay leptonically. Smaller contributions come from events with top-quark pairs produced in association with a W or Z boson, and from triboson production. Isolated but non-prompt lepton candidates misidentified as prompt arise in Drell–Yan events produced in association with a photon that converts in the detector and is reconstructed as an electron. Prompt but non-isolated leptons misidentified as isolated can arise from Dalitz decays [20, 21]. Additional non-prompt, non-isolated leptons arise from heavy-flavor decays and from mesons that decay in flight. Fake leptons can arise from hadrons that satisfy the lepton identification criteria.

This paper presents a search for the anomalous production of events with at least three charged leptons in the final state. The search uses a data set collected in 2011 by the ATLAS detector at the CERN Large Hadron Collider (LHC) corresponding to 4.6 fb^{-1} of pp collisions at a center-of-mass energy of $\sqrt{s} = 7$ TeV. Events are required to have at least two isolated electrons or muons, or one of each, while the third lepton may be either an additional electron or muon or a hadronically decaying tau lepton ($\tau_{\rm had}$).

Searches for new phenomena at the LHC are challenged by large cross-section Standard Model processes that overwhelm any events from rare interactions. Such backgrounds must be reduced by triggers before storing event data for future study; these triggers should be highly efficient at selecting processes of interest while reducing the overall rate of events by orders of magnitude. Additional requirements made on either leptons or event kinematics must likewise have both large background rejection factors and high efficiencies for events with real leptons. The reconstruction and identification of $\tau_{\rm had}$ candidates in a busy hadronic environment is particularly challenging, requiring the use of sophisticated analysis techniques to reduce backgrounds from parton-initiated jets. The analysis presented here attempts to reduce the backgrounds from Standard Model processes as much as possible, while retaining events that are potentially interesting for broad classes of new physics models.

Selected events are grouped into four categories by the presence or absence of a $\tau_{\rm had}$ candidate and by the presence or absence of a combination of leptons consistent with a Z-boson decay. The search is carried out separately in each category by inspecting several variables of interest. The results of the search are presented as model-independent limits. Efficiencies for selecting leptons within the fiducial volume are also presented in order to aid the interpretation of the results in the context of specific models of new phenomena.

Related searches for new phenomena in events with multilepton final states have not shown any significant deviation from Standard Model expectations. The CMS Collaboration has conducted a search similar to the one presented here using 4.98 fb^{-1} of 7 TeV data [22]. The ATLAS Collaboration has performed a search for supersymmetry in final states with three leptons [23], as have experiments at the Tevatron [24, 25]. The search presented here complements the previous searches by providing limits outside of the context of a specific model of

new phenomena.

This paper is organized as follows: the ATLAS detector is described in Section II, followed by a description of the samples and event selection in Sections III and IV, respectively. The categorization of events and definition of signal regions is presented in Section V. The background estimation techniques and the results of the application of those techniques in control regions are described in Section VI. Systematic uncertainties are discussed in Section VII. The results of the search are presented in Section VIII. Fiducial efficiencies for model testing are provided in Section IX, and are used to set upper limits on the pair-production of doubly-charged Higgs bosons.

II. THE ATLAS DETECTOR

The ATLAS experiment [26] is a multipurpose particle physics detector with a forward-backward symmetric cylindrical geometry and nearly 4π coverage in solid angle [27]. The inner tracking detector covers the pseudorapidity range $|\eta|< 2.5$, and consists of a silicon pixel detector, a silicon microstrip detector (SCT), and, for $|\eta|< 2.0$, a straw tube transition radiation tracker. The inner detector is surrounded by a thin superconducting solenoid providing a 2 T magnetic field. The calorimeter system covers the pseudorapidity range $|\eta| < 4.9$. Within the region $|\eta| < 3.2$, electromagnetic calorimetry is provided by barrel and end-cap high-granularity lead liquid-argon (LAr) electromagnetic calorimeters, with an additional thin LAr presampler covering $|\eta| < 1.8$, to correct for energy loss in material upstream of the calorimeters. Hadronic calorimetry is provided by the steel/scintillating-tile calorimeter, segmented into three barrel structures within $|\eta| < 1.7$, and two copper/LAr hadronic endcap calorimeters. The solid angle coverage is completed with forward copper/LAr and tungsten/LAr calorimeter modules optimized for electromagnetic and hadronic measurements respectively. The muon spectrometer surrounds the calorimeters. It consists of three large air-core superconducting toroid systems with eight coils each and stations of precision tracking and trigger chambers providing accurate muon tracking for $|\eta| < 2.7$. A three-level trigger system [28] is used to select events for further analysis offline.

III. MONTE CARLO SIMULATION AND DATA SETS

Monte Carlo (MC) simulation samples are used to estimate backgrounds from events with three prompt leptons. The ATLAS detector is simulated using GEANT4 [29], and simulated events are reconstructed using the same software as that used for collision data. Small post-reconstruction corrections are applied to account for differences in efficiency, momentum resolution and scale, and energy resolution and scale between data and simulation [30, 31].

The largest Standard Model backgrounds with at least three prompt leptons are WZ and ZZ production where the bosons decay leptonically. These processes are modeled with SHERPA 1.4.1 [32]. These samples include the case where the Z boson (or γ^*) is off-shell, and the γ^* has an invariant mass above twice the muon (tau) mass for $\gamma^* \to \mu\mu$ ($\gamma^* \to \tau\tau$), and above 100 MeV for $\gamma^* \to ee$. Diagrams where a γ^* is produced as radiation from a final-state lepton and decays to additional leptons, *i.e.* $W \to \ell^*\nu \to \ell\gamma^*\nu \to \ell\ell'\ell'\nu$ and $Z \to \ell\ell^* \to \ell\ell\gamma^* \to \ell\ell\ell'\ell'$, where ℓ and ℓ' need not have the same flavor, are also included. The leading-order predictions from SHERPA are cross-checked with next-to-leading-order calculations from POWHEG-BOX 1.0 [33]. Diagrams including a Standard Model Higgs boson have negligible contributions in all signal regions under study.

The production of $t\bar{t} + W/Z$ processes (also denoted $t\bar{t} + V$) is simulated with MADGRAPH 5.1.3.28 [34] for the matrix element and PYTHIA 6.425 [35] for the parton shower and fragmentation. Corrections to the normalization from higher-order effects for these samples are 20% for $t\bar{t} + W$ [36] and 30% for $t\bar{t} + Z$ [37]. Leptons from Drell–Yan processes produced in association with a photon that converts in the detector (denoted $Z + \gamma$ in the following) are modeled with PYTHIA. Additional samples are used to model dilepton backgrounds for control regions with fewer than three leptons. Events from $t\bar{t}$ production are simulated with MC@NLO 4.01 [38], with HERWIG 6.520 [39] for the parton shower and fragmentation, and JIMMY 4.31 [40] for the underlying event. Events from W+jets and $W+\gamma$ production are simulated with ALPGEN 2.13 [41] for the matrix element, HERWIG for the parton shower and fragmentation, and JIMMY for the underlying event.

Simulated samples of pair-produced doubly-charged Higgs bosons [16, 17, 19] are used to illustrate the results of this search in the context of a specific scenario. The doubly-charged Higgs bosons decay to pairs of same-sign leptons, producing up to four energetic, prompt, isolated charged leptons in the final state. The doubly-charged Higgs bosons are simulated with masses ranging from 100 GeV to 500 GeV. A sample of pair-produced fourth-generation down-type quarks [3] is also considered when estimating fiducial efficiencies and potential contributions from non-Standard-Model processes. In this model, the heavy quarks decay to top quarks and W bosons, producing four W bosons and two bottom quarks. This analysis is sensitive to the subset of such events in which at least three of the W bosons decay leptonically. The heavy quark is assumed to have a mass of 500 GeV, corresponding to the approximate expected experimental limit. The normalization for this sample is provided at approximately next-to-next-to-leading-order accuracy by HATHOR 1.2 [42]. Both the doubly-charged Higgs boson and fourth-generation quark samples are generated with PYTHIA.

The parton distribution functions for the SHERPA and

POWHEG-BOX samples are taken from CT10 [43], and from MRST2007 LO** [44] for the PYTHIA and HERWIG samples. The MADGRAPH and ALPGEN samples use CTEQ6L1 [45]. The MC@NLO sample uses CTEQ6.6 [46].

Additional pp interactions (pileup) in the same or nearby bunch crossings are modeled with PYTHIA. Simulated events are reweighted to reproduce the distribution of pp interactions per crossing observed in data over the course of the 2011 run. The mean number of interactions per bunch crossing for the data was ten. The luminosity has been measured with an uncertainty of $\pm 3.9\%$ [47].

IV. EVENT SELECTION

Events are required to have fired at least one single-electron or single-muon trigger. The electron trigger requires a minimum threshold on the momentum transverse to the beamline (p_{T}) of 20 GeV for data collected in the early part of 2011, and 22 GeV for data collected later in the year. The muon p_{T} threshold is 18 GeV for the full data set. The efficiency of the trigger requirements for events satisfying all selection criteria ranges from 95% to 99% depending on the signal region, and is evaluated with simulated WZ events. In order to ensure that the efficiency is independent of the p_{T} of the leptons, the offline event selection requires that at least one lepton (electron or muon) has $p_{\mathrm{T}} \geq 25$ GeV. At least one such lepton must also be consistent with having fired the relevant single-lepton trigger. A muon associated with the trigger must lie within $|\eta| < 2.4$ due to the limited acceptance of the muon trigger, while triggered electrons must lie within $|\eta| < 2.47$, excluding the calorimeter barrel/end-cap transition region ($1.37 \leq |\eta| < 1.52$). Additional muons in the event must lie within $|\eta| < 2.5$ and have $p_{\mathrm{T}} \geq 10$ GeV. Additional electrons must satisfy the same η requirements as triggered electrons, and must have $p_{\mathrm{T}} \geq 10$ GeV. The third lepton in the event may be an additional electron or muon satisfying the same requirements as the second lepton, or a τ_{had} with $p_{\mathrm{T}}^{\mathrm{vis}} \geq 15$ GeV and $|\eta^{\mathrm{vis}}| < 2.5$, where $p_{\mathrm{T}}^{\mathrm{vis}}$ and η^{vis} denote the p_{T} and η of the visible products of the tau decay, with no corrections for the momentum carried by neutrinos. Throughout this paper the four-momenta of tau candidates are defined only by the visible decay products.

All parts of the detector are required to have been operating properly for the events under study. Events must have a reconstructed primary vertex candidate with at least three associated tracks, where each track must have $p_{\mathrm{T}} > 0.4$ GeV. In events with multiple primary vertex candidates, the primary vertex is chosen to be the one with the largest value of Σp_{T}^2, where the sum is taken over all reconstructed tracks associated with the vertex. Events with pairs of leptons that are of the same flavor but opposite sign and have an invariant mass below 20 GeV are excluded to avoid contributions from low-mass hadronic resonances.

The lepton selection includes requirements to reduce the contributions from non-prompt or fake lepton candidates. These requirements exploit the transverse and longitudinal impact parameters of their tracks with respect to the primary vertex, the isolation of the lepton candidates from nearby hadronic activity, and in the case of electron and τ_{had} candidates, the lateral and longitudinal profiles of the shower in the electromagnetic calorimeter. There are also requirements for electrons on the quality of the reconstructed track and its match to the cluster in the calorimeter. These requirements are described in more detail below.

Electron candidates are required to satisfy the "tight" identification criteria described in Ref. [30], updated for the increased pileup in the 2011 data set. Muons must have tracks with hits in both the inner tracking detector and muon spectrometer, and must satisfy criteria on track quality described in Ref. [31].

The transverse impact parameter significance is defined as $|d_0/\sigma(d_0)|$, where d_0 is the transverse impact parameter of the reconstructed track with respect to the primary vertex and $\sigma(d_0)$ is the estimated uncertainty on d_0. This quantity must be less than 3.0 for muon candidates. Electrons must satisfy a looser cut of $|d_0/\sigma(d_0)| < 10$, since interactions with material in the inner tracking detector often reduce the quality of the reconstructed track. The longitudinal impact parameter z_0 must satisfy $|z_0 \sin(\theta)| < 1$ mm for both electrons and muons.

Electrons and muons are required to be isolated through the use of two variables sensitive to the amount of hadronic activity near the candidate. The first, $p_{\mathrm{T,track}}^{\mathrm{iso}}$, is the scalar sum of the transverse momenta of all tracks with $p_{\mathrm{T}} \geq 1$ GeV in a cone of $\Delta R < 0.3$ around the lepton axis. The sum excludes the track associated with the lepton candidate, and also excludes tracks inconsistent with originating from the primary vertex. The second, $E_{\mathrm{T,cal}}^{\mathrm{iso}}$, is the sum of the transverse energies of cells in the electromagnetic and hadronic calorimeters in a cone of the same size. For electron candidates this sum excludes a rectangular region around the candidate axis of 0.125×0.172 in $\eta \times \phi$ (corresponding to 5×7 cells in the main sampling layer of the electromagnetic calorimeter) and is corrected for the imperfect containment of the electron transverse energy within the excluded region. For muons, the sum only includes cells above a certain threshold in order to suppress noise, and does not include cells with energy deposits from the muon candidate. For both electrons and muons, the value of $E_{\mathrm{T,cal}}^{\mathrm{iso}}$ is corrected for the expected effects of pileup interactions. Muon candidates are required to have $p_{\mathrm{T,track}}^{\mathrm{iso}}/p_{\mathrm{T}} < 0.13$ and $E_{\mathrm{T,cal}}^{\mathrm{iso}}/p_{\mathrm{T}} < 0.14$, while electron candidates are required to have $p_{\mathrm{T,track}}^{\mathrm{iso}}/p_{\mathrm{T}} < 0.15$ and $E_{\mathrm{T,cal}}^{\mathrm{iso}}/p_{\mathrm{T}} < 0.14$; see Ref. [48] for the optimization of these requirements.

Jets in the event are reconstructed using the FASTJET [49] implementation of the anti-k_t algorithm [50], with distance parameter $R = 0.4$. The jet four-momenta are corrected for the non-compensating nature of the calorimeter, for inactive material in front of the calorime-

ters, and for pileup [51, 52]. Jets used in this analysis are required to have $p_{\mathrm{T}} \geq 25$ GeV and lie within $|\eta| < 4.9$. Jets within the acceptance of the inner tracking detector must fulfill a requirement, based on tracking information, that they originate from the primary vertex. The missing transverse momentum, $\mathbf{p}_{\mathrm{T}}^{\mathrm{miss}}$, is defined as the negative vector sum of the transverse momenta of reconstructed jets, leptons, and any remaining calorimeter clusters unassociated with reconstructed objects. The magnitude of $\mathbf{p}_{\mathrm{T}}^{\mathrm{miss}}$ is denoted $E_{\mathrm{T}}^{\mathrm{miss}}$.

Tau leptons decaying to an electron (muon) and neutrinos are selected with the nominal identification criteria described above, and are classified as electrons (muons). Hadronically decaying tau candidates are constructed from jet candidates and are then selected using a boosted decision tree (BDT), which is trained to distinguish hadronically decaying tau leptons from quark- and gluon-initiated jets [53]. The BDT is trained separately for tau candidates with one and three charged decay products, referred to as "one-prong" and "three-prong" taus, respectively. In this analysis, only one-prong τ_{had} candidates satisfying the "tight" working point criteria are considered. This working point is roughly 35% efficient for one-prong τ_{had} candidates originating from W-boson or Z-boson decays, and has a jet rejection factor of roughly 300. Additional requirements to remove τ_{had} candidates initiated by prompt electrons or muons are also imposed. A BDT trained to discriminate between electron-initiated τ_{had} candidates and true τ_{had} candidates provides a factor of roughly 400 in rejection at 90% efficiency. Muon-initiated τ_{had} candidates are identified with a cut-based method, which achieves a factor of two in rejection at 96% efficiency. The identification of both electron- and muon-initiated τ_{had} candidates is discussed further in Ref. [53].

Since lepton and jet candidates can be reconstructed as multiple objects, the following logic is applied to remove overlaps. If two electrons are separated by $\Delta R < 0.1$, the candidate with lower p_{T} is neglected. If a jet lies within $\Delta R = 0.2$ of an electron or τ_{had} candidate, the jet is neglected, while if the separation of the jet from an electron candidate satisfies $0.2 \leq \Delta R < 0.4$, the electron is neglected. In addition, electrons within $\Delta R = 0.1$ of a muon are also neglected, as are τ_{had} candidates within $\Delta R = 0.2$ of electron or muon candidates. Finally, muon candidates with a jet within $\Delta R = 0.4$ are neglected.

V. SIGNAL REGIONS

Events satisfying all selection criteria are classified into four categories. Events in which at least three of the lepton candidates are electrons or muons are selected first, followed by events with two electrons or muons, or one of each, and at least one τ_{had} candidate. These two categories are referred to as $\geq 3e/\mu$ and $2e/\mu+ \geq 1\tau_{\mathrm{had}}$ respectively. Next, events in each of those two categories are sub-divided by the presence or absence of a reconstructed Z-boson candidate, which is defined as an opposite-sign same-flavor pair of lepton candidates with a total invariant mass within ± 20 GeV of the Z-boson mass [54]. An additional electron may also be included in the combination with the same-flavor opposite-sign pair to satisfy the invariant mass requirement, to handle cases where an energetic photon from final-state radiation converts in the detector and is reconstructed as a prompt electron. Events with a reconstructed Z-boson candidate are referred to as on-Z, and those without such a candidate are referred to as off-Z. The resulting four categories are mutually exclusive, and are chosen to isolate the contributions from backgrounds such as jets faking τ_{had} candidates, and events with Z bosons produced in association with a jet that fakes a prompt lepton. In order to remain independent of the Z+jets control region described in Section VI, the on-Z regions have a minimum $E_{\mathrm{T}}^{\mathrm{miss}}$ requirement of 20 GeV.

TABLE I. Kinematic signal regions defined in the analysis. The on-Z regions have an additional requirement of $E_{\mathrm{T}}^{\mathrm{miss}} > 20$ GeV.

Variable	Lower Bounds [GeV]	Additional Requirement
$H_{\mathrm{T}}^{\mathrm{leptons}}$	0, 100, 150, 200, 300	
$E_{\mathrm{T}}^{\mathrm{miss}}$	0, 50, 75	$H_{\mathrm{T}}^{\mathrm{jets}} < 100$ GeV
$E_{\mathrm{T}}^{\mathrm{miss}}$	0, 50, 75	$H_{\mathrm{T}}^{\mathrm{jets}} \geq 100$ GeV
m_{eff}	0, 150, 300, 500	
m_{eff}	0, 150, 300, 500	$E_{\mathrm{T}}^{\mathrm{miss}} \geq 75$ GeV

Several kinematic variables are used to characterize the events that satisfy all selection criteria. The variable $H_{\mathrm{T}}^{\mathrm{leptons}}$ is defined as the scalar sum of transverse momenta, or $p_{\mathrm{T}}^{\mathrm{vis}}$ for τ_{had} candidates, of the three leading leptons. The variable $H_{\mathrm{T}}^{\mathrm{jets}}$ is defined as the sum of transverse momenta of all selected jets in the event. The "effective mass", m_{eff}, is the scalar sum of $E_{\mathrm{T}}^{\mathrm{miss}}$, $H_{\mathrm{T}}^{\mathrm{jets}}$, and the transverse momenta of all identified leptons in the event.

Subsets of selected events are defined based on kinematic properties. The $H_{\mathrm{T}}^{\mathrm{leptons}}$ distribution is considered for all events in each category. The $E_{\mathrm{T}}^{\mathrm{miss}}$ distribution is considered separately for events with $H_{\mathrm{T}}^{\mathrm{jets}}$ below and above 100 GeV, which serves to separate events produced through weak and strong interactions. The m_{eff} distribution is considered for events with and without a requirement of $E_{\mathrm{T}}^{\mathrm{miss}} \geq 75$ GeV. Increasing lower bounds on the value of each kinematic variable define signal regions; the lower bounds are shown in Table I.

VI. BACKGROUND ESTIMATION

Standard Model processes that produce events with three lepton candidates fall into three classes. The first consists of events in which prompt leptons are produced

in the hard interaction, including the WZ, ZZ, and $t\bar{t}+W/Z$ processes. A second class of events includes Drell–Yan production in association with an energetic γ, which then converts in the detector to produce a single reconstructed electron. A third class of events arises from non-prompt, non-isolated, or fake lepton candidates satisfying the identification criteria described in Section IV.

The first class of backgrounds is dominated by $WZ \to \ell\nu\ell'\ell'$ and $ZZ \to \ell\ell\ell'\ell'$ events. Smaller contributions come from $t\bar{t}+W \to b\bar{b}\ell\nu\ell'\nu\ell''\nu$ and $t\bar{t}+Z \to b\bar{b}\ell\nu\ell'\nu\ell''\ell''$ events. Contributions from triboson events, such as $WWW \to \ell\nu\ell'\nu\ell''\nu$ production, are negligible. All such processes are modeled with the dedicated MC samples described in Section III. Reconstructed leptons in the simulated samples are required to be consistent with the decay of a vector boson or tau lepton from the hard interaction. The second class of backgrounds, from Drell–Yan production in association with a hard photon, is also modeled with MC simulation.

The class of events that includes non-prompt or fake leptons, referred to here as the reducible background, is estimated using *in-situ* techniques which rely minimally on simulation. Such backgrounds for muons arise from semi-leptonic b- or c-hadron decays, from in-flight decays of pions or kaons, and from energetic jets that reach the muon spectrometer. Electron candidates can also arise from misidentified hadrons or jets. Hadronically decaying taus have large backgrounds from narrow, low-track-multiplicity jets that mimic $\tau_{\rm had}$ signatures.

Relaxed criteria are defined for each lepton flavor. These criteria, in combination with a requirement that candidates fail the nominal identification criteria, produce samples of lepton candidates that are rich in background with minimal contributions from misidentified prompt leptons. For electrons and muons, the isolation criteria are relaxed to accept non-isolated leptons. Electrons are also allowed to fail the "tight" electron identification criteria, provided they satisfy the "medium" criteria [30]. The relaxed $\tau_{\rm had}$ identification loosens the requirement on the BDT score.

These samples of events are used to measure the ratio of the number of leptons satisfying the nominal identification criteria to the number that fail the nominal criteria but satisfy the relaxed criteria. This ratio can then be applied as a scale factor – referred to here as a "fake factor" – to multilepton events satisfying the relaxed criteria to estimate the background in signal regions. For electron and muon candidates, the sample used to measure the fake factor consists of events that pass the high-$p_{\rm T}$ single-lepton triggers described in Section IV. Events with more than one selected lepton are removed from the sample to avoid overlap with the signal region, and to reduce the contamination from Drell–Yan processes. Muons must also fail the nominal requirement on $|d_0/\sigma(d_0)|$ to further remove prompt contributions. Finally, events where the transverse mass ($m_{\rm T}$) of the electron combined with the $E_{\rm T}^{\rm miss}$ is larger than 25 GeV are also rejected to avoid contamination from W+jets, where $m_{\rm T}$ is defined as:

$$m_{\rm T} \equiv \sqrt{(E_{\rm T}^{\ell} + E_{\rm T}^{\rm miss})^2 - |\mathbf{p}_{\rm T}^{\ell} + \mathbf{p}_{\rm T}^{\rm miss}|^2}. \quad (1)$$

For events with muons the transverse mass requirement is relaxed to 40 GeV since the inversion of the $|d_0/\sigma(d_0)|$ requirement is sufficient to remove most of the contributions from W-boson decays.

For $\tau_{\rm had}$ candidates, a sample of γ+jet events is used to measure the fake factors. The production of prompt photons in pp collisions is dominated by the Compton process $qg \to q\gamma$, yielding a sample of γ+jet events that is rich in quark-initiated jets. In the events considered here, an energetic photon is used to tag the event, and the $\tau_{\rm had}$ candidate is the away-side jet. The photon is required to have $p_{\rm T} > 40$ GeV, and satisfy the "tight" identification criteria [55]. The photon candidate is also required to have $E_{\rm T,cal}^{\rm iso} < 5$ GeV. These criteria have been shown to yield a mostly pure sample of photon candidates, with the remainder largely consisting of events in which a jet fragments into a leading π^0 that then decays to two photons. The resulting sample suffers from minimal contamination from true $\tau_{\rm had}$ candidates, with the largest contribution from $W(\to \tau_{\rm had}\nu)$+jet events, where the jet is identified as a photon, contributing less than 1% to the total sample.

The fake factors for all flavors are parameterized as functions of the $p_{\rm T}$ and $|\eta|$ of the candidates, to account for changes in the composition of the nominal and relaxed samples in different kinematic ranges. For electrons and muons with $p_{\rm T} > 100$ GeV, the fake factor is computed from a linear extrapolation of the fake factors between 35 GeV and 100 GeV. An additional parameterization is added to account for the heavy-flavor content of the event based on the output of the MV1 b-tagging algorithm. The MV1 algorithm uses a neural network to identify b-jets based on the outputs of several secondary-vertex and three-dimensional-impact-parameter taggers, which are described in detail in Ref [56]. The largest MV1 score associated with any jet in the event is used to parameterize the fake factors. The correlation of this variable with the use of the inverted $|d_0/\sigma(d_0)|$ requirement when estimating the muon fake factors leads to a bias in events with large MV1 scores, causing the muon fake factors to be underestimated by a factor of two. This bias is corrected using MC simulated samples.

Contributions from prompt leptons can bias the reducible background estimates in two ways. The first arises when prompt leptons populate either the tight or relaxed regions when deriving the fake factors. The second arises when prompt leptons populate the relaxed region when applying the fake factors. In all cases, the effects of prompt leptons on the reducible background estimates are evaluated and corrected using MC simulation.

The background estimates are tested in several control regions. A control region rich in events with a Z boson produced in association with a jet is defined to test the

reducible background estimates. Events in this region have three identified lepton candidates, with the requirement that a pair of opposite-sign, same-flavor leptons has an invariant mass within ±20 GeV of the Z-boson mass. The additional requirement that the $E_{\mathrm{T}}^{\mathrm{miss}}$ does not exceed 20 GeV avoids overlap with the signal regions. This is referred to as the Z+jets region.

A second control region, also consisting of events with three lepton candidates, is defined using the low-mass Drell–Yan events rejected by the requirement that no opposite-sign, same-flavor lepton pair have $m(\ell^+\ell^-) < 20$ GeV. This region is referred to as the low-mass Drell–Yan region.

A third region is defined in order to probe the estimates of backgrounds from non-prompt and non-isolated sources in events rich in heavy-flavor decays. Events are required to have exactly two same-sign leptons and $E_{\mathrm{T}}^{\mathrm{miss}} > 40$ GeV. Events are further required to have a b-jet candidate selected by the MV1 tagging algorithm, using a working point that is 60% efficient and that has a light-jet mis-tag rate of less than 1% for jets with $p_{\mathrm{T}} < 100$ GeV. This sample is estimated to be primarily composed of lepton+jets $t\bar{t}$ events. The same-sign requirement suppresses events where both W bosons decay leptonically, and enhances the contributions from events where one lepton candidate originates from semileptonic b decay. This region is referred to as the $t\bar{t}$ region. An upper limit on $H_{\mathrm{T}}^{\mathrm{jets}}$ of 300 GeV reduces potential contamination from new phenomena.

Good agreement between the expected and observed event yields is seen in all control regions as shown in Table II. Figure 1 shows the m_{T} distribution of the $E_{\mathrm{T}}^{\mathrm{miss}}$ and the lepton not associated with the Z boson candidate in the $\geq 3e/\mu$ channel of the Z+jets region. Figure 2 shows the p_{T} distribution for the third lepton candidate in the Z+jets region. The p_{T} distribution for the subleading lepton (τ_{had} candidate) in the $t\bar{t}$ region is shown in Fig. 3. The p_{T} distribution for the third lepton in the low-mass Drell–Yan region is shown in Fig. 4. The $H_{\mathrm{T}}^{\mathrm{leptons}}$, $E_{\mathrm{T}}^{\mathrm{miss}}$, and m_{eff} distributions are not shown here, but also are in good agreement in the control regions. The contributions from new phenomena in the control regions are estimated with doubly-charged Higgs and fourth-generation quark events. An example of such contamination is shown with fourth-generation quark events in Fig. 3(a), where the contamination is small. The contributions in all other control regions from events with pair-produced doubly-charged Higgs bosons or fourth-generation quarks are negligible.

TABLE II. The predicted and observed number of events in the Z+jets, low-mass Drell–Yan, and $t\bar{t}$ control regions. The Z+jets and low-mass Drell–Yan regions are populated by trilepton events, while the $t\bar{t}$ region is composed of same-sign dilepton events. Statistical and systematic uncertainties on the expected event yields are combined as described in Section VII.

Channel	Irreducible	Reducible	Total	Observed
		Z+jets		
$\geq 3e/\mu$	165 ± 26	160 ± 50	320 ± 60	359
$2e/\mu+ \geq 1\tau_{\mathrm{had}}$	3.0 ± 0.6	1480 ± 360	1480 ± 360	1696
		Low-mass Drell–Yan		
$\geq 3e/\mu$	55 ± 9	34 ± 12	89 ± 15	101
$2e/\mu+ \geq 1\tau_{\mathrm{had}}$	0.5 ± 0.1	91 ± 23	92 ± 23	96
		$t\bar{t}$		
$2e/\mu$	25 ± 4	58 ± 23	83 ± 23	87
$1e/\mu + 1\tau_{\mathrm{had}}$	1.9 ± 0.4	107 ± 27	109 ± 27	103

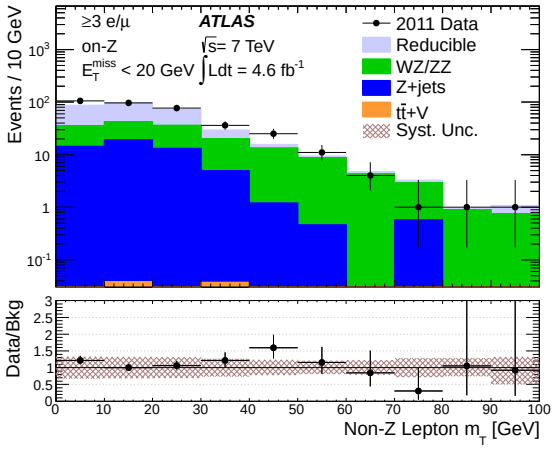

FIG. 1. The m_{T} distribution of the $E_{\mathrm{T}}^{\mathrm{miss}}$ and the lepton not associated with the Z-boson candidate decay in $\geq 3e/\mu$ events in the Z+jets control region. The last bin shows the integral of events above 90 GeV. The bottom panel shows the ratio of events observed in data to those expected from background sources for each bin.

VII. SYSTEMATIC UNCERTAINTIES

Systematic uncertainties on the predicted backgrounds come from several sources. These uncertainties are summarized in Table III, presented as ranges of relative uncertainties on the total expected background yields across all signal regions and channels.

The backgrounds modeled with simulated samples have uncertainties associated with trigger efficiencies, lepton efficiencies, lepton momentum scales and resolution, and jet energy scales and resolution. The uncertainty on the $E_{\mathrm{T}}^{\mathrm{miss}}$ in simulation is computed from varying the inputs to the $E_{\mathrm{T}}^{\mathrm{miss}}$ calculation within their uncertainties on the energy/momentum scale and resolution, and is thus strongly correlated with the other uncertainties and not presented separately. Contributions to the $E_{\mathrm{T}}^{\mathrm{miss}}$ from soft activity not associated with high-p_{T} objects are presented separately. Uncertainties on the jet energy scale and resolution are significant in regions re-

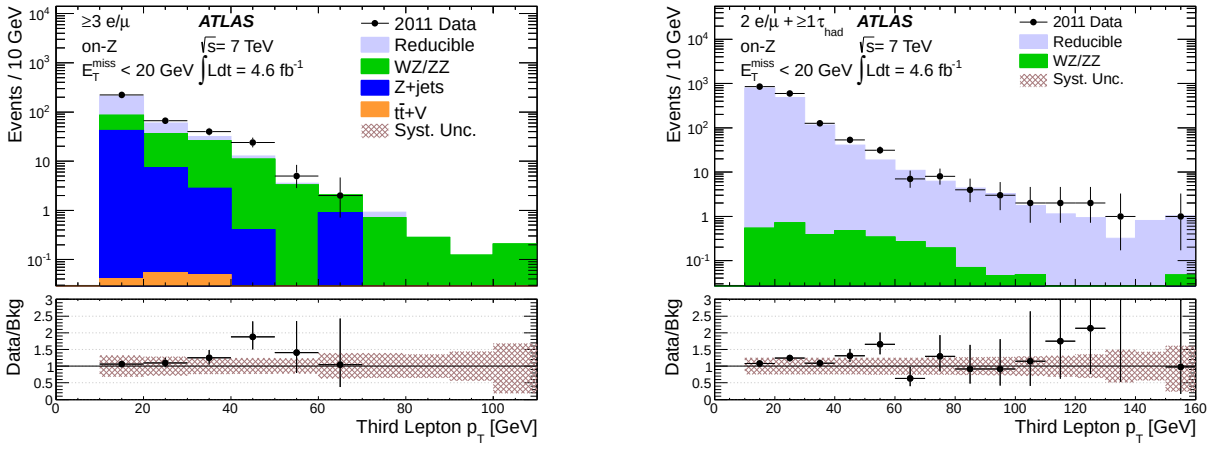

(a) (b)

FIG. 2. The p_{T} distribution of the third lepton candidate in (a) $\geq 3e/\mu$ events and (b) $2e/\mu+ \geq 1\tau_{\mathrm{had}}$ events in the Z+jets control region. The last bin in the left (right) plot shows the integral of events above 100 GeV (150 GeV). The bottom panel shows the ratio of events observed in data to those expected from background sources for each bin.

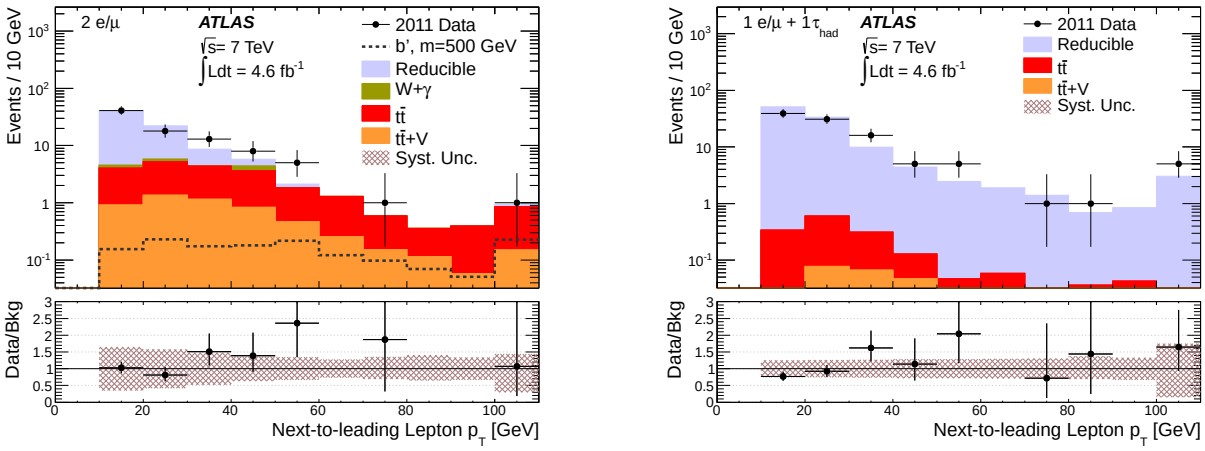

(a) (b)

FIG. 3. The p_{T} distribution of the (a) subleading lepton in $2e/\mu$ events and (b) τ_{had} in $1e/\mu + 1\tau_{\mathrm{had}}$ events in the $t\bar{t}$ control region. The expected contribution from non-Standard-Model processes is illustrated in the left figure by events with fourth-generation down-type quarks (b'). The contribution from b' events in the right figure is negligible. The last bin in each plot shows the integral of events above 100 GeV. The bottom panel shows the ratio of events observed in data to those expected from background sources for each bin.

quiring large values of $H_{\mathrm{T}}^{\mathrm{jets}}$ or m_{eff}, and are small otherwise.

Uncertainties on the cross sections of the different Standard Model processes modeled by simulation are also considered. The SHERPA predictions of the WZ and ZZ processes are cross-checked with the next-to-leading-order predictions from POWHEG-BOX in a kinematic region similar to the signal regions considered in this search, resulting in 10% and 25% uncertainties in the normalization, respectively. Uncertainties from renormalization and factorization scale variations, as well as the variation of the parton distribution functions, contribute an additional 10% and 7% respectively, taken from Ref. [57]. The $t\bar{t}+W$ and $t\bar{t}+Z$ backgrounds carry a total uncertainty of 50% based on parton distribution function and scale variations, and on large higher-order corrections [36, 37]. The Drell–Yan samples have a total uncertainty of 7% [58].

The reducible background estimates carry large uncertainties from several sources. A 40% uncertainty is assigned to the fake factors used to estimate the reducible electron and muon backgrounds, based on closure stud-

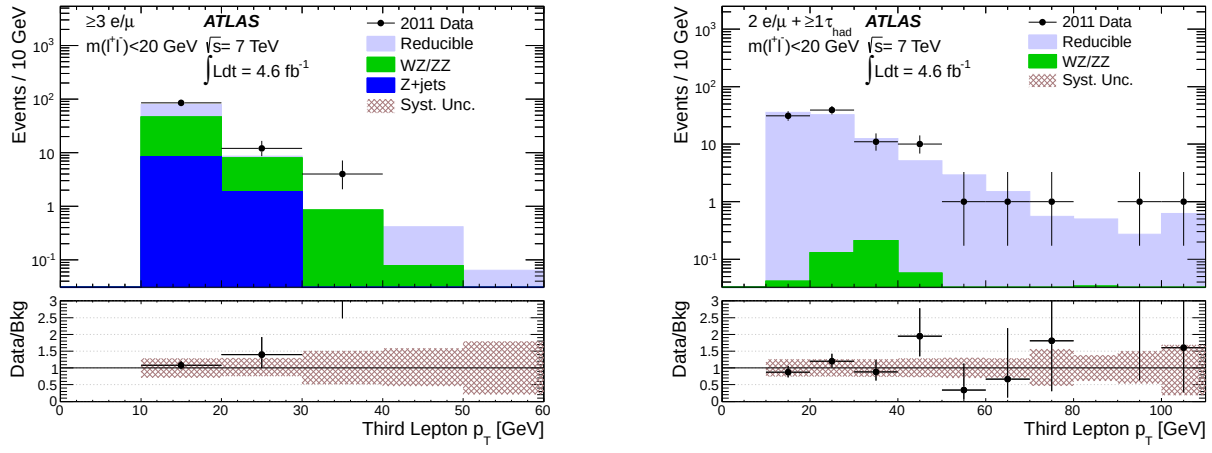

(a) (b)

FIG. 4. The p_{T} distribution of the (a) third lepton candidate in $\geq 3e/\mu$ events and (b) τ_{had} in $2e/\mu+ \geq 1\tau_{\mathrm{had}}$ events in the low-mass Drell–Yan control region. The last bin shows the integral of events above 50 GeV (100 GeV) in the left (right) figure. The bottom panel shows the ratio of events observed in data to those expected from background sources for each bin.

ies in MC samples and cross-checks in control regions. For electrons and muons with $p_{\mathrm{T}} > 100$ GeV, where the fake factors are extrapolated from the values at lower p_{T}, a 100% uncertainty is assigned. A 100% uncertainty is also assigned to the fake factors for muons with high b-tagging scores, due to the large correction taken from MC simulation to remove the bias between the b-tagging algorithm and the inverted d_0 requirement. For the τ_{had} fake estimates, a 25% uncertainty on the fake factors is determined by altering the composition of the relaxed sample. In signal regions where the relaxed samples are poorly populated, statistical uncertainties on the reducible background estimates become significant, especially in regions with high $E_{\mathrm{T}}^{\mathrm{miss}}$ or $H_{\mathrm{T}}^{\mathrm{jets}}$ requirements.

In all of the signal regions under study, the dominant systematic uncertainties on the total background estimate arise from the uncertainty associated with the reducible background estimates or from the uncertainty on the cross sections used for backgrounds taken from MC simulation.

Uncertainties on the efficiency for potential sources of new phenomena include contributions from lepton trigger and identification efficiencies, and lepton momentum scale and resolution. Larger uncertainties on the signal efficiency are assigned based on variations observed between several simulated samples, including pair-production of doubly-charged Higgs bosons and of fourth-generation down-type quarks, and are 10% for the $\geq 3e/\mu$ channels, and 20% for the $2e/\mu+ \geq 1\tau_{\mathrm{had}}$ channels.

VIII. RESULTS

Event yields for the most inclusive signal regions in each search channel are presented in Table IV. No significant deviation from the expected background is observed. The yields for all signal regions are presented in Tables VIII–XII of Appendix A.

The $H_{\mathrm{T}}^{\mathrm{leptons}}$ distributions for the two off-Z signal channels are shown in Fig. 5, and the $E_{\mathrm{T}}^{\mathrm{miss}}$ distributions for the same channels are shown in Fig. 6. The m_{eff} distributions for the two on-Z channels are shown in Fig. 7. The m_{eff} distribution for the on-Z, $\geq 3e/\mu$ channel in Fig. 7(a) has 4 events with $m_{\mathrm{eff}} > 1$ TeV where a total of 2.2 events are expected.

The observed event yields in different signal regions are used to constrain contributions from new phenomena. The 95% confidence level (CL) upper limits on the number of events from non-Standard-Model sources (N_{95}) are calculated using the CL$_s$ method [59]. All statistical and systematic uncertainties on estimated backgrounds are incorporated into the limit-setting procedure, with correlations taken into account where appropriate. Systematic uncertainties on the signal efficiency are also included as described in Section VII. The N_{95} limits are then converted into limits on the "visible cross section" ($\sigma_{95}^{\mathrm{vis}}$) using the relationship $\sigma_{95}^{\mathrm{vis}} = N_{95}/\int L\mathrm{d}t$.

Figures 8–12 show the resulting observed limits, along with the median expected limits with $\pm 1\sigma$ and $\pm 2\sigma$ uncertainties. Observed and expected limits are also presented in Tables XIII–XVII of Appendix B. The most inclusive signal regions for the $H_{\mathrm{T}}^{\mathrm{leptons}}$ and m_{eff} variables are composed of the same events within each channel, leading to identical limits.

IX. MODEL TESTING

The $\sigma_{95}^{\mathrm{vis}}$ limits can be converted into upper limits on the cross section of a specific model as follows:

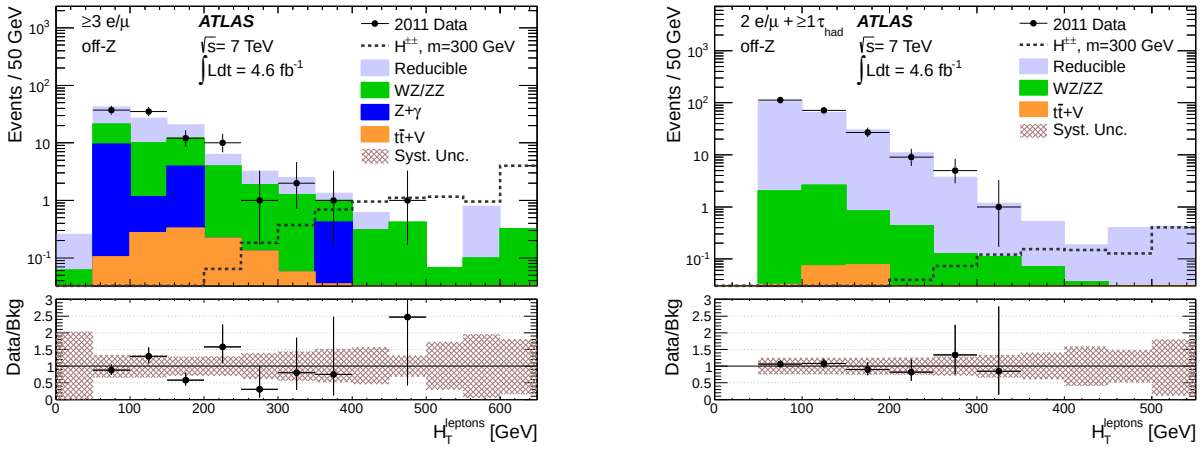

(a) (b)

FIG. 5. The $H_{\mathrm{T}}^{\mathrm{leptons}}$ distribution for the off-Z (a) $\geq 3e/\mu$ and (b) $2e/\mu+ \geq 1\tau_{\mathrm{had}}$ signal channels. The dashed lines represent the expected contributions from events with pair-produced doubly-charged Higgs bosons with masses of 300 GeV. The last bin in the left (right) figure shows the integral of events above 600 GeV (500 GeV). The bottom panel shows the ratio of events observed in data to those expected from background sources for each bin.

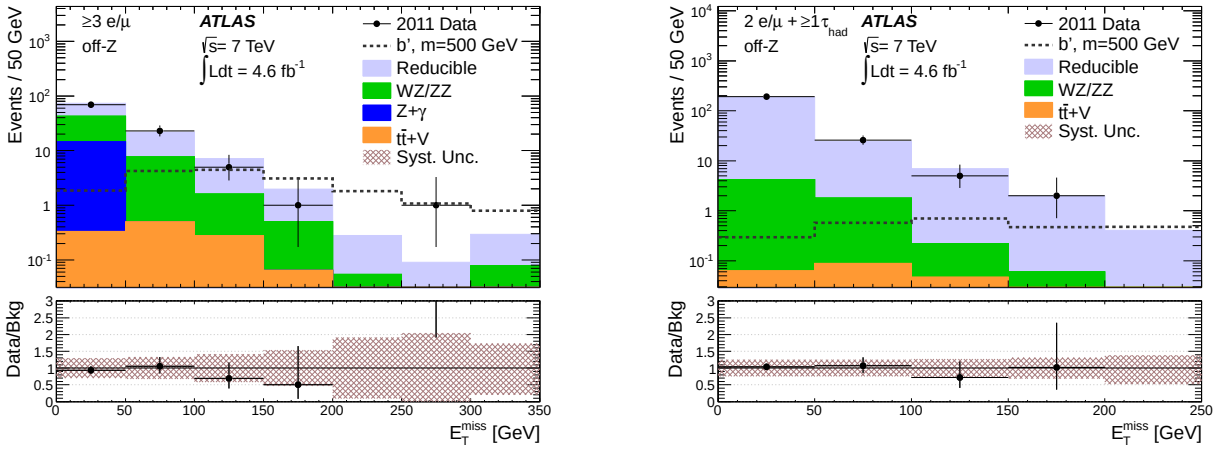

(a) (b)

FIG. 6. The $E_{\mathrm{T}}^{\mathrm{miss}}$ distribution for the off-Z (a) $\geq 3e/\mu$ and (b) $2e/\mu+ \geq 1\tau_{\mathrm{had}}$ signal channels. The dashed lines represent the expected contributions from events with fourth-generation down-type quarks with masses of 500 GeV. The last bin in the left (right) figure shows the integral of events above 300 GeV (200 GeV). The bottom panel shows the ratio of events observed in data to those expected from background sources for each bin.

- Events from the new model are examined at the particle (MC-generator) level and kinematic requirements on the particles are applied. These include the p_{T} and η requirements for leptons and jets, and isolation requirements for the leptons. No special treatment for pileup is necessary.

- The number of events passing this selection determines the cross section for the model given the fiducial constraints, σ^{fid}.

- A correction factor must be applied to take into account detector effects. This correction factor, called ϵ^{fid}, is model-dependent, and is subject to uncertainties from detector resolution, reconstruction efficiency, pileup, and vertex selection. This correction factor represents the ratio of the number of events satisfying the selection criteria after reconstruction to all those satisfying the fiducial acceptance criteria at the particle level. As this correction factor accounts for detector effects, no

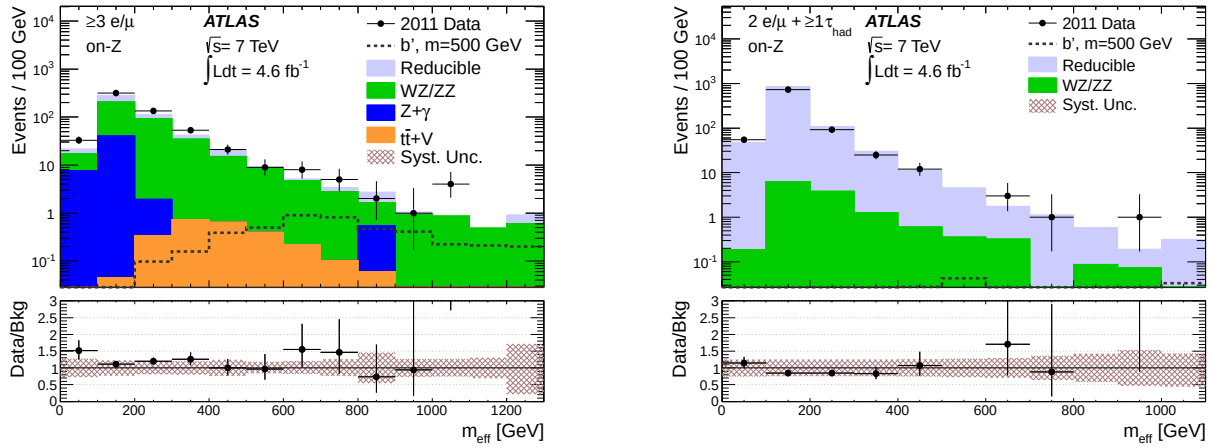

(a) (b)

FIG. 7. The $m_{\rm eff}$ distribution for the on-Z (a) $\geq 3e/\mu$ and (b) $2e/\mu+ \geq 1\tau_{\rm had}$ signal channels. The dashed lines represent the expected contributions from events with fourth-generation down-type quarks with masses of 500 GeV. The last bin in the left (right) figure shows the integral of events above 1.2 TeV (1 TeV). In the $\geq 3e/\mu$ channel, a total of 2.13 events are expected for $m_{\rm eff} > 1$ TeV, and 4 events are observed. The bottom panel shows the ratio of events observed in data to those expected from background sources for each bin.

TABLE III. The range of systematic uncertainties originating from different sources, presented as the relative uncertainty on the total expected background yield in all signal regions under study. In cases where a source of uncertainty contributes less than 1% of total uncertainty in any of the signal regions, the minimum is presented as "$\leq 1\%$".

Source of uncertainty	Uncertainty
Trigger efficiency	(≤ 1) – 1%
Electron energy scale	(≤ 1) – 13%
Electron energy resolution	(≤ 1) – 1%
Electron identification	(≤ 1) – 3%
Electron non-prompt/fake backgrounds	(≤ 1) – 13%
Muon momentum scale	(≤ 1) – 1%
Muon momentum resolution	(≤ 1) – 7%
Muon identification	(≤ 1) – 1%
Muon non-prompt/fake backgrounds	(≤ 1) – 51%
Tau energy scale	(≤ 1) – 4%
Tau identification	(≤ 1) – 4%
Tau non-prompt/fake backgrounds	(≤ 1) – 24%
Jet energy scale	(≤ 1) – 6%
Jet energy resolution	(≤ 1) – 3%
Soft $E_{\rm T}^{\rm miss}$ terms	(≤ 1) – 14%
Luminosity	3.9%
Cross-section uncertainties	(≤ 1) – 14%
Statistical uncertainties	1 – 25%
Total uncertainty	11 – 56%

TABLE IV. The expected and observed event yields for all inclusive signal channels. The expected yields are presented with two uncertainties, the first is the statistical uncertainty, and the second is the systematic uncertainty.

Flavor Chan.	Z Chan.	Expected	Observed
$\geq 3e/\mu$	off-Z	107 ± 7 ± 24	99
$\geq 3e/\mu$	on-Z	510 ± 10 ± 70	588
$2e/\mu+ \geq 1\tau_{\rm had}$	off-Z	220 ± 5 ± 50	226
$2e/\mu+ \geq 1\tau_{\rm had}$	on-Z	1060 ± 10 ± 260	914

unfolding of the reconstructed distributions is necessary.

- A 95% CL upper-limit on the cross section in the new model is then given by:

$$\sigma_{95}^{\rm fid} = \frac{N_{95}}{\epsilon^{\rm fid} \int Ldt} = \frac{\sigma_{95}^{\rm vis}}{\epsilon^{\rm fid}}. \quad (2)$$

The value of $\epsilon^{\rm fid}$ in the $\geq 3e/\mu$ channels ranges from roughly 0.50 for fourth-generation quark models to over 0.70 for doubly-charged Higgs models producing up to four high-$p_{\rm T}$ leptons. In the $2e/\mu+ \geq 1\tau_{\rm had}$ channels, $\epsilon^{\rm fid}$ is roughly 0.10 for a variety of models. Finite momentum resolution in the detector can cause particles with true momenta outside the kinematic acceptance (*e.g.* muons with $p_{\rm T} < 10$ GeV) to be accepted after reconstruction. The fraction of such events after selection is at most 3% for the $\geq 3e/\mu$ channels and 4% for the $2e/\mu+ \geq 1\tau_{\rm had}$ channels.

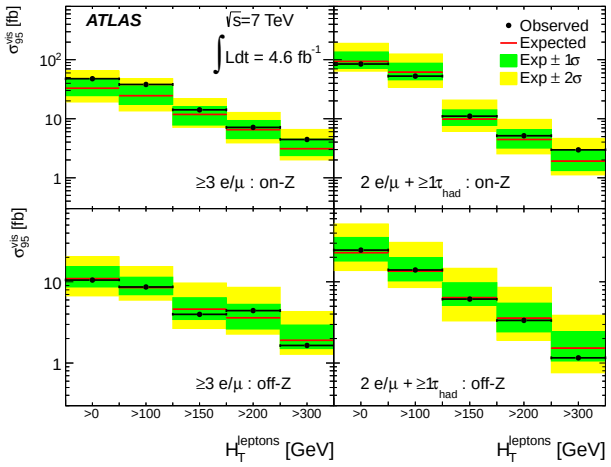

FIG. 8. The observed- and median-expected 95% CL limit on the visible cross section ($\sigma_{95}^{\rm vis}$) in the different signal channels, as functions of increasing lower bounds on $H_{\rm T}^{\rm leptons}$. The $\pm1\sigma$ and $\pm2\sigma$ uncertainties on the median expected limit are indicated by green and yellow bands, respectively.

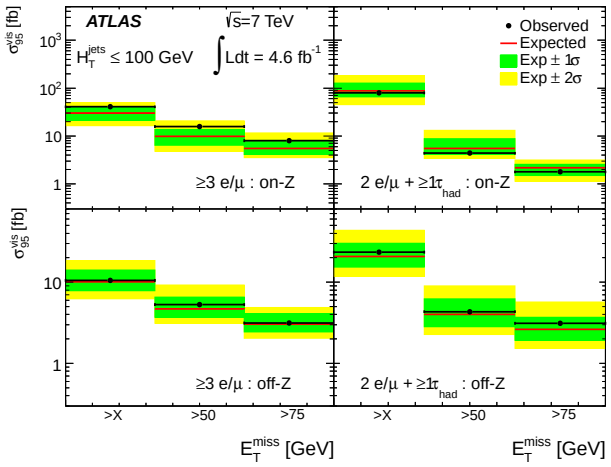

FIG. 9. The observed- and median-expected 95% CL limit on the visible cross section ($\sigma_{95}^{\rm vis}$) in the different signal channels, as functions of increasing lower bounds on $E_{\rm T}^{\rm miss}$, for events with $H_{\rm T}^{\rm jets} < 100$ GeV. The lowest bin boundary X is 0 GeV for the off-Z channels, and 20 GeV for the on-Z channels. The $\pm1\sigma$ and $\pm2\sigma$ uncertainties on the median expected limit are indicated by green and yellow bands, respectively.

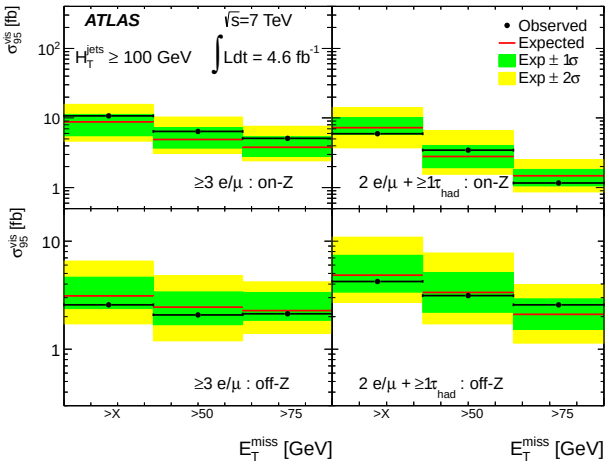

FIG. 10. The observed- and median-expected 95% CL limit on the visible cross section ($\sigma_{95}^{\rm vis}$) in the different signal channels, as functions of increasing lower bounds on $E_{\rm T}^{\rm miss}$, for events with $H_{\rm T}^{\rm jets} \geq 100$ GeV. The lowest bin boundary X is 0 GeV for the off-Z channels, and 20 GeV for the on-Z channels. The $\pm1\sigma$ and $\pm2\sigma$ uncertainties on the median expected limit are indicated by green and yellow bands, respectively.

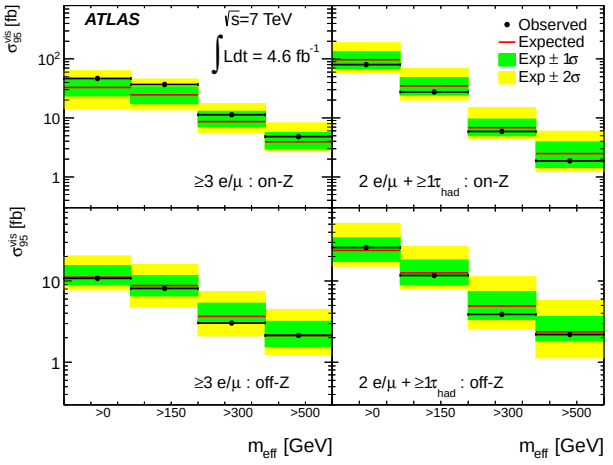

FIG. 11. The observed- and median-expected 95% CL limit on the visible cross section ($\sigma_{95}^{\rm vis}$) in the different signal channels, as functions of increasing lower bounds on $m_{\rm eff}$. The $\pm1\sigma$ and $\pm2\sigma$ uncertainties on the median expected limit are indicated by green and yellow bands, respectively.

In order to determine $\epsilon^{\rm fid}$ for unexplored models of new phenomena producing at least three prompt, isolated, and charged leptons in the final state, per-lepton efficiencies parameterized by the lepton kinematics are provided here. While the experimental results are based on reconstructed quantities, all requirements in the following are defined at the particle level. The per-lepton efficiencies attempt to emulate the ATLAS detector response, thereby allowing a comparison of the yields from particle-level event samples with the cross-section limits provided above without the need for a detector simulation.

Electrons at the particle level are required to have $p_{\rm T} \geq 10$ GeV, and to satisfy $|\eta| < 2.47$ and $|\eta| \notin (1.37, 1.52)$. Particle-level muons are required to have $p_{\rm T} \geq 10$ GeV, and to have $|\eta| < 2.5$. Electrons and muons are both required to be prompt, and not associated with a secondary vertex, unless they are the product of tau-lepton

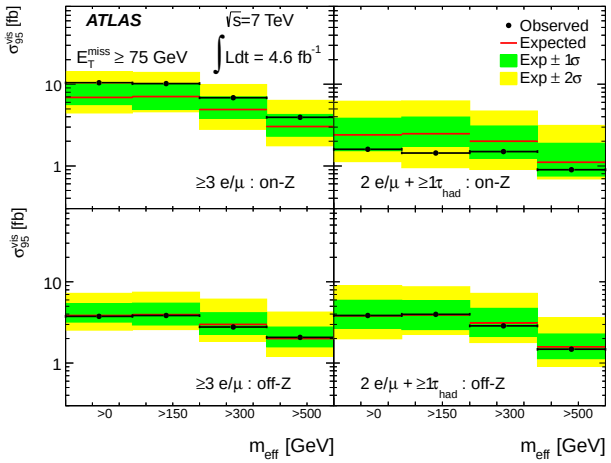

FIG. 12. The observed- and median-expected 95% CL limit on the visible cross section ($\sigma_{95}^{\rm vis}$) in the different signal channels, as functions of increasing lower bounds on $m_{\rm eff}$, for events with $E_{\rm T}^{\rm miss} > 75$ GeV. The $\pm1\sigma$ and $\pm2\sigma$ uncertainties on the median expected limit are indicated by green and yellow bands, respectively.

decays. Leptonically decaying tau candidates are required to produce electrons or muons that satisfy the criteria above. Hadronically decaying tau candidates are required to have $p_{\rm T}^{\rm vis} \geq 10$ GeV and $|\eta^{\rm vis}| < 2.5$, where the visible products of the tau decay include all particles except neutrinos. As with reconstructed tau candidates, the tau four-momentum at the particle level is defined only by the visible decay products.

Generated electrons and muons are further required to be isolated. A track isolation energy at the particle level corresponding to $p_{\rm T,track}^{\rm iso}$, denoted $p_{\rm T,true}^{\rm iso}$, is defined as the scalar sum of transverse momenta of charged particles within a cone of $\Delta R < 0.3$ around the lepton axis. Particles used in the sum are included after hadronization and must have $p_{\rm T} > 1$ GeV. A fiducial isolation energy corresponding to $E_{\rm T,cal}^{\rm iso}$, denoted $E_{\rm T,true}^{\rm iso}$, is defined as the sum of all particles inside the annulus $0.1 < \Delta R < 0.3$ around the lepton axis. Neutrinos and other stable, weakly-interacting particles are excluded from both $p_{\rm T,true}^{\rm iso}$ and $E_{\rm T,true}^{\rm iso}$; muons are excluded from $E_{\rm T,true}^{\rm iso}$. Electrons must satisfy $p_{\rm T,true}^{\rm iso}/p_{\rm T} < 0.13$ and $E_{\rm T,true}^{\rm iso}/p_{\rm T} < 0.2$, while muons must satisfy $p_{\rm T,true}^{\rm iso}/p_{\rm T} < 0.15$ and $E_{\rm T,true}^{\rm iso}/p_{\rm T} < 0.2$.

Events with at least three leptons as defined above must have at least two electrons and/or muons, at least one of which has $p_{\rm T} \geq 25$ GeV. The third lepton is allowed to be an electron or muon, in which case the event is classified as a $\geq 3e/\mu$ event, or a hadronically decaying tau lepton, in which case it is a $2e/\mu+ \geq 1\tau_{\rm had}$ event.

A simulated sample of WZ events is used to determine the per-lepton efficiencies ϵ_ℓ. The leptons above are matched to reconstructed lepton candidates that satisfy the selection criteria defined in Section IV, with ϵ_ℓ defined as the ratio of the number of reconstructed leptons satisfying all selection criteria to the number of generated leptons satisfying the fiducial criteria. Separate values of ϵ_ℓ are measured for each lepton flavor. In the case of electrons and muons, ϵ_ℓ is determined separately for leptons from tau decays.

TABLE V. The fiducial efficiency for electrons and taus in different $p_{\rm T}$ ranges. For tau candidates, $p_{\rm T} \equiv p_{\rm T}^{\rm vis}$.

$p_{\rm T}$ [GeV]	Prompt e	$\tau \to e$	$\tau_{\rm had}$
10–15	0.394±0.003	0.381±0.004	0.025±0.002
15–20	0.510±0.003	0.515±0.005	0.147±0.004
20–25	0.555±0.003	0.542±0.006	0.225±0.005
25–30	0.626±0.002	0.601±0.007	0.229±0.006
30–40	0.691±0.002	0.673±0.006	0.215±0.005
40–50	0.738±0.002	0.729±0.008	0.206±0.006
50–60	0.774±0.002	0.76±0.01	0.202±0.008
60–80	0.796±0.002	0.77±0.01	0.198±0.008
80–100	0.830±0.002	0.82±0.02	0.21±0.01
100–200	0.850±0.003	0.81±0.02	0.23±0.02
200–400	0.878±0.009	0.85±0.07	0.19±0.05

TABLE VI. The fiducial efficiency for electrons and taus in different η ranges. For tau candidates, $\eta \equiv \eta^{\rm vis}$.

$\lvert\eta\rvert$	Prompt e	$\tau \to e$	$\tau_{\rm had}$
0.0–0.1	0.675±0.003	0.52±0.01	0.210±0.009
0.1–0.5	0.757±0.001	0.595±0.005	0.195±0.004
0.5–1.0	0.747±0.001	0.581±0.005	0.179±0.004
1.0–1.5	0.666±0.002	0.494±0.006	0.138±0.004
1.5–2.0	0.607±0.002	0.465±0.006	0.170±0.004
2.0–2.5	0.591±0.002	0.475±0.007	0.163±0.005

All efficiencies are measured as functions of the lepton $p_{\rm T}$ and η. The efficiencies for electrons and taus are shown in Tables V and VI. The η dependence of the muon efficiencies is treated by separate $p_{\rm T}$ efficiency measurements for muons with $|\eta| < 0.1$ and those with $|\eta| \geq 0.1$, and is shown in Table VII. For taus, the efficiency tables include the efficiency for taus generated with $p_{\rm T}^{\rm vis} < 15$ GeV but reconstructed with $p_{\rm T}^{\rm vis} \geq 15$ GeV, due to resolution effects. The corresponding efficiencies for electrons and muons generated below 10 GeV are much smaller, and are not included here. The final per-lepton efficiency for electrons and taus is obtained as $\epsilon_\ell = \epsilon(p_{\rm T}) \cdot \epsilon(\eta)/\langle\epsilon\rangle$, where $\langle\epsilon\rangle$ is 0.69 for prompt electrons, 0.53 for electrons from tau decays, and 0.17 for hadronically decaying taus.

The resulting per-lepton efficiencies are then combined to yield a selection efficiency for a given event satisfying the fiducial acceptance criteria. For events with exactly three leptons, the total efficiency for the event is the product of the individual lepton efficiencies. For events with

TABLE VII. The fiducial efficiency for muons in different p_{T} ranges.

p_{T}	Prompt μ		$\tau \to \mu$	
[GeV]	$\lvert\eta\rvert > 0.1$	$\lvert\eta\rvert < 0.1$	$\lvert\eta\rvert > 0.1$	$\lvert\eta\rvert < 0.1$
10–15	0.852±0.002	0.47±0.02	0.66±0.004	0.36±0.02
15–20	0.896±0.002	0.51±0.01	0.71±0.005	0.38±0.02
20–25	0.912±0.001	0.52±0.01	0.734±0.005	0.43±0.03
25–30	0.921±0.001	0.50±0.01	0.750±0.006	0.39±0.03
30–40	0.927±0.001	0.507±0.007	0.779±0.005	0.46±0.03
40–50	0.928±0.001	0.513±0.008	0.784±0.007	0.45±0.04
50–60	0.932±0.001	0.532±0.009	0.79±0.01	0.37±0.05
60–80	0.932±0.001	0.524±0.009	0.81±0.01	0.43±0.06
80–100	0.932±0.002	0.51±0.01	0.77±0.02	0.53±0.09
100–200	0.930±0.002	0.50±0.01	0.83±0.02	0.47±0.12
200–400	0.919±0.007	0.45±0.05	0.59±0.11	-

more than three leptons, the additional leptons in order of descending p_{T} only contribute to the total efficiency when a lepton with higher p_{T} is not selected, leading to terms like $\epsilon_1\epsilon_2\epsilon_4(1-\epsilon_3)$, where ϵ_i denotes the fiducial efficiency for the i^{th} p_{T}-ordered lepton. The method can be extended to cover the number of leptons expected by the model under consideration.

Jets at the particle level are reconstructed from all stable particles, excluding muons and neutrinos, with the anti-k_t algorithm using a distance parameter $R = 0.4$. Overlaps between jets and leptons are removed as described in Section IV. $E_{\mathrm{T}}^{\mathrm{miss}}$ is defined as the magnitude of the vector sum of the transverse momenta of all stable, weakly-interacting particles, including those produced in models of new phenomena. The kinematic variables used for limit setting are defined as before: $H_{\mathrm{T}}^{\mathrm{leptons}}$ is the scalar sum of the transverse momenta, or $p_{\mathrm{T}}^{\mathrm{vis}}$ for τ_{had} candidates, of the three leptons that define the event; $H_{\mathrm{T}}^{\mathrm{jets}}$ is the scalar sum of all jets surviving overlap removal; $E_{\mathrm{T}}^{\mathrm{miss}}$ is as defined above, and m_{eff} is the sum of $E_{\mathrm{T}}^{\mathrm{miss}}$, $H_{\mathrm{T}}^{\mathrm{jets}}$, and all transverse momenta of selected leptons in the event.

Predictions of the rate and kinematic properties of events with multiple leptons made with the method described above agree well with the same quantities after detector simulation for a variety of models of new phenomena. Uncertainties, based on the level of agreement seen across a variety of models, are estimated at 10% for the $\geq 3e/\mu$ channels, and 20% for the $2e/\mu+ \geq 1\tau_{\mathrm{had}}$ channels. These uncertainties are included in the limits presented in Section VIII.

As an example of the application of the method described in this section, the $\sigma_{95}^{\mathrm{vis}}$ limits can be used to constrain models predicting the pair-production of doubly-charged Higgs bosons. The constraints from dedicated and optimized analyses by ATLAS [60] and CMS [61] are expected to be stronger than the constraints obtained here, but these numbers serve to benchmark the results presented in this paper.

Assuming a branching ratio of 100% for the decay $H^{\pm\pm} \to \mu^{\pm}\mu^{\pm}$, the acceptance of the fiducial selection is 91% and ϵ^{fid} is 71% for $m(H^{\pm\pm}) = 300$ GeV. The resulting 95% CL upper limit on the cross section times branching ratio ($\sigma \cdot \mathrm{BR}$) is 2.5 fb. The observed and median expected upper limits are shown in Fig. 13(a), along with the observed upper limit from the dedicated search by ATLAS [60]. These results are obtained using the $H_{\mathrm{T}}^{\mathrm{leptons}} \geq 300$ GeV signal region in the $\geq 3e/\mu$, off-Z channel. The theoretical cross section for $H^{\pm\pm}$ coupling to left-handed fermions ($H_L^{\pm\pm}$) implies that $H_L^{\pm\pm}$ masses below 330 GeV are excluded at 95% CL for $\mathrm{BR}(H^{\pm\pm} \to \mu^{\pm}\mu^{\pm})$=100%.

For the case with $\mathrm{BR}(H^{\pm\pm} \to \mu^{\pm}\tau^{\pm})$=100%, the acceptance for the $\geq 3e/\mu$ ($2e/\mu+ \geq 1\tau_{\mathrm{had}}$) channel is 24% (49%), and ϵ^{fid} is 59% (13%) for $m(H^{\pm\pm}) = 200$ GeV. The corresponding upper limit on the cross section is 12 (19) fb, with $m(H_L^{\pm\pm}) < 237$ GeV (220 GeV) excluded at 95% CL. In this case, the off-Z $H_{\mathrm{T}}^{\mathrm{leptons}} \geq 300$ GeV signal region is used to calculate the expected limits for all $H^{\pm\pm}$ masses except for $\mathrm{m}(H^{\pm\pm})$=100 GeV where the off-Z, $H_{\mathrm{T}}^{\mathrm{leptons}} \geq 200$ GeV signal region is used. The observed and median expected limits from the $\geq 3e/\mu$ channel are shown in Fig. 13(b).

X. CONCLUSION

A generic search for new phenomena in events with at least three energetic, charged, prompt, and isolated leptons has been presented, using a data sample corresponding to an integrated luminosity of 4.6 fb^{-1} of pp collision data collected by the ATLAS experiment. The search was conducted in separate channels based on the presence or absence of a hadronically decaying tau lepton or reconstructed Z boson, and yielded no significant deviation from background yields expected from the Standard Model. Upper limits at 95% confidence level on event yields due to non-Standard-Model processes were placed as a function of lower bounds on several kinematic variables. Additional information on the fiducial selection of events populating the signal regions under study has been provided. The use of this information in the interpretation of the results in the context of models of new phenomena has been illustrated by setting upper limits on the production of doubly-charged Higgs bosons decaying to same-sign lepton pairs.

ACKNOWLEDGMENTS

We thank CERN for the very successful operation of the LHC, as well as the support staff from our institutions without whom ATLAS could not be operated efficiently.

We acknowledge the support of ANPCyT, Argentina; YerPhI, Armenia; ARC, Australia; BMWF and FWF,

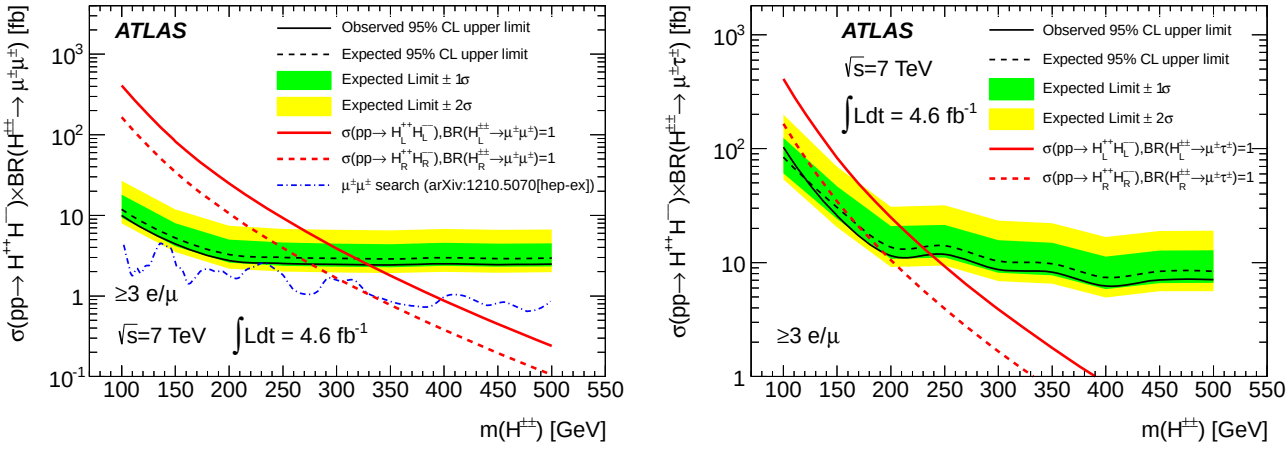

(a)$H^{\pm\pm} \to \mu^{\pm}\mu^{\pm}$ (b)$H^{\pm\pm} \to \mu^{\pm}\tau^{\pm}$

FIG. 13. The expected and observed 95% confidence level upper limits on the cross section times branching ratio of the (a) $H^{\pm\pm} \to \mu^{\pm}\mu^{\pm}$ and (b) $H^{\pm\pm} \to \mu^{\pm}\tau^{\pm}$ final states as a function of the $H^{\pm\pm}$ mass for the $\geq 3e/\mu$ channel. For $H^{\pm\pm} \to \mu^{\pm}\mu^{\pm}$, the median expected limit on the $H_L^{\pm\pm}$ mass is 319 GeV and the corresponding observed limit is 330 GeV; for $H^{\pm\pm} \to \mu^{\pm}\tau^{\pm}$, the median expected limit is 229 GeV and the corresponding observed limit is 237 GeV. Results from the dedicated ATLAS search for $H^{\pm\pm} \to \mu^{\pm}\mu^{\pm}$ [60] are also shown.

Austria; ANAS, Azerbaijan; SSTC, Belarus; CNPq and FAPESP, Brazil; NSERC, NRC and CFI, Canada; CERN; CONICYT, Chile; CAS, MOST and NSFC, China; COLCIENCIAS, Colombia; MSMT CR, MPO CR and VSC CR, Czech Republic; DNRF, DNSRC and Lundbeck Foundation, Denmark; EPLANET, ERC and NSRF, European Union; IN2P3-CNRS, CEA-DSM/IRFU, France; GNSF, Georgia; BMBF, DFG, HGF, MPG and AvH Foundation, Germany; GSRT and NSRF, Greece; ISF, MINERVA, GIF, DIP and Benoziyo Center, Israel; INFN, Italy; MEXT and JSPS, Japan; CNRST, Morocco; FOM and NWO, Netherlands; BRF and RCN, Norway; MNiSW, Poland; GRICES and FCT, Portugal; MERYS (MECTS), Romania; MES of Russia and ROSATOM, Russian Federation; JINR; MSTD, Serbia; MSSR, Slovakia; ARRS and MVZT, Slovenia; DST/NRF, South Africa; MICINN, Spain; SRC and Wallenberg Foundation, Sweden; SER, SNSF and Cantons of Bern and Geneva, Switzerland; NSC, Taiwan; TAEK, Turkey; STFC, the Royal Society and Leverhulme Trust, United Kingdom; DOE and NSF, United States of America.

The crucial computing support from all WLCG partners is acknowledged gratefully, in particular from CERN and the ATLAS Tier-1 facilities at TRIUMF (Canada), NDGF (Denmark, Norway, Sweden), CC-IN2P3 (France), KIT/GridKA (Germany), INFN-CNAF (Italy), NL-T1 (Netherlands), PIC (Spain), ASGC (Taiwan), RAL (UK) and BNL (USA) and in the Tier-2 facilities worldwide.

[1] S. Matsumoto, T. Nabeshima, and K. Yoshioka, J. High Energy Phys. **1006**, 058 (2010), arXiv:1004.3852 [hep-ph].
[2] A. Belyaev, C. Leroy, and R. R. Mehdiyev, Eur. Phys. J. C **41S2**, 1 (2005), arXiv:hep-ph/0401066.
[3] P. H. Frampton, P. Hung, and M. Sher, Phys. Rept. **330**, 263 (2000), arXiv:hep-ph/9903387.
[4] A. Zee, Phys. Lett. B **161**, 141 (1985).
[5] A. Zee, Nucl. Phys. B **264**, 99 (1986).
[6] K. S. Babu, Phys. Lett. B **203**, 132 (1988).
[7] H. Miyazawa, Prog. Theor. Phys. **36 (6)**, 1266 (1966).
[8] P. Ramond, Phys. Rev. D **3**, 2415 (1971).
[9] Y. A. Gol'fand and E. P. Likhtman, JETP Lett. **13**, 323 (1971), [Pisma Zh.Eksp.Teor.Fiz.13:452-455,1971].
[10] A. Neveu and J. H. Schwarz, Nucl. Phys. B **31**, 86 (1971).
[11] A. Neveu and J. H. Schwarz, Phys. Rev. D **4**, 1109 (1971).
[12] J. Gervais and B. Sakita, Nucl. Phys. B **34**, 632 (1971).
[13] D. V. Volkov and V. P. Akulov, Phys. Lett. B **46**, 109 (1973).
[14] J. Wess and B. Zumino, Phys. Lett. B **49**, 52 (1974).
[15] J. Wess and B. Zumino, Nucl. Phys. B **70**, 39 (1974).
[16] T. G. Rizzo, Phys. Rev. D **25**, 1355 (1982).
[17] H. Georgi and M. Machacek, Nucl. Phys. B **262**, 463 (1985).
[18] J. C. Montalvo, N. V. C. Jr., J. S. Borges, and M. D. Tonasse, Nucl. Phys. B **756**, 1 (2006), erratum: ibid. **796** 422 (2008).
[19] J. F. Gunion, R. Vega, and J. Wudka, Phys. Rev. D **42**, 1673 (1990).
[20] R. Dalitz, Proc. Phys. Soc. A **64**, 667 (1951).
[21] N. M. Kroll and W. Wada, Phys. Rev. **98**, 1355 (1955).
[22] CMS Collaboration, J. High Energy Phys. **1206**, 169

(2012), arXiv:1204.5341 [hep-ex].
[23] ATLAS Collaboration, Submitted to Phys. Lett. B (2012), arXiv:1208.3144 [hep-ex].
[24] CDF Collaboration, Phys. Rev. Lett. **101**, 251801 (2008), arXiv:0808.2446 [hep-ex].
[25] D0 Collaboration, Phys. Lett. B **680**, 34 (2009), arXiv:0901.0646 [hep-ex].
[26] ATLAS Collaboration, JINST **3**, S08003 (2008).
[27] ATLAS uses a right-handed coordinate system with its origin at the nominal interaction point (IP) in the center of the detector and the z-axis along the beam pipe. The x-axis points from the IP to the center of the LHC ring, and the y-axis points upward. Cylindrical coordinates (r, ϕ) are used in the transverse plane, ϕ being the azimuthal angle around the beam pipe. The pseudorapidity is defined in terms of the polar angle θ as $\eta = -\ln\tan(\theta/2)$. The variable ΔR is used to evaluate the distance between objects, and is defined as: $\Delta R = \sqrt{(\Delta\phi)^2 + (\Delta\eta)^2}$.
[28] ATLAS Collaboration, Eur. Phys. J. C **72**, 1849 (2012), arXiv:1110.1530 [hep-ex].
[29] S. Agostinelli *et al.*, Nucl. Instrum. Methods **506**, 250 (2003).
[30] ATLAS Collaboration, Eur. Phys. J. C **72**, 1909 (2012), arXiv:1110.3174 [hep-ex].
[31] ATLAS Collaboration, ATLAS-CONF-2011-063 (2011), `https://cdsweb.cern.ch/record/1345743`.
[32] T. Gleisberg, S. Höche, F. Krauss, M. Schönherr, S. Schumann, *et al.*, J. High Energy Phys. **0902**, 007 (2009), arXiv:0811.4622 [hep-ph].
[33] T. Melia, P. Nason, R. Rontsch, and G. Zanderighi, J. High Energy Phys. **1111**, 078 (2011), arXiv:1107.5051 [hep-ph].
[34] J. Alwall, M. Herquet, F. Maltoni, O. Mattelaer, and T. Stelzer, J. High Energy Phys. **1106**, 128 (2011), arXiv:1106.0522 [hep-ph].
[35] T. Sjöstrand, P. Edén, C. Friberg, L. Lönnblad, G. Miu, S. Mrenna, and N. Emanuel, Comput. Phys. Comm. **135**, 238 (2001), arXiv:hep-ph/0010017.
[36] J. M. Campbell and R. K. Ellis, J. High Energy Phys. **1207**, 052 (2012), arXiv:1204.5678 [hep-ph].
[37] M. Garzelli, A. Kardos, C. Papadopoulos, and Z. Trocsanyi, Phys. Rev. D **85**, 074022 (2012), arXiv:1111.1444 [hep-ph].
[38] S. Frixione and B. R. Webber, J. High Energy Phys. **06**, 029 (2002), arXiv:hep-ph/0204244.
[39] G. Corcella, I. Knowles, G. Marchesini, S. Moretti, K. Odagiri, *et al.*, J. High Energy Phys. **0101**, 010 (2001), arXiv:hep-ph/0011363.
[40] J. Butterworth, J. R. Forshaw, and M. Seymour, Z. Phys. C **72**, 637 (1996), arXiv:hep-ph/9601371.
[41] M. L. Mangano, M. Moretti, F. Piccinini, R. Pittau, and A. D. Polosa, J. High Energy Phys. **0307**, 001 (2003), arXiv:hep-ph/0206293.
[42] M. Aliev, H. Lacker, U. Langenfeld, S. Moch, P. Uwer, *et al.*, Comput. Phys. Commun. **182**, 1034 (2011), arXiv:1007.1327 [hep-ph].
[43] H.-L. Lai, M. Guzzi, J. Huston, Z. Li, P. M. Nadolsky, *et al.*, Phys. Rev. D **82**, 074024 (2010), arXiv:1007.2241 [hep-ph].
[44] A. Sherstnev and R. S. Thorne, Eur. Phys. J. C **55**, 553 (2008), arXiv:0711.2473 [hep-ph].
[45] J. Pumplin, D. Stump, J. Huston, H. Lai, P. M. Nadolsky, *et al.*, J. High Energy Phys. **0207**, 012 (2002), arXiv:hep-ph/0201195.
[46] P. M. Nadolsky, H.-L. Lai, Q.-H. Cao, J. Huston, J. Pumplin, *et al.*, Phys. Rev. D **78**, 013004 (2008), arXiv:0802.0007 [hep-ph].
[47] ATLAS Collaboration, Eur. Phys. J. C **71**, 1630 (2011), arXiv:1101.2185 [hep-ex].
[48] ATLAS Collaboration, Submitted to Phys. Lett. B (2012), arXiv:1206.6074 [hep-ex].
[49] M. Cacciari, G. P. Salam, and G. Soyez, Eur. Phys. J. C **72**, 1896 (2012), arXiv:1111.6097 [hep-ph].
[50] M. Cacciari, G. P. Salam, and G. Soyez, J. High Energy Phys. **04**, 063 (2008), arXiv:0802.1189 [hep-ph].
[51] ATLAS Collaboration, Submitted to Eur. Phys. J. C (2011), arXiv:1112.6426 [hep-ex].
[52] ATLAS Collaboration, ATLAS-CONF-2010-054 (2010), `https://cdsweb.cern.ch/record/1281311`.
[53] ATLAS Collaboration, ATLAS-CONF-2011-152 (2011), `https://cdsweb.cern.ch/record/1398195`.
[54] J. Beringer *et al.* (Particle Data Group), Phys. Rev. D **86**, 010001 (2012).
[55] ATLAS Collaboration, Phys. Rev. D **85**, 092014 (2012).
[56] ATLAS Collaboration, ATLAS-CONF-2011-102 (2011), `https://cdsweb.cern.ch/record/1369219`.
[57] ATLAS Collaboration, Phys. Rev. D **85**, 032004 (2012).
[58] ATLAS Collaboration, Phys. Rev. Lett. **107**, 272002 (2011).
[59] A. L. Read, J. of Phys. G **28**, 2693 (2002).
[60] ATLAS Collaboration, Submitted to the Eur. Phys. J. C (2012), arXiv:1210.5070 [hep-ex].
[61] CMS Collaboration, Submitted to the Eur. Phys. J. C (2012), arXiv:1207.2666 [hep-ex].

Appendix A: Tables of expected and observed event yields

The expected and observed event yields for all signal regions under study are shown in Tables VIII-XII.

TABLE VIII. Results for the $H_{\mathrm{T}}^{\mathrm{leptons}}$ signal regions. Irreducible sources include all backgrounds estimated with MC simulation. Results are presented in number of expected events as $N \pm$ (statistical uncertainty) $\pm$ (systematic uncertainty).

$H_{\mathrm{T}}^{\mathrm{leptons}} \geq$	Irreducible	Reducible	Total Exp.	Observed
		$\geq 3e/\mu$, off-Z		
0 GeV	54 ±4 ±7	54 ±6 ±23	107 ±7 ±24	99
100 GeV	32 ±2 ±4	32 ±4 ±16	65 ±4 ±16	62
150 GeV	22 ±1 ±3	15 ±2 ±8	37 ±3 ±8	27
200 GeV	9.7 ±0.6 ±1.5	6 ±2 ±4	16 ±2 ±4	15
300 GeV	3.6 ±0.5 ±0.5	2.5 ±1.2 ±1.8	6.2 ±1.3 ±1.9	4
		$2e/\mu+ \geq 1\tau_{\mathrm{had}}$, off-$Z$		
0 GeV	6.4 ±0.4 ±1.0	214 ±5 ±50	220 ±5 ±50	226
100 GeV	4.4 ±0.3 ±0.6	109 ±3 ±26	113 ±3 ±26	113
150 GeV	1.7 ±0.2 ±0.3	46 ±2 ±11	47 ±2 ±11	42
200 GeV	0.8 ±0.1 ±0.1	17 ±1 ±4	17 ±1 ±4	15
300 GeV	0.2 ±0.1 ±0.0	2.5 ±0.4 ±0.6	2.7 ±0.4 ±0.6	1
		$\geq 3e/\mu$, on-Z		
0 GeV	389 ±5 ±50	120 ±8 ±40	508 ±10 ±70	588
100 GeV	285 ±4 ±40	71 ±6 ±26	356 ±7 ±50	422
150 GeV	122 ±2 ±17	14 ±3 ±7	136 ±4 ±18	151
200 GeV	49 ±1 ±7	5 ±2 ±4	54 ±2 ±8	60
300 GeV	12.3 ±0.7 ±1.6	0.5 ±0.5 ±0.5	12.7 ±0.9 ±1.7	18
		$2e/\mu+ \geq 1\tau_{\mathrm{had}}$, on-$Z$		
0 GeV	13.2 ±0.5 ±2.2	1050 ±10 ±260	1060 ±10 ±260	914
100 GeV	11.1 ±0.5 ±1.9	670 ±10 ±160	680 ±10 ±160	587
150 GeV	4.5 ±0.3 ±0.8	66 ±2 ±16	71 ±2 ±16	75
200 GeV	1.8 ±0.2 ±0.3	19 ±1 ±5	21 ±1 ±5	24
300 GeV	0.5 ±0.1 ±0.1	3.0 ±0.5 ±0.8	3.5 ±0.5 ±0.8	7

TABLE IX. Results for the $E_{\mathrm{T}}^{\mathrm{miss}}$, $H_{\mathrm{T}}^{\mathrm{jets}}$<100 GeV signal regions. Irreducible sources include all backgrounds estimated with MC simulation. Results are presented in number of expected events as $N \pm$ (statistical uncertainty) $\pm$ (systematic uncertainty).

$E_{\mathrm{T}}^{\mathrm{miss}} \geq$	Irreducible	Reducible	Total Exp.	Observed
		$\geq 3e/\mu$, off-Z		
0 GeV	46 ±4 ±6	41 ±5 ±16	86 ±6 ±17	89
20 GeV	28 ±4 ±3	28 ±4 ±12	56 ±6 ±12	65
50 GeV	7.5 ±0.5 ±1.0	15 ±2 ±7	22 ±2 ±7	25
75 GeV	3.0 ±0.3 ±0.4	7 ±2 ±4	10 ±2 ±4	10
		$2e/\mu+ \geq 1\tau_{\mathrm{had}}$, off-$Z$		
0 GeV	5.3 ±0.4 ±0.9	184 ±4 ±40	190 ±4 ±40	202
20 GeV	4.4 ±0.3 ±0.7	93 ±3 ±20	98 ±3 ±20	91
50 GeV	1.5 ±0.2 ±0.2	17 ±1 ±4	19 ±1 ±4	20
75 GeV	0.6 ±0.1 ±0.1	8.0 ±0.8 ±1.8	8.5 ±0.8 ±1.8	10
		$\geq 3e/\mu$, on-Z		
20 GeV	340 ±5 ±50	100 ±7 ±31	439 ±9 ±60	509
50 GeV	105 ±2 ±14	14 ±3 ±5	119 ±3 ±14	144
75 GeV	40 ±1 ±5	5 ±1 ±2	46 ±2 ±6	57
		$2e/\mu+ \geq 1\tau_{\mathrm{had}}$, on-$Z$		
20 GeV	11.3 ±0.5 ±1.9	984 ±10 ±240	1000 ±10 ±240	862
50 GeV	4.6 ±0.3 ±0.7	43 ±2 ±11	48 ±2 ±11	33
75 GeV	2.0 ±0.2 ±0.3	4.1 ±0.6 ±1.0	6.1 ±0.6 ±1.0	4

TABLE X. Results for the $E_{\mathrm{T}}^{\mathrm{miss}}$, $H_{\mathrm{T}}^{\mathrm{jets}} \geq$ 100GeV signal regions. Irreducible sources include all backgrounds estimated with MC simulation. Results are presented in number of expected events as $N \pm$ (statistical uncertainty) $\pm$ (systematic uncertainty).

$E_{\mathrm{T}}^{\mathrm{miss}} \geq$	Irreducible	Reducible	Total Exp.	Observed
$\geq 3e/\mu$, off-Z				
0 GeV	7.7 ±0.8 ±1.2	13 ±2 ±7	21 ±2 ±7	10
20 GeV	6.0 ±0.6 ±0.9	12 ±2 ±6	18 ±2 ±6	8
50 GeV	3.2 ±0.3 ±0.5	8 ±2 ±5	11 ±2 ±5	5
75 GeV	2.2 ±0.2 ±0.3	7 ±2 ±4	9 ±2 ±4	5
$2e/\mu+ \geq 1\tau_{\mathrm{had}}$, off-$Z$				
0 GeV	1.1 ±0.1 ±0.2	30 ±2 ±7	31 ±2 ±7	24
20 GeV	1.1 ±0.1 ±0.2	23 ±1 ±6	25 ±1 ±6	20
50 GeV	0.7 ±0.1 ±0.1	14.5 ±1.1 ±3.4	15.2 ±1.1 ±3.4	13
75 GeV	0.5 ±0.1 ±0.1	9.3 ±0.8 ±2.2	9.8 ±0.8 ±2.3	8
$\geq 3e/\mu$, on-Z				
20 GeV	49 ±1 ±7	20 ±4 ±10	69 ±4 ±12	79
50 GeV	29 ±1 ±4	7 ±2 ±3	36 ±2 ±5	43
75 GeV	17.4 ±0.7 ±2.1	5 ±1 ±2	22 ±2 ±3	28
$2e/\mu+ \geq 1\tau_{\mathrm{had}}$, on-$Z$				
20 GeV	1.9 ±0.2 ±0.4	61 ±2 ±15	63 ±2 ±15	52
50 GeV	1.1 ±0.1 ±0.2	7.8 ±0.8 ±1.9	8.9 ±0.8 ±1.9	11
75 GeV	0.7 ±0.1 ±0.1	2.7 ±0.4 ±0.7	3.4 ±0.5 ±0.7	1

TABLE XI. Results for the m_{eff} signal regions. Irreducible sources include all backgrounds estimated with MC simulation. Results are presented in number of expected events as $N \pm$ (statistical uncertainty) $\pm$ (systematic uncertainty).

$m_{\mathrm{eff}} \geq$	Irreducible	Reducible	Total Exp.	Observed
$\geq 3e/\mu$, off-Z				
0 GeV	54 ±4 ±7	54 ±6 ±23	107 ±7 ±24	99
150 GeV	32 ±2 ±4	43 ±4 ±20	75 ±4 ±20	64
300 GeV	12.0 ±0.9 ±1.6	16 ±2 ±8	28 ±3 ±8	15
500 GeV	3.3 ±0.2 ±0.5	3.2 ±1.2 ±2.4	6.5 ±1.2 ±2.5	5
$2e/\mu+ \geq 1\tau_{\mathrm{had}}$, off-$Z$				
0 GeV	6.4 ±0.4 ±1.0	214 ±5 ±50	220 ±5 ±50	226
150 GeV	4.4 ±0.3 ±0.7	106 ±3 ±24	111 ±3 ±24	101
300 GeV	1.3 ±0.2 ±0.2	31 ±2 ±7	32 ±2 ±7	25
500 GeV	0.4 ±0.1 ±0.2	6.6 ±0.7 ±1.6	7.0 ±0.7 ±1.6	6
$\geq 3e/\mu$, on-Z				
0 GeV	390 ±5 ±50	120 ±8 ±40	510 ±10 ±70	588
150 GeV	270 ±3 ±40	57 ±6 ±22	330 ±7 ±40	399
300 GeV	73 ±1 ±10	16 ±3 ±8	89 ±4 ±13	103
500 GeV	22.2 ±0.9 ±2.8	3 ±1 ±1	25 ±2 ±3	29
$2e/\mu+ \geq 1\tau_{\mathrm{had}}$, on-$Z$				
0 GeV	13.2 ±0.5 ±2.2	1050 ±10 ±260	1060 ±10 ±260	914
150 GeV	10.7 ±0.5 ±1.8	360 ±5 ±90	370 ±5 ±90	309
300 GeV	2.9 ±0.3 ±0.4	47 ±2 ±12	50 ±2 ±12	42
500 GeV	0.9 ±0.2 ±0.1	7.7 ±0.8 ±1.9	8.7 ±0.8 ±2.0	5

TABLE XII. Results for the $m_{\rm eff}$, high-$E_{\rm T}^{\rm miss}$ signal regions. Irreducible sources include all backgrounds estimated with MC simulation. Results are presented in number of expected events as $N \pm$ (statistical uncertainty) $\pm$ (systematic uncertainty).

$m_{\rm eff} \geq$	Irreducible	Reducible	Total Exp.	Observed
		$\geq 3e/\mu$, off-Z		
0 GeV	5.1 ±0.4 ±0.7	13 ±2 ±8	18 ±2 ±8	15
150 GeV	5.1 ±0.4 ±0.7	13 ±2 ±8	18 ±2 ±8	15
300 GeV	3.7 ±0.3 ±0.5	10 ±2 ±6	13 ±2 ±6	9
500 GeV	1.7 ±0.2 ±0.2	2.9 ±1.1 ±2.3	4.5 ±1.1 ±2.3	4
		$2e/\mu+ \geq 1\tau_{\rm had}$, off-$Z$		
0 GeV	1.0 ±0.2 ±0.1	17 ±1 ±4	18 ±1 ±4	18
150 GeV	1.0 ±0.2 ±0.1	17 ±1 ±4	18 ±1 ±4	18
300 GeV	0.6 ±0.1 ±0.1	11.9 ±0.9 ±2.9	12.4 ±0.9 ±2.9	11
500 GeV	0.2 ±0.1 ±0.1	3.2 ±0.5 ±0.8	3.4 ±0.5 ±0.8	2
		$\geq 3e/\mu$, on-Z		
0 GeV	58 ±1 ±7	10 ±2 ±4	68 ±2 ±8	85
150 GeV	58 ±1 ±7	10 ±2 ±4	68 ±2 ±8	85
300 GeV	32 ±1 ±4	6 ±1 ±2	37 ±2 ±4	47
500 GeV	11.8 ±0.6 ±1.4	2.2 ±1.1 ±0.7	14.0 ±1.3 ±1.6	18
		$2e/\mu+ \geq 1\tau_{\rm had}$, on-$Z$		
0 GeV	2.7 ±0.3 ±0.4	6.8 ±0.7 ±1.6	9.5 ±0.8 ±1.7	5
150 GeV	2.7 ±0.3 ±0.4	6.7 ±0.7 ±1.6	9.4 ±0.8 ±1.7	4
300 GeV	1.6 ±0.2 ±0.2	3.5 ±0.5 ±0.9	5.0 ±0.5 ±0.9	2
500 GeV	0.6 ±0.1 ±0.1	0.4 ±0.1 ±0.1	1.0 ±0.2 ±0.1	0

Appendix B: Tables of expected and observed limits

The expected and observed 95% confidence level upper limits on the expected event yields from new phenomena for all signal regions under study are shown in Tables XIII-XVII.

TABLE XIII. Limits in the $H_{\mathrm{T}}^{\mathrm{leptons}}$ bins shown as the upper limit on the visible cross section ($\sigma_{95}^{\mathrm{vis}} = N_{95}/\int L\mathrm{d}t$).

$H_{\mathrm{T}}^{\mathrm{leptons}}$ [GeV]	Observed [fb]	Expected [fb]	$^{+1\sigma}_{-1\sigma}$ [fb]	$^{+2\sigma}_{-2\sigma}$ [fb]
$\geq 3e/\mu$ off-Z				
> 0	11	11	$^{5}_{2}$	$^{9}_{4}$
> 100	8.7	8.5	$^{2.9}_{1.6}$	$^{6.9}_{2.6}$
> 150	4.0	4.6	$^{1.8}_{1.2}$	$^{5.1}_{1.9}$
> 200	4.4	3.6	$^{1.7}_{1.0}$	$^{4.9}_{1.3}$
> 300	1.6	1.9	$^{1.0}_{0.4}$	$^{2.4}_{0.6}$
$2e/\mu+ \geq 1\tau_{\mathrm{had}}$ off-Z				
> 0	25	23	$^{13}_{5}$	$^{29}_{9}$
> 100	14	14	$^{6}_{3}$	$^{17}_{5}$
> 150	6.1	6.4	$^{3.4}_{1.3}$	$^{8.3}_{3.1}$
> 200	3.3	3.6	$^{1.9}_{1.2}$	$^{5.0}_{1.7}$
> 300	1.2	1.5	$^{1.0}_{0.5}$	$^{2.4}_{0.8}$
$\geq 3e/\mu$ on-Z				
> 0	48	33	$^{15}_{8}$	$^{32}_{14}$
> 100	38	25	$^{11}_{7}$	$^{23}_{11}$
> 150	14	12	$^{4}_{4}$	$^{10}_{5}$
> 200	7.2	6.5	$^{2.8}_{1.9}$	$^{6.2}_{2.6}$
> 300	4.5	3.1	$^{1.4}_{0.7}$	$^{3.5}_{1.1}$
$2e/\mu+ \geq 1\tau_{\mathrm{had}}$ on-Z				
> 0	85	94	$^{41}_{22}$	$^{96}_{30}$
> 100	53	61	$^{26}_{16}$	$^{64}_{27}$
> 150	11.0	9.9	$^{4.3}_{2.2}$	$^{11.0}_{3.7}$
> 200	5.2	4.5	$^{2.0}_{1.3}$	$^{5.3}_{1.9}$
> 300	3.0	1.9	$^{1.0}_{0.6}$	$^{2.7}_{0.8}$

TABLE XIV. Limits in the $E_{\mathrm{T}}^{\mathrm{miss}}$ bins with $H_{\mathrm{T}}^{\mathrm{jets}} \geq 100$ GeV requirement shown as the upper limit on the visible cross section ($\sigma_{95}^{\mathrm{vis}} = N_{95}/\int L\mathrm{d}t$).

$E_{\mathrm{T}}^{\mathrm{miss}}$	Observed	Expected	$^{+1\sigma}_{-1\sigma}$	$^{+2\sigma}_{-2\sigma}$
[GeV]	[fb]	[fb]	[fb]	[fb]
$\geq 3e/\mu$ off-Z				
> 0	2.6	3.1	$^{1.5}_{0.7}$	$^{3.4}_{1.4}$
> 50	2.1	2.4	$^{1.0}_{0.8}$	$^{2.3}_{1.2}$
> 75	2.1	2.3	$^{1.1}_{0.4}$	$^{1.9}_{0.9}$
$2e/\mu+ \geq 1\tau_{\mathrm{had}}$ off-Z				
> 0	4.2	4.8	$^{2.5}_{1.5}$	$^{6.1}_{2.1}$
> 50	3.1	3.3	$^{1.8}_{1.2}$	$^{4.4}_{1.6}$
> 75	2.6	2.1	$^{0.8}_{0.6}$	$^{1.9}_{1.0}$
$\geq 3e/\mu$ on-Z				
> 20	11.0	8.7	$^{2.5}_{3.2}$	$^{7.0}_{4.1}$
> 50	6.4	4.9	$^{2.3}_{1.2}$	$^{5.4}_{1.8}$
> 75	5.1	3.8	$^{1.6}_{1.0}$	$^{3.8}_{1.4}$
$2e/\mu+ \geq 1\tau_{\mathrm{had}}$ on-Z				
> 20	5.9	7.3	$^{2.9}_{1.4}$	$^{6.8}_{3.5}$
> 50	3.4	2.8	$^{1.2}_{0.9}$	$^{3.8}_{1.2}$
> 75	1.2	1.5	$^{0.4}_{0.4}$	$^{1.0}_{0.6}$

TABLE XV. Limits in the $E_{\mathrm{T}}^{\mathrm{miss}}$ bins with $H_{\mathrm{T}}^{\mathrm{jets}} \leq 100$ GeV requirement shown as the upper limit on the visible cross section ($\sigma_{95}^{\mathrm{vis}} = N_{95}/\int L\mathrm{d}t$).

$E_{\mathrm{T}}^{\mathrm{miss}}$	Observed	Expected	$^{+1\sigma}_{-1\sigma}$	$^{+2\sigma}_{-2\sigma}$
[GeV]	[fb]	[fb]	[fb]	[fb]
$\geq 3e/\mu$ off-Z				
> 0	11	10	$^{4}_{2}$	$^{8}_{4}$
> 50	5.3	4.7	$^{1.9}_{1.0}$	$^{4.5}_{1.6}$
> 75	3.1	3.0	$^{1.0}_{0.6}$	$^{1.8}_{1.0}$
$2e/\mu+ \geq 1\tau_{\mathrm{had}}$ off-Z				
> 0	23	21	$^{9}_{6}$	$^{23}_{9}$
> 50	4.3	4.0	$^{2.3}_{1.2}$	$^{5.0}_{1.7}$
> 75	3.1	2.6	$^{1.1}_{0.7}$	$^{3.1}_{1.1}$
$\geq 3e/\mu$ on-Z				
> 20	41	30	$^{10}_{9}$	$^{20}_{14}$
> 50	16	10	$^{4}_{3}$	$^{11}_{5}$
> 75	8.0	5.4	$^{2.6}_{1.3}$	$^{6.2}_{1.9}$
$2e/\mu+ \geq 1\tau_{\mathrm{had}}$ on-Z				
> 20	80	88	$^{39}_{23}$	$^{94}_{43}$
> 50	4.4	5.5	$^{3.2}_{1.4}$	$^{7.6}_{2.1}$
> 75	1.8	2.2	$^{0.4}_{0.7}$	$^{1.0}_{1.0}$

TABLE XVI. Limits in the $m_{\rm eff}$ bins shown as the upper limit on the visible cross section ($\sigma_{95}^{\rm vis} = N_{95}/\int L{\rm d}t$).

$m_{\rm eff}$	Observed	Expected	$^{+1\sigma}_{-1\sigma}$	$^{+2\sigma}_{-2\sigma}$
[GeV]	[fb]	[fb]	[fb]	[fb]
$\geq 3e/\mu$ off-Z				
> 0	11	11	$^{5}_{2}$	$^{9}_{4}$
> 150	8.1	8.8	$^{3.0}_{2.2}$	$^{7.2}_{3.9}$
> 300	3.1	3.7	$^{1.7}_{0.7}$	$^{3.8}_{1.6}$
> 500	2.1	2.1	$^{1.1}_{0.6}$	$^{2.3}_{0.9}$
$2e/\mu+ \geq 1\tau_{\rm had}$ off-Z				
> 0	25	23	$^{13}_{5}$	$^{29}_{9}$
> 150	12	13	$^{6}_{4}$	$^{14}_{5}$
> 300	3.9	4.9	$^{2.5}_{1.5}$	$^{6.4}_{2.3}$
> 500	2.2	2.4	$^{1.3}_{0.5}$	$^{3.4}_{1.2}$
$\geq 3e/\mu$ on-Z				
> 0	48	33	$^{15}_{8}$	$^{32}_{14}$
> 150	37	25	$^{9}_{7}$	$^{21}_{11}$
> 300	11	9	$^{4}_{2}$	$^{9}_{3}$
> 500	4.8	3.9	$^{1.7}_{1.0}$	$^{4.3}_{1.1}$
$2e/\mu+ \geq 1\tau_{\rm had}$ on-Z				
> 0	85	94	$^{41}_{22}$	$^{96}_{30}$
> 150	28	35	$^{13}_{11}$	$^{34}_{15}$
> 300	5.9	6.8	$^{2.8}_{1.8}$	$^{8.1}_{2.4}$
> 500	1.9	2.5	$^{1.4}_{1.0}$	$^{3.5}_{1.2}$

TABLE XVII. Limits in the $m_{\rm eff}$ bins with $E_{\rm T}^{\rm miss} \geq 75$ GeV requirement shown as the upper limit on the visible cross section ($\sigma_{95}^{\rm vis} = N_{95}/\int L{\rm d}t$).

$m_{\rm eff}$ [GeV]	Observed [fb]	Expected [fb]	$^{+1\sigma}_{-1\sigma}$ [fb]	$^{+2\sigma}_{-2\sigma}$ [fb]
$\geq 3e/\mu$ off-Z				
> 0	3.8	3.9	$^{1.5}_{0.7}$	$^{3.4}_{1.3}$
> 150	3.8	3.9	$^{1.5}_{1.0}$	$^{3.6}_{1.3}$
> 300	2.8	3.0	$^{1.2}_{0.7}$	$^{3.2}_{1.1}$
> 500	2.1	2.0	$^{0.8}_{0.4}$	$^{2.2}_{0.8}$
$2e/\mu+ \geq 1\tau_{\rm had}$ off-Z				
> 0	3.9	3.8	$^{2.1}_{1.2}$	$^{5.2}_{1.8}$
> 150	4.0	3.9	$^{2.0}_{1.3}$	$^{4.8}_{1.7}$
> 300	2.9	3.1	$^{1.6}_{1.0}$	$^{4.1}_{1.3}$
> 500	1.5	1.6	$^{0.7}_{0.5}$	$^{2.1}_{0.7}$
$\geq 3e/\mu$ on-Z				
> 0	10.0	6.9	$^{3.0}_{1.3}$	$^{7.4}_{2.5}$
> 150	10.0	7.1	$^{2.8}_{2.2}$	$^{7.0}_{2.5}$
> 300	6.8	4.9	$^{2.1}_{1.0}$	$^{5.1}_{2.1}$
> 500	3.9	3.0	$^{1.2}_{0.7}$	$^{3.4}_{1.3}$
$2e/\mu+ \geq 1\tau_{\rm had}$ on-Z				
> 0	1.6	2.4	$^{1.4}_{0.9}$	$^{3.8}_{1.3}$
> 150	1.4	2.5	$^{1.5}_{0.8}$	$^{3.8}_{1.5}$
> 300	1.5	2.0	$^{1.1}_{0.8}$	$^{2.7}_{1.1}$
> 500	0.9	1.1	$^{0.8}_{0.4}$	$^{2.0}_{0.4}$

The ATLAS Collaboration

G. Aad[48], T. Abajyan[21], B. Abbott[111], J. Abdallah[12], S. Abdel Khalek[115], A.A. Abdelalim[49], O. Abdinov[11], R. Aben[105], B. Abi[112], M. Abolins[88], O.S. AbouZeid[158], H. Abramowicz[153], H. Abreu[136], B.S. Acharya[164a,164b,a], L. Adamczyk[38], D.L. Adams[25], T.N. Addy[56], J. Adelman[176], S. Adomeit[98], P. Adragna[75], T. Adye[129], S. Aefsky[23], J.A. Aguilar-Saavedra[124b,b], M. Agustoni[17], M. Aharrouche[81], S.P. Ahlen[22], F. Ahles[48], A. Ahmad[148], M. Ahsan[41], G. Aielli[133a,133b], T.P.A. Åkesson[79], G. Akimoto[155], A.V. Akimov[94], M.S. Alam[2], M.A. Alam[76], J. Albert[169], S. Albrand[55], M. Aleksa[30], I.N. Aleksandrov[64], F. Alessandria[89a], C. Alexa[26a], G. Alexander[153], G. Alexandre[49], T. Alexopoulos[10], M. Alhroob[164a,164c], M. Aliev[16], G. Alimonti[89a], J. Alison[120], B.M.M. Allbrooke[18], P.P. Allport[73], S.E. Allwood-Spiers[53], J. Almond[82], A. Aloisio[102a,102b], R. Alon[172], A. Alonso[79], F. Alonso[70], A. Altheimer[35], B. Alvarez Gonzalez[88], M.G. Alviggi[102a,102b], K. Amako[65], C. Amelung[23], V.V. Ammosov[128,*], S.P. Amor Dos Santos[124a], A. Amorim[124a,c], N. Amram[153], C. Anastopoulos[30], L.S. Ancu[17], N. Andari[115], T. Andeen[35], C.F. Anders[58b], G. Anders[58a], K.J. Anderson[31], A. Andreazza[89a,89b], V. Andrei[58a], M-L. Andrieux[55], X.S. Anduaga[70], S. Angelidakis[9], P. Anger[44], A. Angerami[35], F. Anghinolfi[30], A. Anisenkov[107], N. Anjos[124a], A. Annovi[47], A. Antonaki[9], M. Antonelli[47], A. Antonov[96], J. Antos[144b], F. Anulli[132a], M. Aoki[101], S. Aoun[83], L. Aperio Bella[5], R. Apolle[118,d], G. Arabidze[88], I. Aracena[143], Y. Arai[65], A.T.H. Arce[45], S. Arfaoui[148], J-F. Arguin[93], S. Argyropoulos[42], E. Arik[19a,*], M. Arik[19a], A.J. Armbruster[87], O. Arnaez[81], V. Arnal[80], A. Artamonov[95], G. Artoni[132a,132b], D. Arutinov[21], S. Asai[155], S. Ask[28], B. Åsman[146a,146b], L. Asquith[6], K. Assamagan[25,e], A. Astbury[169], M. Atkinson[165], B. Aubert[5], E. Auge[115], K. Augsten[126], M. Aurousseau[145a], G. Avolio[30], D. Axen[168], G. Azuelos[93,f], Y. Azuma[155], M.A. Baak[30], G. Baccaglioni[89a], C. Bacci[134a,134b], A.M. Bach[15], H. Bachacou[136], K. Bachas[154], M. Backes[49], M. Backhaus[21], J. Backus Mayes[143], E. Badescu[26a], P. Bagnaia[132a,132b], S. Bahinipati[3], Y. Bai[33a], D.C. Bailey[158], T. Bain[158], J.T. Baines[129], O.K. Baker[176], M.D. Baker[25], S. Baker[77], P. Balek[127], E. Banas[39], P. Banerjee[93], Sw. Banerjee[173], D. Banfi[30], A. Bangert[150], V. Bansal[169], H.S. Bansil[18], L. Barak[172], S.P. Baranov[94], A. Barbaro Galtieri[15], T. Barber[48], E.L. Barberio[86], D. Barberis[50a,50b], M. Barbero[21], D.Y. Bardin[64], T. Barillari[99], M. Barisonzi[175], T. Barklow[143], N. Barlow[28], B.M. Barnett[129], R.M. Barnett[15], A. Baroncelli[134a], G. Barone[49], A.J. Barr[118], F. Barreiro[80], J. Barreiro Guimarães da Costa[57], R. Bartoldus[143], A.E. Barton[71], V. Bartsch[149], A. Basye[165], R.L. Bates[53], L. Batkova[144a], J.R. Batley[28], A. Battaglia[17], M. Battistin[30], F. Bauer[136], H.S. Bawa[143,g], S. Beale[98], T. Beau[78], P.H. Beauchemin[161], R. Beccherle[50a], P. Bechtle[21], H.P. Beck[17], K. Becker[175], S. Becker[98], M. Beckingham[138], K.H. Becks[175], A.J. Beddall[19c], A. Beddall[19c], S. Bedikian[176], V.A. Bednyakov[64], C.P. Bee[83], L.J. Beemster[105], M. Begel[25], S. Behar Harpaz[152], P.K. Behera[62], M. Beimforde[99], C. Belanger-Champagne[85], P.J. Bell[49], W.H. Bell[49], G. Bella[153], L. Bellagamba[20a], M. Bellomo[30], A. Belloni[57], O. Beloborodova[107,h], K. Belotskiy[96], O. Beltramello[30], O. Benary[153], D. Benchekroun[135a], K. Bendtz[146a,146b], N. Benekos[165], Y. Benhammou[153], E. Benhar Noccioli[49], J.A. Benitez Garcia[159b], D.P. Benjamin[45], M. Benoit[115], J.R. Bensinger[23], K. Benslama[130], S. Bentvelsen[105], D. Berge[30], E. Bergeaas Kuutmann[42], N. Berger[5], F. Berghaus[169], E. Berglund[105], J. Beringer[15], P. Bernat[77], R. Bernhard[48], C. Bernius[25], T. Berry[76], C. Bertella[83], A. Bertin[20a,20b], F. Bertolucci[122a,122b], M.I. Besana[89a,89b], G.J. Besjes[104], N. Besson[136], S. Bethke[99], W. Bhimji[46], R.M. Bianchi[30], L. Bianchini[23], M. Bianco[72a,72b], O. Biebel[98], S.P. Bieniek[77], K. Bierwagen[54], J. Biesiada[15], M. Biglietti[134a], H. Bilokon[47], M. Bindi[20a,20b], S. Binet[115], A. Bingul[19c], C. Bini[132a,132b], C. Biscarat[178], B. Bittner[99], C.W. Black[150], K.M. Black[22], R.E. Blair[6], J.-B. Blanchard[136], G. Blanchot[30], T. Blazek[144a], I. Bloch[42], C. Blocker[23], J. Blocki[39], A. Blondel[49], W. Blum[81], U. Blumenschein[54], G.J. Bobbink[105], V.S. Bobrovnikov[107], S.S. Bocchetta[79], A. Bocci[45], C.R. Boddy[118], M. Boehler[48], J. Boek[175], T.T. Boek[175], N. Boelaert[36], J.A. Bogaerts[30], A. Bogdanchikov[107], A. Bogouch[90,*], C. Bohm[146a], J. Bohm[125], V. Boisvert[76], T. Bold[38], V. Boldea[26a], N.M. Bolnet[136], M. Bomben[78], M. Bona[75], M. Boonekamp[136], S. Bordoni[78], C. Borer[17], A. Borisov[128], G. Borissov[71], I. Borjanovic[13a], M. Borri[82], S. Borroni[87], J. Bortfeldt[98], V. Bortolotto[134a,134b], K. Bos[105], D. Boscherini[20a], M. Bosman[12], H. Boterenbrood[105], J. Bouchami[93], J. Boudreau[123], E.V. Bouhova-Thacker[71], D. Boumediene[34], C. Bourdarios[115], N. Bousson[83], A. Boveia[31], J. Boyd[30], I.R. Boyko[64], I. Bozovic-Jelisavcic[13b], J. Bracinik[18], P. Branchini[134a], A. Brandt[8], G. Brandt[118], O. Brandt[54], U. Bratzler[156], B. Brau[84], J.E. Brau[114], H.M. Braun[175,*], S.F. Brazzale[164a,164c], B. Brelier[158], J. Bremer[30], K. Brendlinger[120], R. Brenner[166], S. Bressler[172], D. Britton[53], F.M. Brochu[28], I. Brock[21], R. Brock[88], F. Broggi[89a], C. Bromberg[88], J. Bronner[99], G. Brooijmans[35], T. Brooks[76], W.K. Brooks[32b], G. Brown[82], P.A. Bruckman de Renstrom[39], D. Bruncko[144b], R. Bruneliere[48], S. Brunet[60], A. Bruni[20a], G. Bruni[20a], M. Bruschi[20a], L. Bryngemark[79], T. Buanes[14], Q. Buat[55], F. Bucci[49], J. Buchanan[118], P. Buchholz[141], R.M. Buckingham[118], A.G. Buckley[46], S.I. Buda[26a], I.A. Budagov[64], B. Budick[108], V. Büscher[81], L. Bugge[117], O. Bulekov[96], A.C. Bundock[73], M. Bunse[43], T. Buran[117], H. Burckhart[30], S. Burdin[73], T. Burgess[14], S. Burke[129], E. Busato[34], P. Bussey[53], C.P. Buszello[166], B. Butler[143], J.M. Butler[22], C.M. Buttar[53], J.M. Butterworth[77], W. Buttinger[28], S. Cabrera Urbán[167], D. Caforio[20a,20b], O. Cakir[4a], P. Calafiura[15], G. Calderini[78], P. Calfayan[98], R. Calkins[106], L.P. Caloba[24a], R. Caloi[132a,132b], D. Calvet[34], S. Calvet[34], R. Camacho Toro[34], P. Camarri[133a,133b], D. Cameron[117], L.M. Caminada[15], R. Caminal Armadans[12], S. Campana[30], M. Campanelli[77], V. Canale[102a,102b],

F. Canelli[31], A. Canepa[159a], J. Cantero[80], R. Cantrill[76], L. Capasso[102a,102b], M.D.M. Capeans Garrido[30], I. Caprini[26a], M. Caprini[26a], D. Capriotti[99], M. Capua[37a,37b], R. Caputo[81], R. Cardarelli[133a], T. Carli[30], G. Carlino[102a], L. Carminati[89a,89b], B. Caron[85], S. Caron[104], E. Carquin[32b], G.D. Carrillo-Montoya[145b], A.A. Carter[75], J.R. Carter[28], J. Carvalho[124a,i], D. Casadei[108], M.P. Casado[12], M. Cascella[122a,122b], C. Caso[50a,50b,*], A.M. Castaneda Hernandez[173,j], E. Castaneda-Miranda[173], V. Castillo Gimenez[167], N.F. Castro[124a], G. Cataldi[72a], P. Catastini[57], A. Catinaccio[30], J.R. Catmore[30], A. Cattai[30], G. Cattani[133a,133b], S. Caughron[88], V. Cavaliere[165], P. Cavalleri[78], D. Cavalli[89a], M. Cavalli-Sforza[12], V. Cavasinni[122a,122b], F. Ceradini[134a,134b], A.S. Cerqueira[24b], A. Cerri[15], L. Cerrito[75], F. Cerutti[15], S.A. Cetin[19b], A. Chafaq[135a], D. Chakraborty[106], I. Chalupkova[127], K. Chan[3], P. Chang[165], B. Chapleau[85], J.D. Chapman[28], J.W. Chapman[87], D.G. Charlton[18], V. Chavda[82], C.A. Chavez Barajas[30], S. Cheatham[85], S. Chekanov[6], S.V. Chekulaev[159a], G.A. Chelkov[64], M.A. Chelstowska[104], C. Chen[63], H. Chen[25], S. Chen[33c], X. Chen[173], Y. Chen[35], Y. Cheng[31], A. Cheplakov[64], R. Cherkaoui El Moursli[135e], V. Chernyatin[25], E. Cheu[7], S.L. Cheung[158], L. Chevalier[136], G. Chiefari[102a,102b], L. Chikovani[51a,*], J.T. Childers[30], A. Chilingarov[71], G. Chiodini[72a], A.S. Chisholm[18], R.T. Chislett[77], A. Chitan[26a], M.V. Chizhov[64], G. Choudalakis[31], S. Chouridou[137], I.A. Christidi[77], A. Christov[48], D. Chromek-Burckhart[30], M.L. Chu[151], J. Chudoba[125], G. Ciapetti[132a,132b], A.K. Ciftci[4a], R. Ciftci[4a], D. Cinca[34], V. Cindro[74], A. Ciocio[15], M. Cirilli[87], P. Cirkovic[13b], Z.H. Citron[172], M. Citterio[89a], M. Ciubancan[26a], A. Clark[49], P.J. Clark[46], R.N. Clarke[15], W. Cleland[123], J.C. Clemens[83], B. Clement[55], C. Clement[146a,146b], Y. Coadou[83], M. Cobal[164a,164c], A. Coccaro[138], J. Cochran[63], L. Coffey[23], J.G. Cogan[143], J. Coggeshall[165], J. Colas[5], S. Cole[106], A.P. Colijn[105], N.J. Collins[18], C. Collins-Tooth[53], J. Collot[55], T. Colombo[119a,119b], G. Colon[84], G. Compostella[99], P. Conde Muiño[124a], E. Coniavitis[166], M.C. Conidi[12], S.M. Consonni[89a,89b], V. Consorti[48], S. Constantinescu[26a], C. Conta[119a,119b], G. Conti[57], F. Conventi[102a,k], M. Cooke[15], B.D. Cooper[77], A.M. Cooper-Sarkar[118], K. Copic[15], T. Cornelissen[175], M. Corradi[20a], F. Corriveau[85,l], A. Cortes-Gonzalez[165], G. Cortiana[99], G. Costa[89a], M.J. Costa[167], D. Costanzo[139], D. Côté[30], L. Courneyea[169], G. Cowan[76], B.E. Cox[82], K. Cranmer[108], F. Crescioli[78], M. Cristinziani[21], G. Crosetti[37a,37b], S. Crépé-Renaudin[55], C.-M. Cuciuc[26a], C. Cuenca Almenar[176], T. Cuhadar Donszelmann[139], J. Cummings[176], M. Curatolo[47], C.J. Curtis[18], C. Cuthbert[150], P. Cwetanski[60], H. Czirr[141], P. Czodrowski[44], Z. Czyczula[176], S. D'Auria[53], M. D'Onofrio[73], A. D'Orazio[132a,132b], M.J. Da Cunha Sargedas De Sousa[124a], C. Da Via[82], W. Dabrowski[38], A. Dafinca[118], T. Dai[87], F. Dallaire[93], C. Dallapiccola[84], M. Dam[36], M. Dameri[50a,50b], D.S. Damiani[137], H.O. Danielsson[30], V. Dao[49], G. Darbo[50a], G.L. Darlea[26b], J.A. Dassoulas[42], W. Davey[21], T. Davidek[127], N. Davidson[86], R. Davidson[71], E. Davies[118,d], M. Davies[93], O. Davignon[78], A.R. Davison[77], Y. Davygora[58a], E. Dawe[142], I. Dawson[139], R.K. Daya-Ishmukhametova[23], K. De[8], R. de Asmundis[102a], S. De Castro[20a,20b], S. De Cecco[78], J. de Graat[98], N. De Groot[104], P. de Jong[105], C. De La Taille[115], H. De la Torre[80], F. De Lorenzi[63], L. de Mora[71], L. De Nooij[105], D. De Pedis[132a], A. De Salvo[132a], U. De Sanctis[164a,164c], A. De Santo[149], J.B. De Vivie De Regie[115], G. De Zorzi[132a,132b], W.J. Dearnaley[71], R. Debbe[25], C. Debenedetti[46], B. Dechenaux[55], D.V. Dedovich[64], J. Degenhardt[120], J. Del Peso[80], T. Del Prete[122a,122b], T. Delemontex[55], M. Deliyergiyev[74], A. Dell'Acqua[30], L. Dell'Asta[22], M. Della Pietra[102a,k], D. della Volpe[102a,102b], M. Delmastro[5], P.A. Delsart[55], C. Deluca[105], S. Demers[176], M. Demichev[64], B. Demirkoz[12,m], S.P. Denisov[128], D. Derendarz[39], J.E. Derkaoui[135d], F. Derue[78], P. Dervan[73], K. Desch[21], E. Devetak[148], P.O. Deviveiros[105], A. Dewhurst[129], B. DeWilde[148], S. Dhaliwal[158], R. Dhullipudi[25,n], A. Di Ciaccio[133a,133b], L. Di Ciaccio[5], C. Di Donato[102a,102b], A. Di Girolamo[30], B. Di Girolamo[30], S. Di Luise[134a,134b], A. Di Mattia[152], B. Di Micco[30], R. Di Nardo[47], A. Di Simone[133a,133b], R. Di Sipio[20a,20b], M.A. Diaz[32a], E.B. Diehl[87], J. Dietrich[42], T.A. Dietzsch[58a], S. Diglio[86], K. Dindar Yagci[40], J. Dingfelder[21], F. Dinut[26a], C. Dionisi[132a,132b], P. Dita[26a], S. Dita[26a], F. Dittus[30], F. Djama[83], T. Djobava[51b], M.A.B. do Vale[24c], A. Do Valle Wemans[124a,o], T.K.O. Doan[5], M. Dobbs[85], D. Dobos[30], E. Dobson[30,p], J. Dodd[35], C. Doglioni[49], T. Doherty[53], Y. Doi[65,*], J. Dolejsi[127], Z. Dolezal[127], B.A. Dolgoshein[96,*], T. Dohmae[155], M. Donadelli[24d], J. Donini[34], J. Dopke[30], A. Doria[102a], A. Dos Anjos[173], A. Dotti[122a,122b], M.T. Dova[70], A.D. Doxiadis[105], A.T. Doyle[53], N. Dressnandt[120], M. Dris[10], J. Dubbert[99], S. Dube[15], E. Duchovni[172], G. Duckeck[98], D. Duda[175], A. Dudarev[30], F. Dudziak[63], M. Dührssen[30], I.P. Duerdoth[82], L. Duflot[115], M-A. Dufour[85], L. Duguid[76], M. Dunford[58a], H. Duran Yildiz[4a], R. Duxfield[139], M. Dwuznik[38], M. Düren[52], W.L. Ebenstein[45], J. Ebke[98], S. Eckweiler[81], K. Edmonds[81], W. Edson[2], C.A. Edwards[76], N.C. Edwards[53], W. Ehrenfeld[42], T. Eifert[143], G. Eigen[14], K. Einsweiler[15], E. Eisenhandler[75], T. Ekelof[166], M. El Kacimi[135c], M. Ellert[166], S. Elles[5], F. Ellinghaus[81], K. Ellis[75], N. Ellis[30], J. Elmsheuser[98], M. Elsing[30], D. Emeliyanov[129], R. Engelmann[148], A. Engl[98], B. Epp[61], J. Erdmann[176], A. Ereditato[17], D. Eriksson[146a], J. Ernst[2], M. Ernst[25], J. Ernwein[136], D. Errede[165], S. Errede[165], E. Ertel[81], M. Escalier[115], H. Esch[43], C. Escobar[123], X. Espinal Curull[12], B. Esposito[47], F. Etienne[83], A.I. Etienvre[136], E. Etzion[153], D. Evangelakou[54], H. Evans[60], L. Fabbri[20a,20b], C. Fabre[30], R.M. Fakhrutdinov[128], S. Falciano[132a], Y. Fang[33a], M. Fanti[89a,89b], A. Farbin[8], A. Farilla[134a], J. Farley[148], T. Farooque[158], S. Farrell[163], S.M. Farrington[170], P. Farthouat[30], F. Fassi[167], P. Fassnacht[30], D. Fassouliotis[9], B. Fatholahzadeh[158], A. Favareto[89a,89b], L. Fayard[115], S. Fazio[37a,37b], P. Federic[144a], O.L. Fedin[121], W. Fedorko[88], M. Fehling-Kaschek[48], L. Feligioni[83], C. Feng[33d], E.J. Feng[6], A.B. Fenyuk[128], J. Ferencei[144b], W. Fernando[6], S. Ferrag[53], J. Ferrando[53],

V. Ferrara[42], A. Ferrari[166], P. Ferrari[105], R. Ferrari[119a], D.E. Ferreira de Lima[53], A. Ferrer[167], D. Ferrere[49], C. Ferretti[87], A. Ferretto Parodi[50a,50b], M. Fiascaris[31], F. Fiedler[81], A. Filipčič[74], F. Filthaut[104], M. Fincke-Keeler[169], M.C.N. Fiolhais[124a,i], L. Fiorini[167], A. Firan[40], G. Fischer[42], M.J. Fisher[109], M. Flechl[48], I. Fleck[141], J. Fleckner[81], P. Fleischmann[174], S. Fleischmann[175], T. Flick[175], A. Floderus[79], L.R. Flores Castillo[173], A.C. Florez Bustos[159b], M.J. Flowerdew[99], T. Fonseca Martin[17], A. Formica[136], A. Forti[82], D. Fortin[159a], D. Fournier[115], A.J. Fowler[45], H. Fox[71], P. Francavilla[12], M. Franchini[20a,20b], S. Franchino[119a,119b], D. Francis[30], T. Frank[172], M. Franklin[57], S. Franz[30], M. Fraternali[119a,119b], S. Fratina[120], S.T. French[28], C. Friedrich[42], F. Friedrich[44], D. Froidevaux[30], J.A. Frost[28], C. Fukunaga[156], E. Fullana Torregrosa[127], B.G. Fulsom[143], J. Fuster[167], C. Gabaldon[30], O. Gabizon[172], T. Gadfort[25], S. Gadomski[49], G. Gagliardi[50a,50b], P. Gagnon[60], C. Galea[98], B. Galhardo[124a], E.J. Gallas[118], V. Gallo[17], B.J. Gallop[129], P. Gallus[125], K.K. Gan[109], Y.S. Gao[143,g], A. Gaponenko[15], F. Garberson[176], M. Garcia-Sciveres[15], C. García[167], J.E. García Navarro[167], R.W. Gardner[31], N. Garelli[30], H. Garitaonandia[105], V. Garonne[30], C. Gatti[47], G. Gaudio[119a], B. Gaur[141], L. Gauthier[136], P. Gauzzi[132a,132b], I.L. Gavrilenko[94], C. Gay[168], G. Gaycken[21], E.N. Gazis[10], P. Ge[33d], Z. Gecse[168], C.N.P. Gee[129], D.A.A. Geerts[105], Ch. Geich-Gimbel[21], K. Gellerstedt[146a,146b], C. Gemme[50a], A. Gemmell[53], M.H. Genest[55], S. Gentile[132a,132b], M. George[54], S. George[76], D. Gerbaudo[12], P. Gerlach[175], A. Gershon[153], C. Geweniger[58a], H. Ghazlane[135b], N. Ghodbane[34], B. Giacobbe[20a], S. Giagu[132a,132b], V. Giangiobbe[12], F. Gianotti[30], B. Gibbard[25], A. Gibson[158], S.M. Gibson[30], M. Gilchriese[15], D. Gillberg[29], A.R. Gillman[129], D.M. Gingrich[3,f], J. Ginzburg[153], N. Giokaris[9], M.P. Giordani[164c], R. Giordano[102a,102b], F.M. Giorgi[16], P. Giovannini[99], P.F. Giraud[136], D. Giugni[89a], M. Giunta[93], B.K. Gjelsten[117], L.K. Gladilin[97], C. Glasman[80], J. Glatzer[21], A. Glazov[42], K.W. Glitza[175], G.L. Glonti[64], J.R. Goddard[75], J. Godfrey[142], J. Godlewski[30], M. Goebel[42], T. Göpfert[44], C. Goeringer[81], C. Gössling[43], S. Goldfarb[87], T. Golling[176], D. Golubkov[128], A. Gomes[124a,c], L.S. Gomez Fajardo[42], R. Gonçalo[76], J. Goncalves Pinto Firmino Da Costa[42], L. Gonella[21], S. González de la Hoz[167], G. Gonzalez Parra[12], M.L. Gonzalez Silva[27], S. Gonzalez-Sevilla[49], J.J. Goodson[148], L. Goossens[30], P.A. Gorbounov[95], H.A. Gordon[25], I. Gorelov[103], G. Gorfine[175], B. Gorini[30], E. Gorini[72a,72b], A. Gorišek[74], E. Gornicki[39], A.T. Goshaw[6], M. Gosselink[105], M.I. Gostkin[64], I. Gough Eschrich[163], M. Gouighri[135a], D. Goujdami[135c], M.P. Goulette[49], A.G. Goussiou[138], C. Goy[5], S. Gozpinar[23], I. Grabowska-Bold[38], P. Grafström[20a,20b], K-J. Grahn[42], E. Gramstad[117], F. Grancagnolo[72a], S. Grancagnolo[16], V. Grassi[148], V. Gratchev[121], N. Grau[35], H.M. Gray[30], J.A. Gray[148], E. Graziani[134a], O.G. Grebenyuk[121], T. Greenshaw[73], Z.D. Greenwood[25,n], K. Gregersen[36], I.M. Gregor[42], P. Grenier[143], J. Griffiths[8], N. Grigalashvili[64], A.A. Grillo[137], S. Grinstein[12], Ph. Gris[34], Y.V. Grishkevich[97], J.-F. Grivaz[115], E. Gross[172], J. Grosse-Knetter[54], J. Groth-Jensen[172], K. Grybel[141], D. Guest[176], C. Guicheney[34], E. Guido[50a,50b], S. Guindon[54], U. Gul[53], J. Gunther[125], B. Guo[158], J. Guo[35], P. Gutierrez[111], N. Guttman[153], O. Gutzwiller[173], C. Guyot[136], C. Gwenlan[118], C.B. Gwilliam[73], A. Haas[108], S. Haas[30], C. Haber[15], H.K. Hadavand[8], D.R. Hadley[18], P. Haefner[21], F. Hahn[30], Z. Hajduk[39], H. Hakobyan[177], D. Hall[118], K. Hamacher[175], P. Hamal[113], K. Hamano[86], M. Hamer[54], A. Hamilton[145b,q], S. Hamilton[161], L. Han[33b], K. Hanagaki[116], K. Hanawa[160], M. Hance[15], C. Handel[81], P. Hanke[58a], J.R. Hansen[36], J.B. Hansen[36], J.D. Hansen[36], P.H. Hansen[36], P. Hansson[143], K. Hara[160], T. Harenberg[175], S. Harkusha[90], D. Harper[87], R.D. Harrington[46], O.M. Harris[138], J. Hartert[48], F. Hartjes[105], T. Haruyama[65], A. Harvey[56], S. Hasegawa[101], Y. Hasegawa[140], S. Hassani[136], S. Haug[17], M. Hauschild[30], R. Hauser[88], M. Havranek[21], C.M. Hawkes[18], R.J. Hawkings[30], A.D. Hawkins[79], T. Hayakawa[66], T. Hayashi[160], D. Hayden[76], C.P. Hays[118], H.S. Hayward[73], S.J. Haywood[129], S.J. Head[18], V. Hedberg[79], L. Heelan[8], S. Heim[120], B. Heinemann[15], S. Heisterkamp[36], L. Helary[22], C. Heller[98], M. Heller[30], S. Hellman[146a,146b], D. Hellmich[21], C. Helsens[12], R.C.W. Henderson[71], M. Henke[58a], A. Henrichs[176], A.M. Henriques Correia[30], S. Henrot-Versille[115], C. Hensel[54], C.M. Hernandez[8], Y. Hernández Jiménez[167], R. Herrberg[16], G. Herten[48], R. Hertenberger[98], L. Hervas[30], G.G. Hesketh[77], N.P. Hessey[105], E. Higón-Rodriguez[167], J.C. Hill[28], K.H. Hiller[42], S. Hillert[21], S.J. Hillier[18], I. Hinchliffe[15], E. Hines[120], M. Hirose[116], F. Hirsch[43], D. Hirschbuehl[175], J. Hobbs[148], N. Hod[153], M.C. Hodgkinson[139], P. Hodgson[139], A. Hoecker[30], M.R. Hoeferkamp[103], J. Hoffman[40], D. Hoffmann[83], M. Hohlfeld[81], M. Holder[141], S.O. Holmgren[146a], T. Holy[126], J.L. Holzbauer[88], T.M. Hong[120], L. Hooft van Huysduynen[108], S. Horner[48], J-Y. Hostachy[55], S. Hou[151], A. Hoummada[135a], J. Howard[118], J. Howarth[82], I. Hristova[16], J. Hrivnac[115], T. Hryn'ova[5], P.J. Hsu[81], S.-C. Hsu[138], D. Hu[35], Z. Hubacek[126], F. Hubaut[83], F. Huegging[21], A. Huettmann[42], T.B. Huffman[118], E.W. Hughes[35], G. Hughes[71], M. Huhtinen[30], M. Hurwitz[15], N. Huseynov[64,r], J. Huston[88], J. Huth[57], G. Iacobucci[49], G. Iakovidis[10], M. Ibbotson[82], I. Ibragimov[141], L. Iconomidou-Fayard[115], J. Idarraga[115], P. Iengo[102a], O. Igonkina[105], Y. Ikegami[65], M. Ikeno[65], D. Iliadis[154], N. Ilic[158], T. Ince[99], P. Ioannou[9], M. Iodice[134a], K. Iordanidou[9], V. Ippolito[132a,132b], A. Irles Quiles[167], C. Isaksson[166], M. Ishino[67], M. Ishitsuka[157], R. Ishmukhametov[109], C. Issever[118], S. Istin[19a], A.V. Ivashin[128], W. Iwanski[39], H. Iwasaki[65], J.M. Izen[41], V. Izzo[102a], B. Jackson[120], J.N. Jackson[73], P. Jackson[1], M.R. Jaekel[30], V. Jain[2], K. Jakobs[48], S. Jakobsen[36], T. Jakoubek[125], J. Jakubek[126], D.O. Jamin[151], D.K. Jana[111], E. Jansen[77], H. Jansen[30], J. Janssen[21], A. Jantsch[99], M. Janus[48], R.C. Jared[173], G. Jarlskog[79], L. Jeanty[57], I. Jen-La Plante[31], G.-Y. Jeng[150], D. Jennens[86], P. Jenni[30], A.E. Loevschall-Jensen[36], P. Ježo[36], S. Jézéquel[5], M.K. Jha[20a], H. Ji[173], W. Ji[81], J. Jia[148], Y. Jiang[33b],

M. Jimenez Belenguer[42], S. Jin[33a], O. Jinnouchi[157], M.D. Joergensen[36], D. Joffe[40], M. Johansen[146a,146b], K.E. Johansson[146a], P. Johansson[139], S. Johnert[42], K.A. Johns[7], K. Jon-And[146a,146b], G. Jones[170], R.W.L. Jones[71], T.J. Jones[73], C. Joram[30], P.M. Jorge[124a], K.D. Joshi[82], J. Jovicevic[147], T. Jovin[13b], X. Ju[173], C.A. Jung[43], R.M. Jungst[30], V. Juranek[125], P. Jussel[61], A. Juste Rozas[12], S. Kabana[17], M. Kaci[167], A. Kaczmarska[39], P. Kadlecik[36], M. Kado[115], H. Kagan[109], M. Kagan[57], E. Kajomovitz[152], S. Kalinin[175], L.V. Kalinovskaya[64], S. Kama[40], N. Kanaya[155], M. Kaneda[30], S. Kaneti[28], T. Kanno[157], V.A. Kantserov[96], J. Kanzaki[65], B. Kaplan[108], A. Kapliy[31], J. Kaplon[30], D. Kar[53], M. Karagounis[21], K. Karakostas[10], M. Karnevskiy[58b], V. Kartvelishvili[71], A.N. Karyukhin[128], L. Kashif[173], G. Kasieczka[58b], R.D. Kass[109], A. Kastanas[14], M. Kataoka[5], Y. Kataoka[155], J. Katzy[42], V. Kaushik[7], K. Kawagoe[69], T. Kawamoto[155], G. Kawamura[81], M.S. Kayl[105], S. Kazama[155], V.F. Kazanin[107], M.Y. Kazarinov[64], R. Keeler[169], P.T. Keener[120], R. Kehoe[40], M. Keil[54], G.D. Kekelidze[64], J.S. Keller[138], M. Kenyon[53], O. Kepka[125], N. Kerschen[30], B.P. Kerševan[74], S. Kersten[175], K. Kessoku[155], J. Keung[158], F. Khalil-zada[11], H. Khandanyan[146a,146b], A. Khanov[112], D. Kharchenko[64], A. Khodinov[96], A. Khomich[58a], T.J. Khoo[28], G. Khoriauli[21], A. Khoroshilov[175], V. Khovanskiy[95], E. Khramov[64], J. Khubua[51b], H. Kim[146a,146b], S.H. Kim[160], N. Kimura[171], O. Kind[16], B.T. King[73], M. King[66], R.S.B. King[118], J. Kirk[129], A.E. Kiryunin[99], T. Kishimoto[66], D. Kisielewska[38], T. Kitamura[66], T. Kittelmann[123], K. Kiuchi[160], E. Kladiva[144b], M. Klein[73], U. Klein[73], K. Kleinknecht[81], M. Klemetti[85], A. Klier[172], P. Klimek[146a,146b], A. Klimentov[25], R. Klingenberg[43], J.A. Klinger[82], E.B. Klinkby[36], T. Klioutchnikova[30], P.F. Klok[104], S. Klous[105], E.-E. Kluge[58a], T. Kluge[73], P. Kluit[105], S. Kluth[99], E. Kneringer[61], E.B.F.G. Knoops[83], A. Knue[54], B.R. Ko[45], T. Kobayashi[155], M. Kobel[44], M. Kocian[143], P. Kodys[127], K. Köneke[30], A.C. König[104], S. Koenig[81], L. Köpke[81], F. Koetsveld[104], P. Koevesarki[21], T. Koffas[29], E. Koffeman[105], L.A. Kogan[118], S. Kohlmann[175], F. Kohn[54], Z. Kohout[126], T. Kohriki[65], T. Koi[143], G.M. Kolachev[107,*], H. Kolanoski[16], V. Kolesnikov[64], I. Koletsou[89a], J. Koll[88], A.A. Komar[94], Y. Komori[155], T. Kondo[65], T. Kono[42,s], A.I. Kononov[48], R. Konoplich[108,t], N. Konstantinidis[77], R. Kopeliansky[152], S. Koperny[38], K. Korcyl[39], K. Kordas[154], A. Korn[118], A. Korol[107], I. Korolkov[12], E.V. Korolkova[139], V.A. Korotkov[128], O. Kortner[99], S. Kortner[99], V.V. Kostyukhin[21], S. Kotov[99], V.M. Kotov[64], A. Kotwal[45], C. Kourkoumelis[9], V. Kouskoura[154], A. Koutsman[159a], R. Kowalewski[169], T.Z. Kowalski[38], W. Kozanecki[136], A.S. Kozhin[128], V. Kral[126], V.A. Kramarenko[97], G. Kramberger[74], M.W. Krasny[78], A. Krasznahorkay[108], J.K. Kraus[21], A. Kravchenko[25], S. Kreiss[108], F. Krejci[126], J. Kretzschmar[73], K. Kreutzfeldt[52], N. Krieger[54], P. Krieger[158], K. Kroeninger[54], H. Kroha[99], J. Kroll[120], J. Kroseberg[21], J. Krstic[13a], U. Kruchonak[64], H. Krüger[21], T. Kruker[17], N. Krumnack[63], Z.V. Krumshteyn[64], M.K. Kruse[45], T. Kubota[86], S. Kuday[4a], S. Kuehn[48], A. Kugel[58c], T. Kuhl[42], D. Kuhn[61], V. Kukhtin[64], Y. Kulchitsky[90], S. Kuleshov[32b], C. Kummer[98], M. Kuna[78], J. Kunkle[120], A. Kupco[125], H. Kurashige[66], M. Kurata[160], Y.A. Kurochkin[90], V. Kus[125], E.S. Kuwertz[147], M. Kuze[157], J. Kvita[142], R. Kwee[16], A. La Rosa[49], L. La Rotonda[37a,37b], L. Labarga[80], S. Lablak[135a], C. Lacasta[167], F. Lacava[132a,132b], J. Lacey[29], H. Lacker[16], D. Lacour[78], V.R. Lacuesta[167], E. Ladygin[64], R. Lafaye[5], B. Laforge[78], T. Lagouri[176], S. Lai[48], E. Laisne[55], L. Lambourne[77], C.L. Lampen[7], W. Lampl[7], E. Lancon[136], U. Landgraf[48], M.P.J. Landon[75], V.S. Lang[58a], C. Lange[42], A.J. Lankford[163], F. Lanni[25], K. Lantzsch[175], A. Lanza[119a], S. Laplace[78], C. Lapoire[21], J.F. Laporte[136], T. Lari[89a], A. Larner[118], M. Lassnig[30], P. Laurelli[47], V. Lavorini[37a,37b], W. Lavrijsen[15], P. Laycock[73], O. Le Dortz[78], E. Le Guirriec[83], E. Le Menedeu[12], T. LeCompte[6], F. Ledroit-Guillon[55], H. Lee[105], J.S.H. Lee[116], S.C. Lee[151], L. Lee[176], M. Lefebvre[169], M. Legendre[136], F. Legger[98], C. Leggett[15], M. Lehmacher[21], G. Lehmann Miotto[30], A.G. Leister[176], M.A.L. Leite[24d], R. Leitner[127], D. Lellouch[172], B. Lemmer[54], V. Lendermann[58a], K.J.C. Leney[145b], T. Lenz[105], G. Lenzen[175], B. Lenzi[30], K. Leonhardt[44], S. Leontsinis[10], F. Lepold[58a], C. Leroy[93], J-R. Lessard[169], C.G. Lester[28], C.M. Lester[120], J. Levêque[5], D. Levin[87], L.J. Levinson[172], A. Lewis[118], G.H. Lewis[108], A.M. Leyko[21], M. Leyton[16], B. Li[33b], B. Li[83], H. Li[148], H.L. Li[31], S. Li[33b,u], X. Li[87], Z. Liang[118,v], H. Liao[34], B. Liberti[133a], P. Lichard[30], M. Lichtnecker[98], K. Lie[165], W. Liebig[14], C. Limbach[21], A. Limosani[86], M. Limper[62], S.C. Lin[151,w], F. Linde[105], J.T. Linnemann[88], E. Lipeles[120], A. Lipniacka[14], T.M. Liss[165], D. Lissauer[25], A. Lister[49], A.M. Litke[137], C. Liu[29], D. Liu[151], J.B. Liu[87], L. Liu[87], M. Liu[33b], Y. Liu[33b], M. Livan[119a,119b], S.S.A. Livermore[118], A. Lleres[55], J. Llorente Merino[80], S.L. Lloyd[75], E. Lobodzinska[42], P. Loch[7], W.S. Lockman[137], T. Loddenkoetter[21], F.K. Loebinger[82], A. Loginov[176], C.W. Loh[168], T. Lohse[16], K. Lohwasser[48], M. Lokajicek[125], V.P. Lombardo[5], R.E. Long[71], L. Lopes[124a], D. Lopez Mateos[57], J. Lorenz[98], N. Lorenzo Martinez[115], M. Losada[162], P. Loscutoff[15], F. Lo Sterzo[132a,132b], M.J. Losty[159a,*], X. Lou[41], A. Lounis[115], K.F. Loureiro[162], J. Love[6], P.A. Love[71], A.J. Lowe[143,g], F. Lu[33a], H.J. Lubatti[138], C. Luci[132a,132b], A. Lucotte[55], A. Ludwig[44], D. Ludwig[42], I. Ludwig[48], J. Ludwig[48], F. Luehring[60], G. Luijckx[105], W. Lukas[61], L. Luminari[132a], E. Lund[117], B. Lund-Jensen[147], B. Lundberg[79], J. Lundberg[146a,146b], O. Lundberg[146a,146b], J. Lundquist[36], M. Lungwitz[81], D. Lynn[25], E. Lytken[79], H. Ma[25], L.L. Ma[173], G. Maccarrone[47], A. Macchiolo[99], B. Maček[74], J. Machado Miguens[124a], D. Macina[30], R. Mackeprang[36], R.J. Madaras[15], H.J. Maddocks[71], W.F. Mader[44], R. Maenner[58c], T. Maeno[25], P. Mättig[175], S. Mättig[42], L. Magnoni[163], E. Magradze[54], K. Mahboubi[48], J. Mahlstedt[105], S. Mahmoud[73], G. Mahout[18], C. Maiani[136], C. Maidantchik[24a], A. Maio[124a,c], S. Majewski[25], Y. Makida[65], N. Makovec[115], P. Mal[136], B. Malaescu[30], Pa. Malecki[39], P. Malecki[39], V.P. Maleev[121], F. Malek[55], U. Mallik[62], D. Malon[6], C. Malone[143],

S. Maltezos[10], V. Malyshev[107], S. Malyukov[30], J. Mamuzic[13b], A. Manabe[65], L. Mandelli[89a], I. Mandić[74], R. Mandrysch[62], J. Maneira[124a], A. Manfredini[99], L. Manhaes de Andrade Filho[24b], J.A. Manjarres Ramos[136], A. Mann[98], P.M. Manning[137], A. Manousakis-Katsikakis[9], B. Mansoulie[136], A. Mapelli[30], L. Mapelli[30], L. March[167], J.F. Marchand[29], F. Marchese[133a,133b], G. Marchiori[78], M. Marcisovsky[125], C.P. Marino[169], F. Marroquim[24a], Z. Marshall[30], L.F. Marti[17], S. Marti-Garcia[167], B. Martin[30], B. Martin[88], J.P. Martin[93], T.A. Martin[18], V.J. Martin[46], B. Martin dit Latour[49], S. Martin-Haugh[149], M. Martinez[12], V. Martinez Outschoorn[57], A.C. Martyniuk[169], M. Marx[82], F. Marzano[132a], A. Marzin[111], L. Masetti[81], T. Mashimo[155], R. Mashinistov[94], J. Masik[82], A.L. Maslennikov[107], I. Massa[20a,20b], G. Massaro[105], N. Massol[5], P. Mastrandrea[148], A. Mastroberardino[37a,37b], T. Masubuchi[155], H. Matsunaga[155], T. Matsushita[66], C. Mattravers[118,d], J. Maurer[83], S.J. Maxfield[73], D.A. Maximov[107,h], A. Mayne[139], R. Mazini[151], M. Mazur[21], L. Mazzaferro[133a,133b], M. Mazzanti[89a], J. Mc Donald[85], S.P. Mc Kee[87], A. McCarn[165], R.L. McCarthy[148], T.G. McCarthy[29], N.A. McCubbin[129], K.W. McFarlane[56,*], J.A. Mcfayden[139], G. Mchedlidze[51b], T. Mclaughlan[18], S.J. McMahon[129], R.A. McPherson[169,l], A. Meade[84], J. Mechnich[105], M. Mechtel[175], M. Medinnis[42], S. Meehan[31], R. Meera-Lebbai[111], T. Meguro[116], S. Mehlhase[36], A. Mehta[73], K. Meier[58a], B. Meirose[79], C. Melachrinos[31], B.R. Mellado Garcia[173], F. Meloni[89a,89b], L. Mendoza Navas[162], Z. Meng[151,x], A. Mengarelli[20a,20b], S. Menke[99], E. Meoni[161], K.M. Mercurio[57], P. Mermod[49], L. Merola[102a,102b], C. Meroni[89a], F.S. Merritt[31], H. Merritt[109], A. Messina[30,y], J. Metcalfe[25], A.S. Mete[163], C. Meyer[81], C. Meyer[31], J-P. Meyer[136], J. Meyer[174], J. Meyer[54], S. Michal[30], L. Micu[26a], R.P. Middleton[129], S. Migas[73], L. Mijović[136], G. Mikenberg[172], M. Mikestikova[125], M. Mikuž[74], D.W. Miller[31], R.J. Miller[88], W.J. Mills[168], C. Mills[57], A. Milov[172], D.A. Milstead[146a,146b], D. Milstein[172], A.A. Minaenko[128], M. Miñano Moya[167], I.A. Minashvili[64], A.I. Mincer[108], B. Mindur[38], M. Mineev[64], Y. Ming[173], L.M. Mir[12], G. Mirabelli[132a], J. Mitrevski[137], V.A. Mitsou[167], S. Mitsui[65], P.S. Miyagawa[139], J.U. Mjörnmark[79], T. Moa[146a,146b], V. Moeller[28], K. Mönig[42], N. Möser[21], S. Mohapatra[148], W. Mohr[48], R. Moles-Valls[167], A. Molfetas[30], J. Monk[77], E. Monnier[83], J. Montejo Berlingen[12], F. Monticelli[70], S. Monzani[20a,20b], R.W. Moore[3], G.F. Moorhead[86], C. Mora Herrera[49], A. Moraes[53], N. Morange[136], J. Morel[54], G. Morello[37a,37b], D. Moreno[81], M. Moreno Llácer[167], P. Morettini[50a], M. Morgenstern[44], M. Morii[57], A.K. Morley[30], G. Mornacchi[30], J.D. Morris[75], L. Morvaj[101], H.G. Moser[99], M. Mosidze[51b], J. Moss[109], R. Mount[143], E. Mountricha[10,z], S.V. Mouraviev[94,*], E.J.W. Moyse[84], F. Mueller[58a], J. Mueller[123], K. Mueller[21], T.A. Müller[98], T. Mueller[81], D. Muenstermann[30], Y. Munwes[153], W.J. Murray[129], I. Mussche[105], E. Musto[152], A.G. Myagkov[128], M. Myska[125], O. Nackenhorst[54], J. Nadal[12], K. Nagai[160], R. Nagai[157], K. Nagano[65], A. Nagarkar[109], Y. Nagasaka[59], M. Nagel[99], A.M. Nairz[30], Y. Nakahama[30], K. Nakamura[155], T. Nakamura[155], I. Nakano[110], G. Nanava[21], A. Napier[161], R. Narayan[58b], M. Nash[77,d], T. Nattermann[21], T. Naumann[42], G. Navarro[162], H.A. Neal[87], P.Yu. Nechaeva[94], T.J. Neep[82], A. Negri[119a,119b], G. Negri[30], M. Negrini[20a], S. Nektarijevic[49], A. Nelson[163], T.K. Nelson[143], S. Nemecek[125], P. Nemethy[108], A.A. Nepomuceno[24a], M. Nessi[30,aa], M.S. Neubauer[165], M. Neumann[175], A. Neusiedl[81], R.M. Neves[108], P. Nevski[25], F.M. Newcomer[120], P.R. Newman[18], V. Nguyen Thi Hong[136], R.B. Nickerson[118], R. Nicolaidou[136], B. Nicquevert[30], F. Niedercorn[115], J. Nielsen[137], N. Nikiforou[35], A. Nikiforov[16], V. Nikolaenko[128], I. Nikolic-Audit[78], K. Nikolics[49], K. Nikolopoulos[18], H. Nilsen[48], P. Nilsson[8], Y. Ninomiya[155], A. Nisati[132a], R. Nisius[99], T. Nobe[157], L. Nodulman[6], M. Nomachi[116], I. Nomidis[154], S. Norberg[111], M. Nordberg[30], P.R. Norton[129], J. Novakova[127], M. Nozaki[65], L. Nozka[113], I.M. Nugent[159a], A.-E. Nuncio-Quiroz[21], G. Nunes Hanninger[86], T. Nunnemann[98], E. Nurse[77], B.J. O'Brien[46], D.C. O'Neil[142], V. O'Shea[53], L.B. Oakes[98], F.G. Oakham[29,f], H. Oberlack[99], J. Ocariz[78], A. Ochi[66], S. Oda[69], S. Odaka[65], J. Odier[83], H. Ogren[60], A. Oh[82], S.H. Oh[45], C.C. Ohm[30], T. Ohshima[101], W. Okamura[116], H. Okawa[25], Y. Okumura[31], T. Okuyama[155], A. Olariu[26a], A.G. Olchevski[64], S.A. Olivares Pino[32a], M. Oliveira[124a,i], D. Oliveira Damazio[25], E. Oliver Garcia[167], D. Olivito[120], A. Olszewski[39], J. Olszowska[39], A. Onofre[124a,ab], P.U.E. Onyisi[31,ac], C.J. Oram[159a], M.J. Oreglia[31], Y. Oren[153], D. Orestano[134a,134b], N. Orlando[72a,72b], I. Orlov[107], C. Oropeza Barrera[53], R.S. Orr[158], B. Osculati[50a,50b], R. Ospanov[120], C. Osuna[12], G. Otero y Garzon[27], J.P. Ottersbach[105], M. Ouchrif[135d], E.A. Ouellette[169], F. Ould-Saada[117], A. Ouraou[136], Q. Ouyang[33a], A. Ovcharova[15], M. Owen[82], S. Owen[139], V.E. Ozcan[19a], N. Ozturk[8], A. Pacheco Pages[12], C. Padilla Aranda[12], S. Pagan Griso[15], E. Paganis[139], C. Pahl[99], F. Paige[25], P. Pais[84], K. Pajchel[117], G. Palacino[159b], C.P. Paleari[7], S. Palestini[30], D. Pallin[34], A. Palma[124a], J.D. Palmer[18], Y.B. Pan[173], E. Panagiotopoulou[10], J.G. Panduro Vazquez[76], P. Pani[105], N. Panikashvili[87], S. Panitkin[25], D. Pantea[26a], A. Papadelis[146a], Th.D. Papadopoulou[10], A. Paramonov[6], D. Paredes Hernandez[34], W. Park[25,ad], M.A. Parker[28], F. Parodi[50a,50b], J.A. Parsons[35], U. Parzefall[48], S. Pashapour[54], E. Pasqualucci[132a], S. Passaggio[50a], A. Passeri[134a], F. Pastore[134a,134b,*], Fr. Pastore[76], G. Pásztor[49,ae], S. Pataraia[175], N. Patel[150], J.R. Pater[82], S. Patricelli[102a,102b], T. Pauly[30], M. Pecsy[144a], S. Pedraza Lopez[167], M.I. Pedraza Morales[173], S.V. Peleganchuk[107], D. Pelikan[166], H. Peng[33b], B. Penning[31], A. Penson[35], J. Penwell[60], M. Perantoni[24a], K. Perez[35,af], T. Perez Cavalcanti[42], E. Perez Codina[159a], M.T. Pérez García-Estañ[167], V. Perez Reale[35], L. Perini[89a,89b], H. Pernegger[30], R. Perrino[72a], P. Perrodo[5], V.D. Peshekhonov[64], K. Peters[30], B.A. Petersen[30], J. Petersen[30], T.C. Petersen[36], E. Petit[5], A. Petridis[154], C. Petridou[154], E. Petrolo[132a], F. Petrucci[134a,134b], D. Petschull[42], M. Petteni[142], R. Pezoa[32b], A. Phan[86], P.W. Phillips[129], G. Piacquadio[30], A. Picazio[49], E. Piccaro[75],

M. Piccinini[20a,20b], S.M. Piec[42], R. Piegaia[27], D.T. Pignotti[109], J.E. Pilcher[31], A.D. Pilkington[82], J. Pina[124a,c], M. Pinamonti[164a,164c], A. Pinder[118], J.L. Pinfold[3], A. Pingel[36], B. Pinto[124a], C. Pizio[89a,89b], M.-A. Pleier[25], E. Plotnikova[64], A. Poblaguev[25], S. Poddar[58a], F. Podlyski[34], L. Poggioli[115], D. Pohl[21], M. Pohl[49], G. Polesello[119a], A. Policicchio[37a,37b], A. Polini[20a], J. Poll[75], V. Polychronakos[25], D. Pomeroy[23], K. Pommès[30], L. Pontecorvo[132a], B.G. Pope[88], G.A. Popeneciu[26a], D.S. Popovic[13a], A. Poppleton[30], X. Portell Bueso[30], G.E. Pospelov[99], S. Pospisil[126], I.N. Potrap[99], C.J. Potter[149], C.T. Potter[114], G. Poulard[30], J. Poveda[60], V. Pozdnyakov[64], R. Prabhu[77], P. Pralavorio[83], A. Pranko[15], S. Prasad[30], R. Pravahan[25], S. Prell[63], K. Pretzl[17], D. Price[60], J. Price[73], L.E. Price[6], D. Prieur[123], M. Primavera[72a], K. Prokofiev[108], F. Prokoshin[32b], S. Protopopescu[25], J. Proudfoot[6], X. Prudent[44], M. Przybycien[38], H. Przysiezniak[5], S. Psoroulas[21], E. Ptacek[114], E. Pueschel[84], D. Puldon[148], J. Purdham[87], M. Purohit[25,ad], P. Puzo[115], Y. Pylypchenko[62], J. Qian[87], A. Quadt[54], D.R. Quarrie[15], W.B. Quayle[173], M. Raas[104], V. Radeka[25], V. Radescu[42], P. Radloff[114], F. Ragusa[89a,89b], G. Rahal[178], A.M. Rahimi[109], D. Rahm[25], S. Rajagopalan[25], M. Rammensee[48], M. Rammes[141], A.S. Randle-Conde[40], K. Randrianarivony[29], K. Rao[163], F. Rauscher[98], T.C. Rave[48], M. Raymond[30], A.L. Read[117], D.M. Rebuzzi[119a,119b], A. Redelbach[174], G. Redlinger[25], R. Reece[120], K. Reeves[41], A. Reinsch[114], I. Reisinger[43], C. Rembser[30], Z.L. Ren[151], A. Renaud[115], M. Rescigno[132a], S. Resconi[89a], B. Resende[136], P. Reznicek[98], R. Rezvani[158], R. Richter[99], E. Richter-Was[5,ag], M. Ridel[78], M. Rijpstra[105], M. Rijssenbeek[148], A. Rimoldi[119a,119b], L. Rinaldi[20a], R.R. Rios[40], I. Riu[12], G. Rivoltella[89a,89b], F. Rizatdinova[112], E. Rizvi[75], S.H. Robertson[85,l], A. Robichaud-Veronneau[118], D. Robinson[28], J.E.M. Robinson[82], A. Robson[53], J.G. Rocha de Lima[106], C. Roda[122a,122b], D. Roda Dos Santos[30], A. Roe[54], S. Roe[30], O. Røhne[117], S. Rolli[161], A. Romaniouk[96], M. Romano[20a,20b], G. Romeo[27], E. Romero Adam[167], N. Rompotis[138], L. Roos[78], E. Ros[167], S. Rosati[132a], K. Rosbach[49], A. Rose[149], M. Rose[76], G.A. Rosenbaum[158], E.I. Rosenberg[63], P.L. Rosendahl[14], O. Rosenthal[141], L. Rosselet[49], V. Rossetti[12], E. Rossi[132a,132b], L.P. Rossi[50a], M. Rotaru[26a], I. Roth[172], J. Rothberg[138], D. Rousseau[115], C.R. Royon[136], A. Rozanov[83], Y. Rozen[152], X. Ruan[33a,ah], F. Rubbo[12], I. Rubinskiy[42], N. Ruckstuhl[105], V.I. Rud[97], C. Rudolph[44], G. Rudolph[61], F. Rühr[7], A. Ruiz-Martinez[63], L. Rumyantsev[64], Z. Rurikova[48], N.A. Rusakovich[64], A. Ruschke[98], J.P. Rutherfoord[7], P. Ruzicka[125], Y.F. Ryabov[121], M. Rybar[127], G. Rybkin[115], N.C. Ryder[118], A.F. Saavedra[150], I. Sadeh[153], H.F-W. Sadrozinski[137], R. Sadykov[64], F. Safai Tehrani[132a], H. Sakamoto[155], G. Salamanna[75], A. Salamon[133a], M. Saleem[111], D. Salek[30], D. Salihagic[99], A. Salnikov[143], J. Salt[167], B.M. Salvachua Ferrando[6], D. Salvatore[37a,37b], F. Salvatore[149], A. Salvucci[104], A. Salzburger[30], D. Sampsonidis[154], B.H. Samset[117], A. Sanchez[102a,102b], V. Sanchez Martinez[167], H. Sandaker[14], H.G. Sander[81], M.P. Sanders[98], M. Sandhoff[175], T. Sandoval[28], C. Sandoval[162], R. Sandstroem[99], D.P.C. Sankey[129], A. Sansoni[47], C. Santamarina Rios[85], C. Santoni[34], R. Santonico[133a,133b], H. Santos[124a], I. Santoyo Castillo[149], J.G. Saraiva[124a], T. Sarangi[173], E. Sarkisyan-Grinbaum[8], B. Sarrazin[21], F. Sarri[122a,122b], G. Sartisohn[175], O. Sasaki[65], Y. Sasaki[155], N. Sasao[67], I. Satsounkevitch[90], G. Sauvage[5,*], E. Sauvan[5], J.B. Sauvan[115], P. Savard[158,f], V. Savinov[123], D.O. Savu[30], L. Sawyer[25,n], D.H. Saxon[53], J. Saxon[120], C. Sbarra[20a], A. Sbrizzi[20a,20b], D.A. Scannicchio[163], M. Scarcella[150], J. Schaarschmidt[115], P. Schacht[99], D. Schaefer[120], U. Schäfer[81], A. Schaelicke[46], S. Schaepe[21], S. Schaetzel[58b], A.C. Schaffer[115], D. Schaile[98], R.D. Schamberger[148], A.G. Schamov[107], V. Scharf[58a], V.A. Schegelsky[121], D. Scheirich[87], M. Schernau[163], M.I. Scherzer[35], C. Schiavi[50a,50b], J. Schieck[98], M. Schioppa[37a,37b], S. Schlenker[30], E. Schmidt[48], K. Schmieden[21], C. Schmitt[81], S. Schmitt[58b], B. Schneider[17], U. Schnoor[44], L. Schoeffel[136], A. Schoening[58b], A.L.S. Schorlemmer[54], M. Schott[30], D. Schouten[159a], J. Schovancova[125], M. Schram[85], C. Schroeder[81], N. Schroer[58c], M.J. Schultens[21], J. Schultes[175], H.-C. Schultz-Coulon[58a], H. Schulz[16], M. Schumacher[48], B.A. Schumm[137], Ph. Schune[136], A. Schwartzman[143], Ph. Schwegler[99], Ph. Schwemling[78], R. Schwienhorst[88], R. Schwierz[44], J. Schwindling[136], T. Schwindt[21], M. Schwoerer[5], F.G. Sciacca[17], G. Sciolla[23], W.G. Scott[129], J. Searcy[114], G. Sedov[42], E. Sedykh[121], S.C. Seidel[103], A. Seiden[137], F. Seifert[44], J.M. Seixas[24a], G. Sekhniaidze[102a], S.J. Sekula[40], K.E. Selbach[46], D.M. Seliverstov[121], B. Sellden[146a], G. Sellers[73], M. Seman[144b], N. Semprini-Cesari[20a,20b], C. Serfon[98], L. Serin[115], L. Serkin[54], R. Seuster[159a], H. Severini[111], A. Sfyrla[30], E. Shabalina[54], M. Shamim[114], L.Y. Shan[33a], J.T. Shank[22], Q.T. Shao[86], M. Shapiro[15], P.B. Shatalov[95], K. Shaw[164a,164c], D. Sherman[176], P. Sherwood[77], S. Shimizu[101], M. Shimojima[100], T. Shin[56], M. Shiyakova[64], A. Shmeleva[94], M.J. Shochet[31], D. Short[118], S. Shrestha[63], E. Shulga[96], M.A. Shupe[7], P. Sicho[125], A. Sidoti[132a], F. Siegert[48], Dj. Sijacki[13a], O. Silbert[172], J. Silva[124a], Y. Silver[153], D. Silverstein[143], S.B. Silverstein[146a], V. Simak[126], O. Simard[136], Lj. Simic[13a], S. Simion[115], E. Simioni[81], B. Simmons[77], R. Simoniello[89a,89b], M. Simonyan[36], P. Sinervo[158], N.B. Sinev[114], V. Sipica[141], G. Siragusa[174], A. Sircar[25], A.N. Sisakyan[64,*], S.Yu. Sivoklokov[97], J. Sjölin[146a,146b], T.B. Sjursen[14], L.A. Skinnari[15], H.P. Skottowe[57], K. Skovpen[107], P. Skubic[111], M. Slater[18], T. Slavicek[126], K. Sliwa[161], V. Smakhtin[172], B.H. Smart[46], L. Smestad[117], S.Yu. Smirnov[96], Y. Smirnov[96], L.N. Smirnova[97], O. Smirnova[79], B.C. Smith[57], D. Smith[143], K.M. Smith[53], M. Smizanska[71], K. Smolek[126], A.A. Snesarev[94], S.W. Snow[82], J. Snow[111], S. Snyder[25], R. Sobie[169,l], J. Sodomka[126], A. Soffer[153], C.A. Solans[167], M. Solar[126], J. Solc[126], E.Yu. Soldatov[96], U. Soldevila[167], E. Solfaroli Camillocci[132a,132b], A.A. Solodkov[128], O.V. Solovyanov[128], V. Solovyev[121], N. Soni[1], A. Sood[15], V. Sopko[126], B. Sopko[126], M. Sosebee[8], R. Soualah[164a,164c], P. Soueid[93], A. Soukharev[107], S. Spagnolo[72a,72b], F. Spanò[76], R. Spighi[20a], G. Spigo[30],

R. Spiwoks[30], M. Spousta[127,ai], T. Spreitzer[158], B. Spurlock[8], R.D. St. Denis[53], J. Stahlman[120], R. Stamen[58a], E. Stanecka[39], R.W. Stanek[6], C. Stanescu[134a], M. Stanescu-Bellu[42], M.M. Stanitzki[42], S. Stapnes[117], E.A. Starchenko[128], J. Stark[55], P. Staroba[125], P. Starovoitov[42], R. Staszewski[39], A. Staude[98], P. Stavina[144a,*], G. Steele[53], P. Steinbach[44], P. Steinberg[25], I. Stekl[126], B. Stelzer[142], H.J. Stelzer[88], O. Stelzer-Chilton[159a], H. Stenzel[52], S. Stern[99], G.A. Stewart[30], J.A. Stillings[21], M.C. Stockton[85], K. Stoerig[48], G. Stoicea[26a], S. Stonjek[99], P. Strachota[127], A.R. Stradling[8], A. Straessner[44], J. Strandberg[147], S. Strandberg[146a,146b], A. Strandlie[117], M. Strang[109], E. Strauss[143], M. Strauss[111], P. Strizenec[144b], R. Ströhmer[174], D.M. Strom[114], J.A. Strong[76,*], R. Stroynowski[40], B. Stugu[14], I. Stumer[25,*], J. Stupak[148], P. Sturm[175], N.A. Styles[42], D.A. Soh[151,v], D. Su[143], HS. Subramania[3], R. Subramaniam[25], A. Succurro[12], Y. Sugaya[116], C. Suhr[106], M. Suk[127], V.V. Sulin[94], S. Sultansoy[4d], T. Sumida[67], X. Sun[55], J.E. Sundermann[48], K. Suruliz[139], G. Susinno[37a,37b], M.R. Sutton[149], Y. Suzuki[65], Y. Suzuki[66], M. Svatos[125], S. Swedish[168], I. Sykora[144a], T. Sykora[127], J. Sánchez[167], D. Ta[105], K. Tackmann[42], A. Taffard[163], R. Tafirout[159a], N. Taiblum[153], Y. Takahashi[101], H. Takai[25], R. Takashima[68], H. Takeda[66], T. Takeshita[140], Y. Takubo[65], M. Talby[83], A. Talyshev[107,h], M.C. Tamsett[25], K.G. Tan[86], J. Tanaka[155], R. Tanaka[115], S. Tanaka[131], S. Tanaka[65], A.J. Tanasijczuk[142], K. Tani[66], N. Tannoury[83], S. Tapprogge[81], D. Tardif[158], S. Tarem[152], F. Tarrade[29], G.F. Tartarelli[89a], P. Tas[127], M. Tasevsky[125], E. Tassi[37a,37b], Y. Tayalati[135d], C. Taylor[77], F.E. Taylor[92], G.N. Taylor[86], W. Taylor[159b], M. Teinturier[115], F.A. Teischinger[30], M. Teixeira Dias Castanheira[75], P. Teixeira-Dias[76], K.K. Temming[48], H. Ten Kate[30], P.K. Teng[151], S. Terada[65], K. Terashi[155], J. Terron[80], M. Testa[47], R.J. Teuscher[158,l], J. Therhaag[21], T. Theveneaux-Pelzer[78], S. Thoma[48], J.P. Thomas[18], E.N. Thompson[35], P.D. Thompson[18], P.D. Thompson[158], A.S. Thompson[53], L.A. Thomsen[36], E. Thomson[120], M. Thomson[28], W.M. Thong[86], R.P. Thun[87], F. Tian[35], M.J. Tibbetts[15], T. Tic[125], V.O. Tikhomirov[94], Y.A. Tikhonov[107,h], S. Timoshenko[96], E. Tiouchichine[83], P. Tipton[176], S. Tisserant[83], T. Todorov[5], S. Todorova-Nova[161], B. Toggerson[163], J. Tojo[69], S. Tokár[144a], K. Tokushuku[65], K. Tollefson[88], M. Tomoto[101], L. Tompkins[31], K. Toms[103], A. Tonoyan[14], C. Topfel[17], N.D. Topilin[64], E. Torrence[114], H. Torres[78], E. Torró Pastor[167], J. Toth[83,ae], F. Touchard[83], D.R. Tovey[139], T. Trefzger[174], L. Tremblet[30], A. Tricoli[30], I.M. Trigger[159a], S. Trincaz-Duvoid[78], M.F. Tripiana[70], N. Triplett[25], W. Trischuk[158], B. Trocmé[55], C. Troncon[89a], M. Trottier-McDonald[142], P. True[88], M. Trzebinski[39], A. Trzupek[39], C. Tsarouchas[30], J.C-L. Tseng[118], M. Tsiakiris[105], P.V. Tsiareshka[90], D. Tsionou[5,aj], G. Tsipolitis[10], S. Tsiskaridze[12], V. Tsiskaridze[48], E.G. Tskhadadze[51a], I.I. Tsukerman[95], V. Tsulaia[15], J.-W. Tsung[21], S. Tsuno[65], D. Tsybychev[148], A. Tua[139], A. Tudorache[26a], V. Tudorache[26a], J.M. Tuggle[31], M. Turala[39], D. Turecek[126], I. Turk Cakir[4e], E. Turlay[105], R. Turra[89a,89b], P.M. Tuts[35], A. Tykhonov[74], M. Tylmad[146a,146b], M. Tyndel[129], G. Tzanakos[9], K. Uchida[21], I. Ueda[155], R. Ueno[29], M. Ughetto[83], M. Ugland[14], M. Uhlenbrock[21], M. Uhrmacher[54], F. Ukegawa[160], G. Unal[30], A. Undrus[25], G. Unel[163], Y. Unno[65], D. Urbaniec[35], P. Urquijo[21], G. Usai[8], M. Uslenghi[119a,119b], L. Vacavant[83], V. Vacek[126], B. Vachon[85], S. Vahsen[15], J. Valenta[125], S. Valentinetti[20a,20b], A. Valero[167], S. Valkar[127], E. Valladolid Gallego[167], S. Vallecorsa[152], J.A. Valls Ferrer[167], R. Van Berg[120], P.C. Van Der Deijl[105], R. van der Geer[105], H. van der Graaf[105], R. Van Der Leeuw[105], E. van der Poel[105], D. van der Ster[30], N. van Eldik[30], P. van Gemmeren[6], J. Van Nieuwkoop[142], I. van Vulpen[105], M. Vanadia[99], W. Vandelli[30], A. Vaniachine[6], P. Vankov[42], F. Vannucci[78], R. Vari[132a], E.W. Varnes[7], T. Varol[84], D. Varouchas[15], A. Vartapetian[8], K.E. Varvell[150], V.I. Vassilakopoulos[56], F. Vazeille[34], T. Vazquez Schroeder[54], G. Vegni[89a,89b], J.J. Veillet[115], F. Veloso[124a], R. Veness[30], S. Veneziano[132a], A. Ventura[72a,72b], D. Ventura[84], M. Venturi[48], N. Venturi[158], V. Vercesi[119a], M. Verducci[138], W. Verkerke[105], J.C. Vermeulen[105], A. Vest[44], M.C. Vetterli[142,f], I. Vichou[165], T. Vickey[145b,ak], O.E. Vickey Boeriu[145b], G.H.A. Viehhauser[118], S. Viel[168], M. Villa[20a,20b], M. Villaplana Perez[167], E. Vilucchi[47], M.G. Vincter[29], E. Vinek[30], V.B. Vinogradov[64], M. Virchaux[136,*], J. Virzi[15], O. Vitells[172], M. Viti[42], I. Vivarelli[48], F. Vives Vaque[3], S. Vlachos[10], D. Vladoiu[98], M. Vlasak[126], A. Vogel[21], P. Vokac[126], G. Volpi[47], M. Volpi[86], G. Volpini[89a], H. von der Schmitt[99], H. von Radziewski[48], E. von Toerne[21], V. Vorobel[127], V. Vorwerk[12], M. Vos[167], R. Voss[30], J.H. Vossebeld[73], N. Vranjes[136], M. Vranjes Milosavljevic[105], V. Vrba[125], M. Vreeswijk[105], T. Vu Anh[48], R. Vuillermet[30], I. Vukotic[31], W. Wagner[175], P. Wagner[120], H. Wahlen[175], S. Wahrmund[44], J. Wakabayashi[101], S. Walch[87], J. Walder[71], R. Walker[98], W. Walkowiak[141], R. Wall[176], P. Waller[73], B. Walsh[176], C. Wang[45], H. Wang[173], H. Wang[40], J. Wang[151], J. Wang[33a], R. Wang[103], S.M. Wang[151], T. Wang[21], A. Warburton[85], C.P. Ward[28], D.R. Wardrope[77], M. Warsinsky[48], A. Washbrook[46], C. Wasicki[42], I. Watanabe[66], P.M. Watkins[18], A.T. Watson[18], I.J. Watson[150], M.F. Watson[18], G. Watts[138], S. Watts[82], A.T. Waugh[150], B.M. Waugh[77], M.S. Weber[17], J.S. Webster[31], A.R. Weidberg[118], P. Weigell[99], J. Weingarten[54], C. Weiser[48], P.S. Wells[30], T. Wenaus[25], D. Wendland[16], Z. Weng[151,v], T. Wengler[30], S. Wenig[30], N. Wermes[21], M. Werner[48], P. Werner[30], M. Werth[163], M. Wessels[58a], J. Wetter[161], C. Weydert[55], K. Whalen[29], A. White[8], M.J. White[86], S. White[122a,122b], S.R. Whitehead[118], D. Whiteson[163], D. Whittington[60], D. Wicke[175], F.J. Wickens[129], W. Wiedenmann[173], M. Wielers[129], P. Wienemann[21], C. Wiglesworth[75], L.A.M. Wiik-Fuchs[21], P.A. Wijeratne[77], A. Wildauer[99], M.A. Wildt[42,s], I. Wilhelm[127], H.G. Wilkens[30], J.Z. Will[98], E. Williams[35], H.H. Williams[120], S. Williams[28], W. Willis[35], S. Willocq[84], J.A. Wilson[18], M.G. Wilson[143], A. Wilson[87], I. Wingerter-Seez[5], S. Winkelmann[48], F. Winklmeier[30], M. Wittgen[143], S.J. Wollstadt[81], M.W. Wolter[39],

H. Wolters[124a,i], W.C. Wong[41], G. Wooden[87], B.K. Wosiek[39], J. Wotschack[30], M.J. Woudstra[82], K.W. Wozniak[39], K. Wraight[53], M. Wright[53], B. Wrona[73], S.L. Wu[173], X. Wu[49], Y. Wu[33b,al], E. Wulf[35], B.M. Wynne[46], S. Xella[36], M. Xiao[136], S. Xie[48], C. Xu[33b,z], D. Xu[33a], L. Xu[33b], B. Yabsley[150], S. Yacoob[145a,am], M. Yamada[65], H. Yamaguchi[155], A. Yamamoto[65], K. Yamamoto[63], S. Yamamoto[155], T. Yamamura[155], T. Yamanaka[155], T. Yamazaki[155], Y. Yamazaki[66], Z. Yan[22], H. Yang[87], U.K. Yang[82], Y. Yang[109], Z. Yang[146a,146b], S. Yanush[91], L. Yao[33a], Y. Yasu[65], E. Yatsenko[42], J. Ye[40], S. Ye[25], A.L. Yen[57], M. Yilmaz[4c], R. Yoosoofmiya[123], K. Yorita[171], R. Yoshida[6], K. Yoshihara[155], C. Young[143], C.J. Young[118], S. Youssef[22], D. Yu[25], D.R. Yu[15], J. Yu[8], J. Yu[112], L. Yuan[66], A. Yurkewicz[106], M. Byszewski[30], B. Zabinski[39], R. Zaidan[62], A.M. Zaitsev[128], L. Zanello[132a,132b], D. Zanzi[99], A. Zaytsev[25], C. Zeitnitz[175], M. Zeman[125], A. Zemla[39], O. Zenin[128], T. Ženiš[144a], Z. Zinonos[122a,122b], D. Zerwas[115], G. Zevi della Porta[57], D. Zhang[87], H. Zhang[88], J. Zhang[6], X. Zhang[33d], Z. Zhang[115], L. Zhao[108], Z. Zhao[33b], A. Zhemchugov[64], J. Zhong[118], B. Zhou[87], N. Zhou[163], Y. Zhou[151], C.G. Zhu[33d], H. Zhu[42], J. Zhu[87], Y. Zhu[33b], X. Zhuang[98], V. Zhuravlov[99], A. Zibell[98], D. Zieminska[60], N.I. Zimin[64], R. Zimmermann[21], S. Zimmermann[21], S. Zimmermann[48], M. Ziolkowski[141], R. Zitoun[5], L. Živković[35], V.V. Zmouchko[128,*], G. Zobernig[173], A. Zoccoli[20a,20b], M. zur Nedden[16], V. Zutshi[106], L. Zwalinski[30].

[1] School of Chemistry and Physics, University of Adelaide, Adelaide, Australia
[2] Physics Department, SUNY Albany, Albany NY, United States of America
[3] Department of Physics, University of Alberta, Edmonton AB, Canada
[4] [(a)]Department of Physics, Ankara University, Ankara; [(b)]Department of Physics, Dumlupinar University, Kutahya; [(c)]Department of Physics, Gazi University, Ankara; [(d)]Division of Physics, TOBB University of Economics and Technology, Ankara; [(e)]Turkish Atomic Energy Authority, Ankara, Turkey
[5] LAPP, CNRS/IN2P3 and Université de Savoie, Annecy-le-Vieux, France
[6] High Energy Physics Division, Argonne National Laboratory, Argonne IL, United States of America
[7] Department of Physics, University of Arizona, Tucson AZ, United States of America
[8] Department of Physics, The University of Texas at Arlington, Arlington TX, United States of America
[9] Physics Department, University of Athens, Athens, Greece
[10] Physics Department, National Technical University of Athens, Zografou, Greece
[11] Institute of Physics, Azerbaijan Academy of Sciences, Baku, Azerbaijan
[12] Institut de Física d'Altes Energies and Departament de Física de la Universitat Autònoma de Barcelona and ICREA, Barcelona, Spain
[13] [(a)]Institute of Physics, University of Belgrade, Belgrade; [(b)]Vinca Institute of Nuclear Sciences, University of Belgrade, Belgrade, Serbia
[14] Department for Physics and Technology, University of Bergen, Bergen, Norway
[15] Physics Division, Lawrence Berkeley National Laboratory and University of California, Berkeley CA, United States of America
[16] Department of Physics, Humboldt University, Berlin, Germany
[17] Albert Einstein Center for Fundamental Physics and Laboratory for High Energy Physics, University of Bern, Bern, Switzerland
[18] School of Physics and Astronomy, University of Birmingham, Birmingham, United Kingdom
[19] [(a)]Department of Physics, Bogazici University, Istanbul; [(b)]Division of Physics, Dogus University, Istanbul; [(c)]Department of Physics Engineering, Gaziantep University, Gaziantep; [(d)]Department of Physics, Istanbul Technical University, Istanbul, Turkey
[20] [(a)]INFN Sezione di Bologna; [(b)]Dipartimento di Fisica, Università di Bologna, Bologna, Italy
[21] Physikalisches Institut, University of Bonn, Bonn, Germany
[22] Department of Physics, Boston University, Boston MA, United States of America
[23] Department of Physics, Brandeis University, Waltham MA, United States of America
[24] [(a)]Universidade Federal do Rio De Janeiro COPPE/EE/IF, Rio de Janeiro; [(b)]Federal University of Juiz de Fora (UFJF), Juiz de Fora; [(c)]Federal University of Sao Joao del Rei (UFSJ), Sao Joao del Rei; [(d)]Instituto de Fisica, Universidade de Sao Paulo, Sao Paulo, Brazil
[25] Physics Department, Brookhaven National Laboratory, Upton NY, United States of America
[26] [(a)]National Institute of Physics and Nuclear Engineering, Bucharest; [(b)]University Politehnica Bucharest, Bucharest; [(c)]West University in Timisoara, Timisoara, Romania
[27] Departamento de Física, Universidad de Buenos Aires, Buenos Aires, Argentina
[28] Cavendish Laboratory, University of Cambridge, Cambridge, United Kingdom
[29] Department of Physics, Carleton University, Ottawa ON, Canada
[30] CERN, Geneva, Switzerland
[31] Enrico Fermi Institute, University of Chicago, Chicago IL, United States of America
[32] [(a)]Departamento de Física, Pontificia Universidad Católica de Chile, Santiago; [(b)]Departamento de Física,

Universidad Técnica Federico Santa María, Valparaíso, Chile
[33] [(a)]Institute of High Energy Physics, Chinese Academy of Sciences, Beijing; [(b)]Department of Modern Physics, University of Science and Technology of China, Anhui; [(c)]Department of Physics, Nanjing University, Jiangsu; [(d)]School of Physics, Shandong University, Shandong; [(e)]Physics Department, Shanghai Jiao Tong University, Shanghai, China
[34] Laboratoire de Physique Corpusculaire, Clermont Université and Université Blaise Pascal and CNRS/IN2P3, Clermont-Ferrand, France
[35] Nevis Laboratory, Columbia University, Irvington NY, United States of America
[36] Niels Bohr Institute, University of Copenhagen, Kobenhavn, Denmark
[37] [(a)]INFN Gruppo Collegato di Cosenza; [(b)]Dipartimento di Fisica, Università della Calabria, Arcavata di Rende, Italy
[38] AGH University of Science and Technology, Faculty of Physics and Applied Computer Science, Krakow, Poland
[39] The Henryk Niewodniczanski Institute of Nuclear Physics, Polish Academy of Sciences, Krakow, Poland
[40] Physics Department, Southern Methodist University, Dallas TX, United States of America
[41] Physics Department, University of Texas at Dallas, Richardson TX, United States of America
[42] DESY, Hamburg and Zeuthen, Germany
[43] Institut für Experimentelle Physik IV, Technische Universität Dortmund, Dortmund, Germany
[44] Institut für Kern-und Teilchenphysik, Technical University Dresden, Dresden, Germany
[45] Department of Physics, Duke University, Durham NC, United States of America
[46] SUPA - School of Physics and Astronomy, University of Edinburgh, Edinburgh, United Kingdom
[47] INFN Laboratori Nazionali di Frascati, Frascati, Italy
[48] Fakultät für Mathematik und Physik, Albert-Ludwigs-Universität, Freiburg, Germany
[49] Section de Physique, Université de Genève, Geneva, Switzerland
[50] [(a)]INFN Sezione di Genova; [(b)]Dipartimento di Fisica, Università di Genova, Genova, Italy
[51] [(a)]E. Andronikashvili Institute of Physics, Iv. Javakhishvili Tbilisi State University, Tbilisi; [(b)]High Energy Physics Institute, Tbilisi State University, Tbilisi, Georgia
[52] II Physikalisches Institut, Justus-Liebig-Universität Giessen, Giessen, Germany
[53] SUPA - School of Physics and Astronomy, University of Glasgow, Glasgow, United Kingdom
[54] II Physikalisches Institut, Georg-August-Universität, Göttingen, Germany
[55] Laboratoire de Physique Subatomique et de Cosmologie, Université Joseph Fourier and CNRS/IN2P3 and Institut National Polytechnique de Grenoble, Grenoble, France
[56] Department of Physics, Hampton University, Hampton VA, United States of America
[57] Laboratory for Particle Physics and Cosmology, Harvard University, Cambridge MA, United States of America
[58] [(a)]Kirchhoff-Institut für Physik, Ruprecht-Karls-Universität Heidelberg, Heidelberg; [(b)]Physikalisches Institut, Ruprecht-Karls-Universität Heidelberg, Heidelberg; [(c)]ZITI Institut für technische Informatik, Ruprecht-Karls-Universität Heidelberg, Mannheim, Germany
[59] Faculty of Applied Information Science, Hiroshima Institute of Technology, Hiroshima, Japan
[60] Department of Physics, Indiana University, Bloomington IN, United States of America
[61] Institut für Astro-und Teilchenphysik, Leopold-Franzens-Universität, Innsbruck, Austria
[62] University of Iowa, Iowa City IA, United States of America
[63] Department of Physics and Astronomy, Iowa State University, Ames IA, United States of America
[64] Joint Institute for Nuclear Research, JINR Dubna, Dubna, Russia
[65] KEK, High Energy Accelerator Research Organization, Tsukuba, Japan
[66] Graduate School of Science, Kobe University, Kobe, Japan
[67] Faculty of Science, Kyoto University, Kyoto, Japan
[68] Kyoto University of Education, Kyoto, Japan
[69] Department of Physics, Kyushu University, Fukuoka, Japan
[70] Instituto de Física La Plata, Universidad Nacional de La Plata and CONICET, La Plata, Argentina
[71] Physics Department, Lancaster University, Lancaster, United Kingdom
[72] [(a)]INFN Sezione di Lecce; [(b)]Dipartimento di Matematica e Fisica, Università del Salento, Lecce, Italy
[73] Oliver Lodge Laboratory, University of Liverpool, Liverpool, United Kingdom
[74] Department of Physics, Jožef Stefan Institute and University of Ljubljana, Ljubljana, Slovenia
[75] School of Physics and Astronomy, Queen Mary University of London, London, United Kingdom
[76] Department of Physics, Royal Holloway University of London, Surrey, United Kingdom
[77] Department of Physics and Astronomy, University College London, London, United Kingdom
[78] Laboratoire de Physique Nucléaire et de Hautes Energies, UPMC and Université Paris-Diderot and CNRS/IN2P3, Paris, France
[79] Fysiska institutionen, Lunds universitet, Lund, Sweden

[80] Departamento de Fisica Teorica C-15, Universidad Autonoma de Madrid, Madrid, Spain
[81] Institut für Physik, Universität Mainz, Mainz, Germany
[82] School of Physics and Astronomy, University of Manchester, Manchester, United Kingdom
[83] CPPM, Aix-Marseille Université and CNRS/IN2P3, Marseille, France
[84] Department of Physics, University of Massachusetts, Amherst MA, United States of America
[85] Department of Physics, McGill University, Montreal QC, Canada
[86] School of Physics, University of Melbourne, Victoria, Australia
[87] Department of Physics, The University of Michigan, Ann Arbor MI, United States of America
[88] Department of Physics and Astronomy, Michigan State University, East Lansing MI, United States of America
[89] [(a)]INFN Sezione di Milano; [(b)]Dipartimento di Fisica, Università di Milano, Milano, Italy
[90] B.I. Stepanov Institute of Physics, National Academy of Sciences of Belarus, Minsk, Republic of Belarus
[91] National Scientific and Educational Centre for Particle and High Energy Physics, Minsk, Republic of Belarus
[92] Department of Physics, Massachusetts Institute of Technology, Cambridge MA, United States of America
[93] Group of Particle Physics, University of Montreal, Montreal QC, Canada
[94] P.N. Lebedev Institute of Physics, Academy of Sciences, Moscow, Russia
[95] Institute for Theoretical and Experimental Physics (ITEP), Moscow, Russia
[96] Moscow Engineering and Physics Institute (MEPhI), Moscow, Russia
[97] Skobeltsyn Institute of Nuclear Physics, Lomonosov Moscow State University, Moscow, Russia
[98] Fakultät für Physik, Ludwig-Maximilians-Universität München, München, Germany
[99] Max-Planck-Institut für Physik (Werner-Heisenberg-Institut), München, Germany
[100] Nagasaki Institute of Applied Science, Nagasaki, Japan
[101] Graduate School of Science and Kobayashi-Maskawa Institute, Nagoya University, Nagoya, Japan
[102] [(a)]INFN Sezione di Napoli; [(b)]Dipartimento di Scienze Fisiche, Università di Napoli, Napoli, Italy
[103] Department of Physics and Astronomy, University of New Mexico, Albuquerque NM, United States of America
[104] Institute for Mathematics, Astrophysics and Particle Physics, Radboud University Nijmegen/Nikhef, Nijmegen, Netherlands
[105] Nikhef National Institute for Subatomic Physics and University of Amsterdam, Amsterdam, Netherlands
[106] Department of Physics, Northern Illinois University, DeKalb IL, United States of America
[107] Budker Institute of Nuclear Physics, SB RAS, Novosibirsk, Russia
[108] Department of Physics, New York University, New York NY, United States of America
[109] Ohio State University, Columbus OH, United States of America
[110] Faculty of Science, Okayama University, Okayama, Japan
[111] Homer L. Dodge Department of Physics and Astronomy, University of Oklahoma, Norman OK, United States of America
[112] Department of Physics, Oklahoma State University, Stillwater OK, United States of America
[113] Palacký University, RCPTM, Olomouc, Czech Republic
[114] Center for High Energy Physics, University of Oregon, Eugene OR, United States of America
[115] LAL, Université Paris-Sud and CNRS/IN2P3, Orsay, France
[116] Graduate School of Science, Osaka University, Osaka, Japan
[117] Department of Physics, University of Oslo, Oslo, Norway
[118] Department of Physics, Oxford University, Oxford, United Kingdom
[119] [(a)]INFN Sezione di Pavia; [(b)]Dipartimento di Fisica, Università di Pavia, Pavia, Italy
[120] Department of Physics, University of Pennsylvania, Philadelphia PA, United States of America
[121] Petersburg Nuclear Physics Institute, Gatchina, Russia
[122] [(a)]INFN Sezione di Pisa; [(b)]Dipartimento di Fisica E. Fermi, Università di Pisa, Pisa, Italy
[123] Department of Physics and Astronomy, University of Pittsburgh, Pittsburgh PA, United States of America
[124] [(a)]Laboratorio de Instrumentacao e Fisica Experimental de Particulas - LIP, Lisboa, Portugal; [(b)]Departamento de Fisica Teorica y del Cosmos and CAFPE, Universidad de Granada, Granada, Spain
[125] Institute of Physics, Academy of Sciences of the Czech Republic, Praha, Czech Republic
[126] Czech Technical University in Prague, Praha, Czech Republic
[127] Faculty of Mathematics and Physics, Charles University in Prague, Praha, Czech Republic
[128] State Research Center Institute for High Energy Physics, Protvino, Russia
[129] Particle Physics Department, Rutherford Appleton Laboratory, Didcot, United Kingdom
[130] Physics Department, University of Regina, Regina SK, Canada
[131] Ritsumeikan University, Kusatsu, Shiga, Japan
[132] [(a)]INFN Sezione di Roma I; [(b)]Dipartimento di Fisica, Università La Sapienza, Roma, Italy
[133] [(a)]INFN Sezione di Roma Tor Vergata; [(b)]Dipartimento di Fisica, Università di Roma Tor Vergata, Roma, Italy
[134] [(a)]INFN Sezione di Roma Tre; [(b)]Dipartimento di Fisica, Università Roma Tre, Roma, Italy

[135] [(a)]Faculté des Sciences Ain Chock, Réseau Universitaire de Physique des Hautes Energies - Université Hassan II, Casablanca; [(b)]Centre National de l'Energie des Sciences Techniques Nucleaires, Rabat; [(c)]Faculté des Sciences Semlalia, Université Cadi Ayyad, LPHEA-Marrakech; [(d)]Faculté des Sciences, Université Mohamed Premier and LPTPM, Oujda; [(e)]Faculté des sciences, Université Mohammed V-Agdal, Rabat, Morocco
[136] DSM/IRFU (Institut de Recherches sur les Lois Fondamentales de l'Univers), CEA Saclay (Commissariat à l'Energie Atomique et aux Energies Alternatives), Gif-sur-Yvette, France
[137] Santa Cruz Institute for Particle Physics, University of California Santa Cruz, Santa Cruz CA, United States of America
[138] Department of Physics, University of Washington, Seattle WA, United States of America
[139] Department of Physics and Astronomy, University of Sheffield, Sheffield, United Kingdom
[140] Department of Physics, Shinshu University, Nagano, Japan
[141] Fachbereich Physik, Universität Siegen, Siegen, Germany
[142] Department of Physics, Simon Fraser University, Burnaby BC, Canada
[143] SLAC National Accelerator Laboratory, Stanford CA, United States of America
[144] [(a)]Faculty of Mathematics, Physics & Informatics, Comenius University, Bratislava; [(b)]Department of Subnuclear Physics, Institute of Experimental Physics of the Slovak Academy of Sciences, Kosice, Slovak Republic
[145] [(a)]Department of Physics, University of Johannesburg, Johannesburg; [(b)]School of Physics, University of the Witwatersrand, Johannesburg, South Africa
[146] [(a)]Department of Physics, Stockholm University; [(b)]The Oskar Klein Centre, Stockholm, Sweden
[147] Physics Department, Royal Institute of Technology, Stockholm, Sweden
[148] Departments of Physics & Astronomy and Chemistry, Stony Brook University, Stony Brook NY, United States of America
[149] Department of Physics and Astronomy, University of Sussex, Brighton, United Kingdom
[150] School of Physics, University of Sydney, Sydney, Australia
[151] Institute of Physics, Academia Sinica, Taipei, Taiwan
[152] Department of Physics, Technion: Israel Institute of Technology, Haifa, Israel
[153] Raymond and Beverly Sackler School of Physics and Astronomy, Tel Aviv University, Tel Aviv, Israel
[154] Department of Physics, Aristotle University of Thessaloniki, Thessaloniki, Greece
[155] International Center for Elementary Particle Physics and Department of Physics, The University of Tokyo, Tokyo, Japan
[156] Graduate School of Science and Technology, Tokyo Metropolitan University, Tokyo, Japan
[157] Department of Physics, Tokyo Institute of Technology, Tokyo, Japan
[158] Department of Physics, University of Toronto, Toronto ON, Canada
[159] [(a)]TRIUMF, Vancouver BC; [(b)]Department of Physics and Astronomy, York University, Toronto ON, Canada
[160] Faculty of Pure and Applied Sciences, University of Tsukuba, Tsukuba, Japan
[161] Department of Physics and Astronomy, Tufts University, Medford MA, United States of America
[162] Centro de Investigaciones, Universidad Antonio Narino, Bogota, Colombia
[163] Department of Physics and Astronomy, University of California Irvine, Irvine CA, United States of America
[164] [(a)]INFN Gruppo Collegato di Udine; [(b)]ICTP, Trieste; [(c)]Dipartimento di Chimica, Fisica e Ambiente, Università di Udine, Udine, Italy
[165] Department of Physics, University of Illinois, Urbana IL, United States of America
[166] Department of Physics and Astronomy, University of Uppsala, Uppsala, Sweden
[167] Instituto de Física Corpuscular (IFIC) and Departamento de Física Atómica, Molecular y Nuclear and Departamento de Ingeniería Electrónica and Instituto de Microelectrónica de Barcelona (IMB-CNM), University of Valencia and CSIC, Valencia, Spain
[168] Department of Physics, University of British Columbia, Vancouver BC, Canada
[169] Department of Physics and Astronomy, University of Victoria, Victoria BC, Canada
[170] Department of Physics, University of Warwick, Coventry, United Kingdom
[171] Waseda University, Tokyo, Japan
[172] Department of Particle Physics, The Weizmann Institute of Science, Rehovot, Israel
[173] Department of Physics, University of Wisconsin, Madison WI, United States of America
[174] Fakultät für Physik und Astronomie, Julius-Maximilians-Universität, Würzburg, Germany
[175] Fachbereich C Physik, Bergische Universität Wuppertal, Wuppertal, Germany
[176] Department of Physics, Yale University, New Haven CT, United States of America
[177] Yerevan Physics Institute, Yerevan, Armenia
[178] Centre de Calcul de l'Institut National de Physique Nucléaire et de Physique des Particules (IN2P3), Villeurbanne, France
[a] Also at Department of Physics, King's College London, London, United Kingdom

[b] Also at Laboratorio de Instrumentacao e Fisica Experimental de Particulas - LIP, Lisboa, Portugal
[c] Also at Faculdade de Ciencias and CFNUL, Universidade de Lisboa, Lisboa, Portugal
[d] Also at Particle Physics Department, Rutherford Appleton Laboratory, Didcot, United Kingdom
[e] Also at Department of Physics, University of Johannesburg, Johannesburg, South Africa
[f] Also at TRIUMF, Vancouver BC, Canada
[g] Also at Department of Physics, California State University, Fresno CA, United States of America
[h] Also at Novosibirsk State University, Novosibirsk, Russia
[i] Also at Department of Physics, University of Coimbra, Coimbra, Portugal
[j] Also at Department of Physics, UASLP, San Luis Potosi, Mexico
[k] Also at Università di Napoli Parthenope, Napoli, Italy
[l] Also at Institute of Particle Physics (IPP), Canada
[m] Also at Department of Physics, Middle East Technical University, Ankara, Turkey
[n] Also at Louisiana Tech University, Ruston LA, United States of America
[o] Also at Dep Fisica and CEFITEC of Faculdade de Ciencias e Tecnologia, Universidade Nova de Lisboa, Caparica, Portugal
[p] Also at Department of Physics and Astronomy, University College London, London, United Kingdom
[q] Also at Department of Physics, University of Cape Town, Cape Town, South Africa
[r] Also at Institute of Physics, Azerbaijan Academy of Sciences, Baku, Azerbaijan
[s] Also at Institut für Experimentalphysik, Universität Hamburg, Hamburg, Germany
[t] Also at Manhattan College, New York NY, United States of America
[u] Also at CPPM, Aix-Marseille Université and CNRS/IN2P3, Marseille, France
[v] Also at School of Physics and Engineering, Sun Yat-sen University, Guanzhou, China
[w] Also at Academia Sinica Grid Computing, Institute of Physics, Academia Sinica, Taipei, Taiwan
[x] Also at School of Physics, Shandong University, Shandong, China
[y] Also at Dipartimento di Fisica, Università La Sapienza, Roma, Italy
[z] Also at DSM/IRFU (Institut de Recherches sur les Lois Fondamentales de l'Univers), CEA Saclay (Commissariat à l'Energie Atomique et aux Energies Alternatives), Gif-sur-Yvette, France
[aa] Also at Section de Physique, Université de Genève, Geneva, Switzerland
[ab] Also at Departamento de Fisica, Universidade de Minho, Braga, Portugal
[ac] Also at Department of Physics, The University of Texas at Austin, Austin TX, United States of America
[ad] Also at Department of Physics and Astronomy, University of South Carolina, Columbia SC, United States of America
[ae] Also at Institute for Particle and Nuclear Physics, Wigner Research Centre for Physics, Budapest, Hungary
[af] Also at California Institute of Technology, Pasadena CA, United States of America
[ag] Also at Institute of Physics, Jagiellonian University, Krakow, Poland
[ah] Also at LAL, Université Paris-Sud and CNRS/IN2P3, Orsay, France
[ai] Also at Nevis Laboratory, Columbia University, Irvington NY, United States of America
[aj] Also at Department of Physics and Astronomy, University of Sheffield, Sheffield, United Kingdom
[ak] Also at Department of Physics, Oxford University, Oxford, United Kingdom
[al] Also at Department of Physics, The University of Michigan, Ann Arbor MI, United States of America
[am] Also at Discipline of Physics, University of KwaZulu-Natal, Durban, South Africa
[*] Deceased